Multiple Swing Out-of-Step Relaying

Francisco G. Velez Cedeno

Dissertation submitted to the faculty of the Virginia Polytechnic Institute and State University in partial fulfillment of the requirements for the degree of

Doctor of Philosophy
in
Electrical Engineering

Committee Members

Virgilio A. Centeno (Chairman)
Jaime De La Ree Lopez
Arun G. Phadke
James S. Thorp
Douglas K. Lindner
Werner E. Kohler

December 6th, 2010
Blacksburg, Virginia

Keywords: wide area measurements, power system stability, out-of-step protection, forecasting, multiple-swing

Multiple Swing Out-of-Step Relaying

Francisco G. Velez Cedeno

Abstract

The reduced stability margin, at which power systems are being operated these days, has encouraged the power industry to come up with new ideas to guarantee a continuous and reliable operation of the bulk interconnected system. The development of the synchronized Phasor Measurement technology, and its deployment in several locations in the network, has introduced a promising means to protect power systems from undesired conditions.

This research effort describes a methodology to handle transient stability in power systems using Wide Area Measurements. A correct identification of transiently stable and unstable power oscillations can be achieved with the use of the Out-of-Step protection technique presented in this document. The development of this idea is explained through the analysis of small power system models, and tested in three different operating conditions of the state of California.

The main contribution of this research work, to the Out-of-Step relaying theory, is the identification of multiple unstable swings after a given disturbance. In other words, an Out-of-Step protection scheme that handles a network that behaves as a multi-machine system is presented.

This dissertation is dedicated to my parents, Francisco Vélez and Velia Cedeño. For the encouragement, support and love they always manifested during this period of time.

Acknowledgments

I would like to thank Dr. Virgilio Centeno, my academic advisor, for his continuous guidance, support and encouragement throughout my research work. Dr. Centeno has proved to be a valuable mentor and I will always be thankful for all his help and advice. I would also like to thank Dr. Jaime De La Ree who gave me the opportunity to be part of the Power Engineering program at Virginia Tech; his assistance and guidance is truly appreciated. Special thanks go to Dr. Arun Phadke and Dr. James Thorp for the contributions and comments they kindly extended to this research effort. The interest of Dr. Werner Kohler and Dr. Douglas Lindner in this endeavor is also appreciated.

Table of Contents

List of Figures

List of Tables

Chapter 1 Introduction

At their inception, power systems were built to deliver power at locations geographically close to the generation stations. This characteristic made power systems very robust, which means that power systems were operated way below their stability limits. A small or large disturbance would not upset the system and the ability to deliver power was not compromised. As the use of electrical power became more popular in the early 20th century, the need to transmit power over long distances became imminent. This along with the increase in the network size has changed the way power systems are being operated. Nowadays power grids are pushed to operate closer to their stability limits. Increase in energy demand, hence increase in generation, and lack of new transmission lines have caused the system reach stressed conditions more often and system collapses, such as the 2003 northeastern blackout, are not unlikely to happen anymore. In fact there are references that describe how the probability of a cascading event becomes larger as the loading in the system increases [1].

Government agencies have imposed constrains on power utilities and system operators making them comply with regulations that try to assure a reliable operation of the bulk power system. This is one of the reasons why control and protection of the network has become an important field of study over the past years. With the invention and deployment of Phasor Measurement Units (PMUs), throughout the grid, new and more accurate protection philosophies and operational guidelines are being implemented. This document focuses on the use of this technology to handle transient stability in power systems.

In this dissertation a new Out-of-Step protection scheme is presented. This scheme makes use of phasor measurement data collected in different parts of the system to predict loss of synchronism between generating groups. This protection scheme was tested on different dynamic models in order to evaluate its performance during stable and unstable swings.

1.1 Power System Stability

Power system stability refers to the capacity of a power system to regain an acceptable operating condition after it has been subjected to normal or abnormal perturbations [2], this operating condition is achieved if the system frequency and voltage levels stay close to their nominal values. The study of power system stability is divided into two categories, voltage stability and angular stability.

1.2 Voltage Stability

Voltage Stability is the ability of the power system to maintain acceptable voltage levels throughout the grid as the system suffers modifications in its operating condition; these changes usually take place in the form of load increments. Voltage instability is a complicated phenomenon that normally occurs when the system is heavily loaded with insufficient reactive support [3]. Under these conditions voltage, in parts of the network, begins to drop drastically giving rise to what is called voltage collapse.

1.2.1 Angular Stability

Angular Stability refers to the property of a power system to stay in synchronous operation after being affected by a system disturbance. These perturbations can be of different nature and magnitude, such as load changes, three phase faults, transmission line tripping, loss of generating units, etc. After a given disturbance, angular stability is achieved if all generating units remain in synchronism with each other.

These perturbations are divided into small and large disturbances, and the concepts of Steady State Stability and Transient Stability are studied separately.

1.2.2 Steady State Stability

Steady State Stability, also called small signal stability, is the power system's ability to withstand small perturbations. Small random changes in load and generation account for the majority of these disturbances. Whether or not the system reaches an acceptable operating point after one of these events depends on different system

parameters such as, generation reserves, availability of synchronizing and damping torque, and the power-angle curve operating point at the time of the disturbance.

Steady state instability is not a relaying problem, small signal instability initiates with small oscillations in the power system that are not properly damped by the system controls such as excitation systems and power system stabilizers. In order to avoid this kind of instability configuration of control devices has to be tracked and updated according to system's needs.

1.2.3 Transient Stability

Transient Stability is the ability of a power system to survive and recover from a large system disturbance, e.g. three phase faults or loss of transmission lines. During the transient period machines in the system start swinging against each other and stability is more difficult to predict than in the steady state stability problem. The magnitude and location of the disturbance play an important role in the response of the system [4]. This response is governed by nonlinear differential equations that have to be solved for different system disturbances, these equations are solved in the form of time-domain simulations. After the simulations are run and the desired output is obtained, rotor angles are plotted against time and synchronism in the system is then evaluated. In general transient stability studies, or dynamic simulations, are performed in order to determine if the generators will stay in synchronism after the system is subjected to a given disturbance [5].

This dissertation focuses in this kind of stability. Several time-domain simulations were run, in the system under study, to determine the dynamic behavior of the network when it was subjected to different perturbations. With this information an Out-of-Step protection scheme was developed and tested for different transiently stable and unstable cases.

1.3 Power Swings

The dynamic behavior of the generators is governed by Newton's second law of motion. The difference between mechanical and electrical power in the units, after the system has been disturbed, accelerates or decelerates the machines at different rates, causing the machines to oscillate (or swing) against each other. A power swing is the variation in power flow that occurs as a consequence of this oscillatory movement.

The equation that describes the motion of the generators rotors, hence the power oscillation in the system, is the swing equation; equation (1.1). A more comprehensive treatment of this expression is presented in Chapter 3.

$$\frac{2H}{\omega_s}\frac{d^2\delta}{dt^2} = P_m - P_e = P_a \tag{1.1}$$

Depending on the location and magnitude of the disturbance power swings can be either stable or unstable, as shown in Figure 1-1. Whether or not the machines remain in synchronism is what determines the nature of the swing.

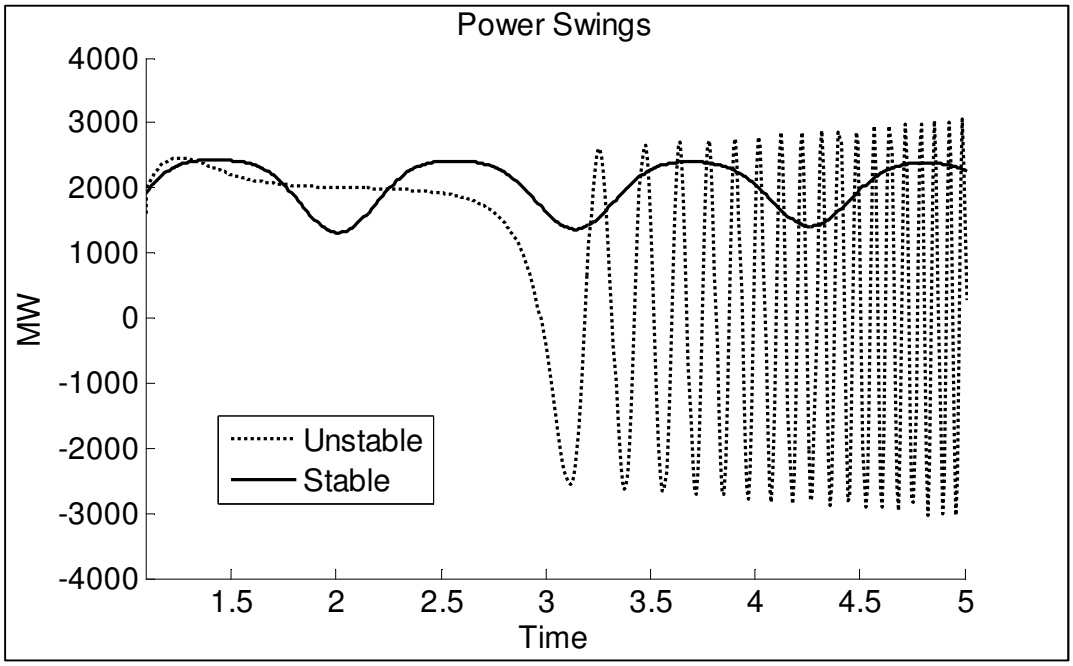

Figure 1-1. Power Oscillation after a System Disturbance

1.4 Out-of-Step Condition

Out-of-Step condition, or unstable power swing, refers to the operating situation when a group of generators is not synchronized with the rest of the machines in the system. This state of the power system is highly undesirable due to the stress it brings to the system; large cyclic power flows, high currents in the network and cyclic torque oscillations in the generators are some effects of this phenomenon [6]. When this situation is detected corrective actions should be initiated in order to separate the portions of the network operating asynchronously.

Separation of the system should occur at preselected locations which are determined by system planners and protection engineers. Transient stability studies are also conducted to verify the correct position of Out-of-Step relays and to decide if more relays are needed in the system.

1.5 Out-of-Step Relying

When generating units in the system start to swing against each other, due to a system perturbation, Out-of-Step relays have to determine whether the system will remain in synchronism or experience an unstable swing (an Out-of-Step condition), this is one of the two functions this kind of protection devices have to perform; they also execute what it is called power swing blocking.

1.5.1 Power Swing Blocking

Power swing blocking function refers to the capability of the Out-of-Step relay to differentiate between faults and power swings. Whit this function protection elements can be blocked from tripping when the system is undergoing a power swing. Tripping under stable swings is highly undesirable since the system will be able to recuperate by itself and no action is needed. However some protection schemes can be mislead into operation by stable swings. For example an impedance locus encroaching a protection zone, as shown in Figure 1-2.

Instantaneous phase over-current relays, directional instantaneous over-current relays and distance relays are some of the protection elements that are prone to false-operate during a power swing [7]. Blocking signals, from the Out-of-Step relay, can be sent to these devices to prevent their operation.

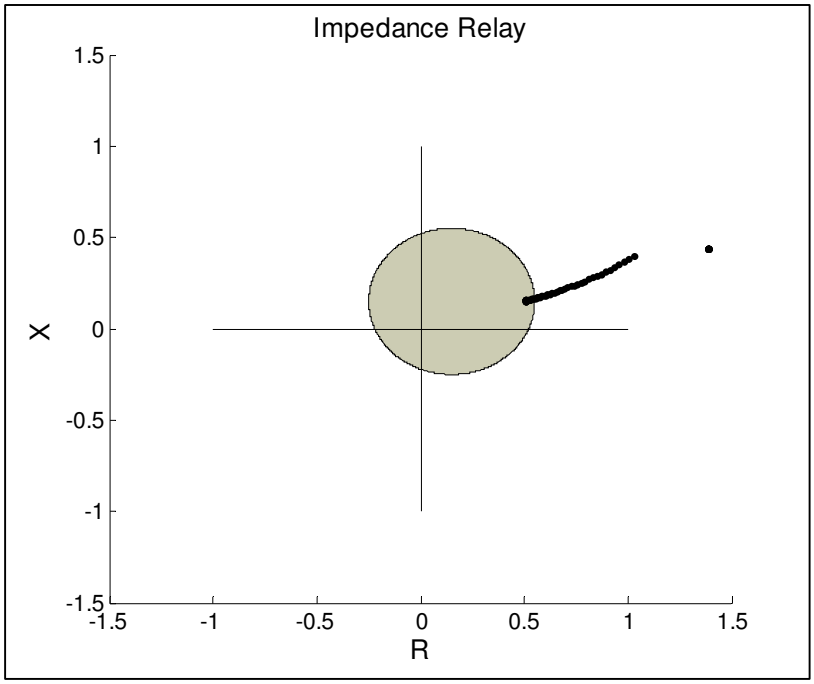

Figure 1-2. Power Swing Encroachment

1.5.2 Out-of-Step Trip

Once the system event has properly been identified as a power swing, by the aforementioned function, the Out-of-Step relay has to accurately discriminate between stable and unstable swings. This function is called Out-of-Step Trip, and it is the most important function in regards to this dissertation. When the relay identifies a given event as a stable swing no action is needed in terms of transmission line tripping. However, system separation should be conducted when an unstable swing is recognized. Different methods can be implemented to perform this function; some of them are discussed in Chapter 2.

1.6 Synchronized Phasor Measurements in Power System Stability

Introduction of PMUs in power systems have made the stability phenomenon easier to understand and handle. Thanks to synchronized phasors (or synchrophasors), oscillations in the system can be monitored in real-time and recorded for post-event analysis, something that was impossible before the development of the PMU technology.

Research at Virginia Tech in the 1990's proved that the observation of oscillations was feasible [8]. This marked the beginning of multiple PMU applications that today are becoming extraordinary tools for power system stability engineers.

One example of these applications is the monitoring of voltage magnitude in real-time, allowing system operators to know and visualize voltage levels throughout the network. Alarms can be set up to indicate low voltage levels in the system allowing the control centers to start preventive actions before the grid reaches its voltage stability limit. Reference [9] describes how with two PMU's measuring voltage magnitude and voltage phase angles in two parts of the network an accurate assessment of voltage stability can be performed for a small power system. Even though the use of synchrophasors is not critical for voltage stability monitoring, their advantage over traditional SCADA systems is evident.

Frequency, which can be obtained as a sub-product in PMUs [10], can also be monitored and compared in different parts of the power system in real-time. It is well known that a deviation from nominal frequency is an indicator of generation excess/deficit in the network. After a disturbance has occurred, operators can turn to frequency measurements in order to assess the severity of the disturbance and direct load or generation curtailment if necessary. Frequency measurements can also be used in order to evaluate interconnection status and identify locations where the system can be separated (islanding) in case of a loss of synchronism [11].

Probably one of the most interesting PMU applications is the monitoring of power system oscillations. PMUs are the only devices capable of providing fast and accurate streaming data necessary for this application, making the observation of inter-area

modes of oscillations possible. Small signal oscillations that occur naturally in the power system can be tracked and controlled with damping mechanisms before they become too large and system separation is required. Several tools have been tested and implemented in different USA power utilities with promising results to face the small signal stability problem. One example is the tool, developed by Southern California Edison (SCE), Power System Outlook which can identify modes of oscillations among other variables present in the interconnection system [12].

PMU applications for transient stability, on the other hand, are still in a developing stage. Even though several ideas have been proposed thorough the years [13-15], they have not become a reality for different reasons. In specific this application faces the challenge that the decision making has to be faster than in the voltage and small signal stability case. When handling this kind of problem, system operators generally have couple of seconds to assess whether or not the system will reach its stability limit. In this dissertation an application for handling transient stability with PMUs is presented.

1.7 Outline of this Dissertation

A brief description of the methods that have been used, by different power utilities, to face the Out-of-Step phenomenon is provided in Chapter 2. In addition, some of the ideas that have been proposed in the literature to handle transient stability are also mentioned.

Chapter 3 discusses the main ideas behind the Equal Area Criterion. This theoretical concept provides an excellent means to understand the transient stability problem. The expansion of the Equal Area Criterion for a multi-machine system which is called Extended Equal Area Criterion is also discussed.

The concept of time series analysis and forecasting is presented in Chapter 4. These methods are used in order to predict the evolution of voltage angle oscillations. The outcome of these predictions is fed to the Out-of-Step protection scheme in order to assess the transient stability of the system.

Chapter 5 mentions the key concepts and ideas behind the proposed Out-of-Step protection philosophy. As previously mentioned, this Out-of-Step protection scheme uses Wide Area Measurements and time series analysis to send the correct tripping/blocking signals to the relays in the field.

Simulations results are presented in Chapter 6. The proposed protection scheme was tested in 5 different power system models and its performance in the detection of unstable power swings is discussed at the end of this Chapter.

Chapter 7 presents the main contribution of this research effort to the power system protection theory. Conclusions of this research project are listed; and future work that can possible enhance the performance of this scheme are mentioned.

Chapter 2 Literature Review

The prediction of an Out-of-Step condition is in general not an easy task to achieve. Throughout the years different protection schemes, that aim to protect the system from this situation, have been proposed and implemented in different power utilities around the world. The following sections provide a brief description of some of these schemes.

2.1 Impedance Relays

This is probably the most common and mature relaying philosophy for Out-of-Step protection in the power system industry. It uses regular impedance elements, concentric circles or blinders characteristics, and timers in order to accomplish the identification of faults, stable and unstable swings.

In order to differentiate between power swings and faults these devices take into consideration that the apparent impedance seen by the relays would change almost instantaneously for a fault. While during a power swing the rate of change of the observed impedance would be significantly smaller.

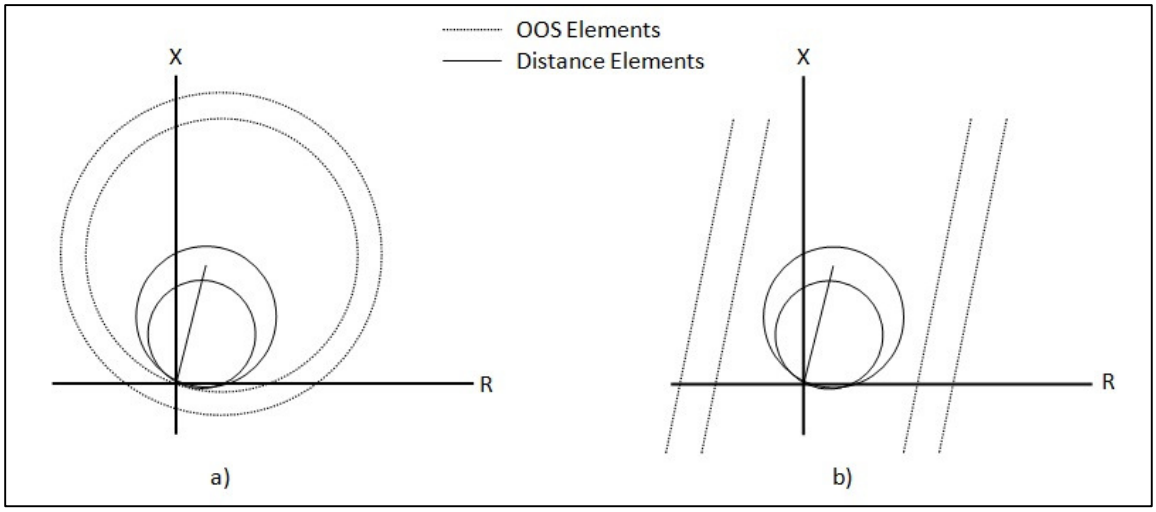

Figure 2-1. a) Concentric Circles b) Double Blinder

The operating principle of these devices is very simple. Looking at Figure 2-1a for example; if the apparent impedance locus crosses both circles practically simultaneously a fault is determined. If the apparent impedance crosses just the outer, or larger, circle a stable swing is stated. To declare a power swing as unstable, the apparent impedance must cross both impedance characteristics and the time between crossings should be smaller than the timer setting [16].

2.2 R-Rdot Scheme

This scheme was proposed by Bonneville Power Administration (BPA) and implemented in the 500 kV AC Pacific Intertie. It uses the apparent resistance seen at the relay's location and its rate of change in order to discriminate between stable and unstable swings. Its operation is very similar to conventional Out-of-Step impedance relays. Tripping would be initiated if the apparent resistance and its rate of change fall inside the unstable section of the R-Rdot plane defined by the following equation [17].

$$U = (R - R_1) + T_1 \frac{dR}{dt} \tag{2.1}$$

In equation (2.1) R is the apparent resistance measured by the relay and R_1 and T_1 are settings of the relay. Figure 2-2 shows the stable and unstable regions for this scheme. The relay does not if the rate of change of the apparent impedance is positive.

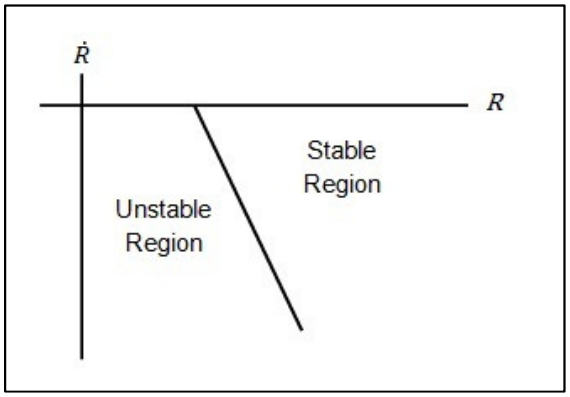

Figure 2-2. R-Rdot Scheme

According to [18], one R-Rdot relay was installed at Malin 500 kV substation only for monitoring of power swings. The relay detected around 150 events in 1983, in all of them the relay reacted accordingly to the systems conditions.

2.3 Tokyo Electric Power Approach

The Tokyo Electric Power system was characterized, in 1990, for having its load centers geographically separated from its generating stations. Generation was also dispersed in the system; groups of machines were located in the northern, eastern, western and southeastern parts of the network, as shown in Figure 2-3. Electrical energy was supplied to the load centers through 500 kV transmission lines [19].

It was discovered, by system operators, that if the system underwent specific events one of the generating groups would lose synchronism with respect to the rest of the system. The system faced uncontrolled small oscillations that would become large in a matter of 10 seconds, small signal instability.

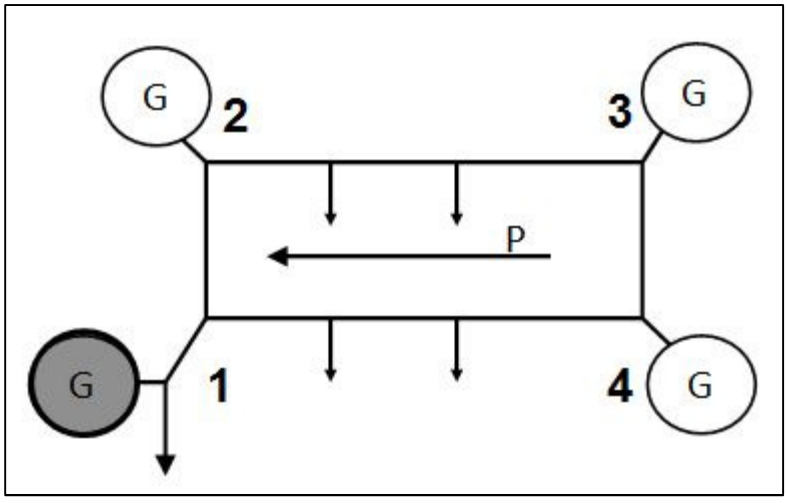

Figure 2-3. Japanese System and Critical Group

The Japanese power utility used the following approach to solve the problem [19]:

1. Measure voltage angles of representative substations for each group of generators.
2. Calculate phase angle differences between the critical group and the rest of the groups (δ_{1-2}, δ_{1-3} and δ_{1-3}).
3. Predict angle differences 200 ms in the future.
4. If two out of the three forecasted angle differences were greater than a threshold value, the power swing was tagged as unstable, and the critical group was separated from the rest of the system.

It is obvious that in order to execute this procedure the measured voltage angles in the different substations had to be synchronized. According to the authors of [19], using microwave telecommunication they could achieve an accuracy of 50 μs.

Step number 3, prediction of the angle difference, was done using the present value and 7 other previous points as shown in Figure 2-4. The threshold value selected was 100 degrees. Only one event is reported in the literature and the relay reacted properly for this disturbance.

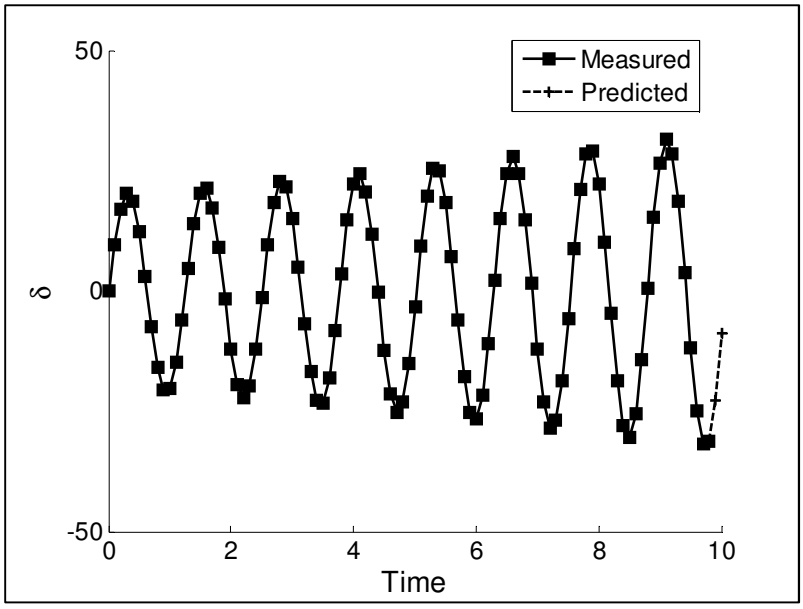

Figure 2-4. Small Signal Stability Prediction

2.4 Equal Area Criterion with PMUs

This scheme was implemented in the Florida (Florida Power and Light) and Georgia (Georgia Power Company) interface. This relay used the Equal Area Criterion principle to determine the nature of the transient power swing. It is well known that for stable swings the decelerating area must be larger than the accelerating area in the $P-\delta$ curve, otherwise the system is considered to be unstable.

An important feature of this proposed relay is the correct approximation of the Florida-Georgia interface as a two machine system, as illustrated in Figure 2-5. The model used comprises two machines connected through 500 kV transmission lines. The parameters of the model were calculated using data provided by the two utilities involved [20].

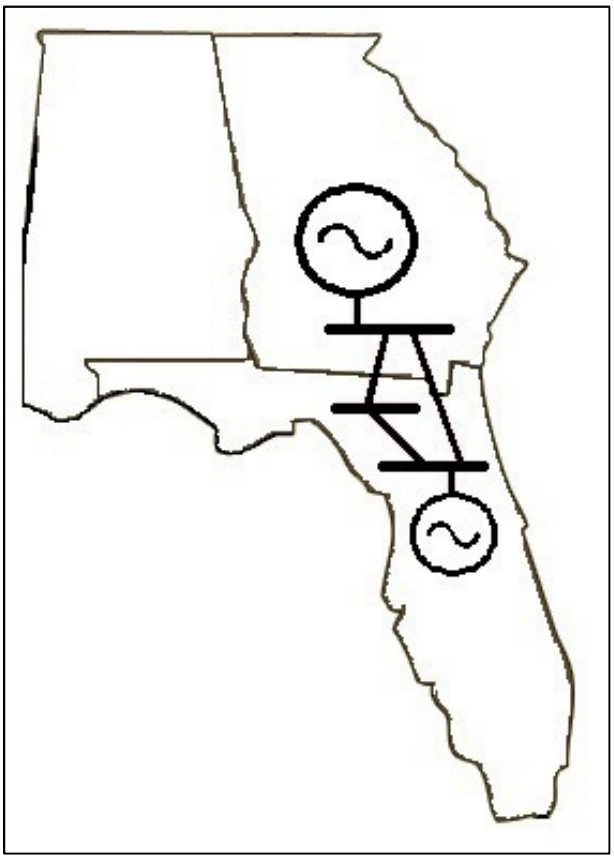

Figure 2-5. Florida-Georgia Interface

With the two machine model approximation and the installation of two PMUs, to represent the angles of the machines in Florida and Eastern USA respectively, the Equal Area Criterion principle was applied as follow.

For a fault case, the pre-disturbance and post-disturbance topology was known due to the continue supervision of the breakers in the 500 kV lines. Knowing that P_m does not change immediately and computing the $P-\delta$ curves beforehand the new operating point could be found, then the two areas were calculated and the stability of the power swing could be assessed. For a loss of generation case the pre-disturbance and post-disturbance $P-\delta$ curves are the same, the change in P_m was estimated using a least square approximation and then the areas were again calculated using the new operating point in the curve [21].

2.4.1 Equal Area Criterion

Equal Area Criterion, which will be fully explained in the next Chapter, has been a topic of research since it was first introduced for transient stability assessment [22]. There have been many research efforts that have tried to implement this kind of analysis in real power systems. Reference [23] uses PMU measurements at every generation station to compute the rotor angle of the machines in the system. It also employs aggregation techniques to reduce the system to a One Machine Infinite Bus equivalent. After the machine angles have been computed, and the equivalent has been created, the equal area criterion is used to assess the transient stability of the system. The main limitation in this Equal Area Criterion method is the need to monitor every generation station in the power system. Most of the techniques that propose this concept, as an on-line tool, to evaluate the system's transient stability face the same issue. This feature makes them inappropriate to be implemented in a real power system.

2.4.2 Equal Area Criterion in Time Domain

Equal Area Criterion is a method which uses power-angle curves to obtain the correct transient stability evaluation of a power system; this is the reason why this concept is

regarded as a stability assessment in the power angle domain. Reference [24] proposes the use of the same method but with a different approach; it suggests the use of the Equal Area Criterion in the time domain. This eliminates the need to compute the different power-angle curves of the network. In this method power output measurements have to be taken at every generation station in the network. When a system disturbance occurs, the algorithm maintains the total system mechanical power constant and equal to its pre-disturbance value. The total instantaneous electrical output power of the system is then compared against the mechanical power at every time step. The difference between these values ($P_m - P_e$) is integrated from the inception of the fault to the time when the maximum angle oscillation occurs. If the value of the total integration is greater than zero, the system is declared to be stable; otherwise the system is will undergo instability.

2.5 Time Derivatives of Voltage Angles

First and second derivatives of voltage angles have also been proposed to assess transient stability in power systems. Reference [25] describes a method in which voltage angle measurements, at a specific location in the network, are used in order to approximate the first and second time derivatives of the position of the rotor angles in a two-machine system equivalent. After a system disturbance, the relay can make a decision regarding system stability using $\delta - \delta'$ and $\delta' - \delta''$ plots. The former plane establishes when a stability assessment can be carried out and the latter determines the nature of the power swing, either stable or unstable. In a similar manner [26] proposes to approximate the acceleration and velocity of the rotor angles using local voltage angle measurements. It is claimed that with these two values an Out-of-Step condition can be detected if the acceleration changes sings in two consecutive measurements and the velocity exceeds a predetermined threshold value.

2.5.1 Swing-Center Voltage

Swing-center refers to the network location, in a two-machine power system equivalent, where the voltage magnitude is zero when the two machine angles are separated by 180 degrees. Under an Out-of-Step condition, in which the difference of angles will monotonically increase, the voltage magnitude at this specific location will vary between zero and one per unit. The voltage magnitude of the swing-center can be approximated using equation (2.2).

$$SCV \approx |V_s| \cos \varphi \tag{2.2}$$

In this equation $|V_s|$ is the voltage magnitude of a bus, located close the swing center, which is being locally measured and φ is the angle difference between this voltage and its associated current vector. Reference [27] calculates the first time derivative of the positive-sequence voltage to approximate the slip frequency between the two systems. A high value of this variable would indicate the presence of a power swing in the network. After the power swing has been correctly identified, this reference uses conventional impedance elements in order to distinguish stable and unstable power swings. It is claimed that with the use of this power swing identification method a more robust decision regarding the transient stability of the system can be accomplished.

2.6 Artificial Intelligence in Out-of-Step Protection

Artificial Intelligence methods such as Decision Trees and Artificial Neural Networks have also been applied to the power system transient stability problem. Artificial Intelligence refers to the ability of a machine or mechanism to interpret information and provide a decision regarding such data.

Decision Trees is data mining process in which a large numbers of stable and unstable cases are input to its logic. These cases have different initial operating conditions and/or different topology configurations. The Decision Tree then analyzes the data and outcomes a set of variables, or “attributes”, and threshold values that can differentiate

between stable and unstable cases at a given probability. Reference [28] uses PMU measurements taken at all machine buses, in the New England 39 bus test system, in order to calculate velocity and acceleration of the rotor angles. Different stable and unstable cases were created to build a decision tree which achieved an accuracy of 97 percent in the detection of instability.

Artificial Neural Networks (ANN) is also a pattern recognition method. It also implies creating a set of learning cases, both unstable and stable, to be supplied to the ANN. With the selection of input and output variables and the appropriate ANN architecture a set of weights and threshold values are adjusted during the training phase to obtain a correct stability assessment [29].

Even though a lot of research has been carried out in this topic, no effort to implement this kind of methods, for Out-of-Step protection, in a real system has been attempted.

2.7 Energy Methods

Transient energy functions are regarded as direct methods for transient stability assessment, since no step-by-step dynamic simulations are employed to evaluate the first swing stability of the system. This method relies in the computation of the transient energy of the system, which is the algebraic summation of its potential and kinetic energy after a given disturbance. This approach establishes that for a system to be stable, its transient energy has to be smaller than potential energy evaluated at the unstable equilibrium point (u.e.p.) [30]. Different kind of functions, depending on the assumptions made to analyze the system, can be used in order to find the correct value of the transient energy and the unstable equilibrium point of the system. Some of these functions for a system with classical machine models are, the energy function which uses relative rotor angles and the one which uses a center of inertia to compute the energies of the system [31]. This kind of analysis was a topic of many articles and research efforts during a long period of time; but its limitations in providing an accurate transient stability assessment in some cases, as shown in [32], make this technique unreliable to be implemented in real power systems.

Chapter 3 Equal Area Criterion

The analysis of transient stability is greatly related to the understanding of the Equal Area Criterion (EAC). A brief summary and some general ideas involving this concept are presented in this Chapter. Extended Equal Area Criterion, which is an expansion of the same method for a multi-machine system, is also discussed. The Equal Area Criterion method, as mentioned in section 2.4, was used in a real Out-of-Step protection scheme in the Florida-Georgia interface in the mid-nineties [33].

The Extended Equal Area Criterion, in this work, attempts to provide a conceptual and theoretical approach to the Out-of-Step protection scheme that will be presented in the following Chapters.

3.1 Machine Dynamics and the Swing Equation

When a major disturbance occurs in the power system, the generator rotors will start moving or oscillating around their synchronous speed. The differential equation that describes the motion of the rotors, as mentioned in section 1.3, is the swing equation (1.1). This equation is a form of Newton's second law of motion for angular movement, which states that the net torque applied to a rotating mass is equal to the product of its moment of inertia and its angular acceleration, equation (3.1). Each machine rotor in the power system is represented by one swing equation and it is important to mention that its solution is not feasible through algebraic methods. The swing equation is actually a non-linear differential equation whose solution needs to be found using numerical methods, a step-by-step computer simulations is the preferred method.

$$T_{net} = J\alpha \tag{3.1}$$

In power system terms, the net torque applied to a given machine is the summation of the mechanical and the electromagnetic torques present in the rotor, as illustrated in Figure 3-1. The mechanical torque is the momentum that the prime mover applies to the

machine and tends to accelerate the generator rotor. The electromagnetic torque is equal to the total output electric energy of the machine and it has the opposite effect on the rotor, it tends to decelerate it.

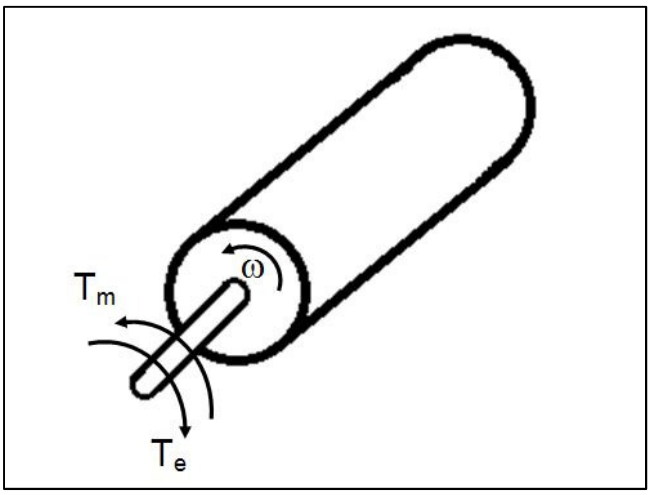

Figure 3-1. Generator Rotor

Under steady state conditions the mechanical and electromagnetic torques are equal to each other, and the angular acceleration and the net torque applied to the shaft are both zero. The same phenomenon occurs in all generators in the network. Since there is no acceleration, in any of the rotors, all machines in the system rotate at synchronous speed ω_s.

When a disturbance occurs in the network, the electromechanical torque applied to the machine suffers a sudden variation. On the other hand, the mechanical torque remains constant in the transient period since the machine controls, e.g. governor, exciter and power system stabilizer, are unable to take any rapid action. This unbalance between the mechanical and electromagnetic torque is what makes the rotor accelerate or decelerate. If the disturbance is large the acceleration will make the angular velocity increase without control and the rotor will not return to synchronous speed. If the rotor is subjected to a small acceleration, the machine's velocity will oscillate around synchronous speed and will settle down at this speed after the transient period is over.

The swing equation for single machine can be expressed as:

$$J\frac{d^2\theta_m}{dt^2} = T_m - T_e - T_D \tag{3.2}$$

where

θ_m	Angular displacement in mechanical radians with respect to a fixed reference
$d\theta_m/dt = \omega$	Angular velocity, in radians per second
$d^2\theta_m/dt^2 = \alpha$	Angular acceleration, in radians per second^2
T_m	Mechanical Torque, in N-m
T_e	Electromagnetic Torque, in N-m
T_D	Damping Torque, in N-m. Neglected in EAC studies
J	Moment of Inertia, in kg-m^2

After some mathematical manipulation the swing equation can be modified and expressed in a more convenient form for transient stability studies. The derivation of the swing equation in per unit system can be found in many references, as in [34].

$$\frac{H}{180f}\frac{d^2\delta}{dt^2} = P_a = P_m - P_e \quad per\ unit \tag{3.3}$$

In this case,

H	Inertia constant of the machine in seconds
f	System frequency
δ	Rotor angular displacement in electrical degrees from a synchronously rotating reference
P_m	Input mechanical power in p.u.
P_e	Output electrical power in p.u.

P_a Accelerating Power in p.u.

3.2 Power-Angle Equation

In order to properly use the EAC in transient stability studies, it is necessary to analyze the power output of a machine after the system has been perturbed. This variable, the output electrical power, is what will determine if the machine accelerates or decelerates; since the input mechanical power will remain constant during the transient period.

For transient stability assessments, generators are usually represented using the classical model for machines. This means each generator is composed by its internal voltage behind its transient reactance. The phase angle of the internal voltage is considered to be the rotor angle of the machine, δ in equation (3.3).

The output electric power of the machines is affected by sudden modifications in the power system. Tripping of transmission lines and system faults, for example, make the electrical output power change immediately. The power-angle equation relates the electrical output power, and the rotor angle, to changes in the system topology. To explain this concept the simple transmission system shown in Figure 3-2 will be used.

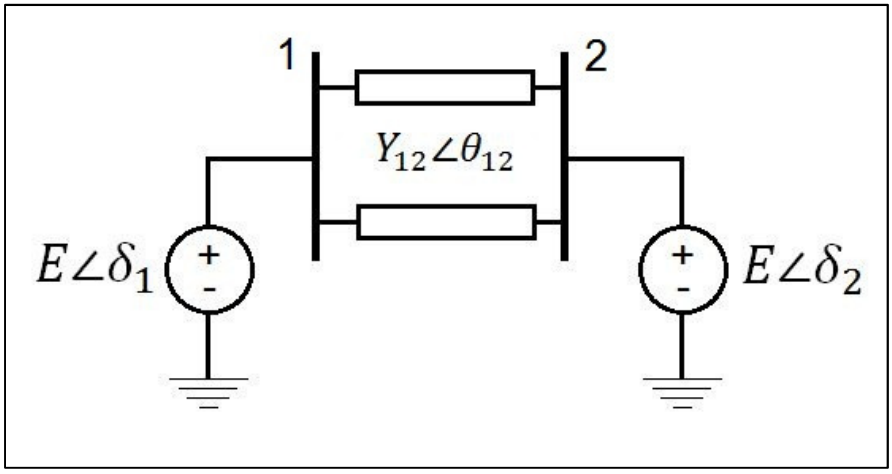

Figure 3-2. Transmission Network

Assuming the machine on the left is supplying power to the system on the right, which in this case is considered to be an infinite bus. And assuming the transient reactance, for both machines is included in Y_{12}, along with the admittance of other power transmission elements such as power lines and power transformers. It can be shown that the output electric power of machine one is defined by equation (3.4).

$$P_1 = |E_1|^2 G_{11} + |E_1||E_2||Y_{12}|\cos(\delta_1 - \delta_2 - \theta_{12}) \tag{3.4}$$

Equation (3.4) can be expressed as:

$$P_1 = P_c + P_{\max}\sin(\delta - \gamma) \tag{3.5}$$

Where

$$\delta = \delta_1 - \delta_2 \qquad \gamma = \theta_{12} - \pi/2$$

$$P_c = |E_1|^2 G_{11} \qquad P_{\max} = |E_1||E_2||Y_{12}|$$

Equation (3.5) is usually called the power-angle equation since it determines the amount of electric power being transferred over the admittance Y_{12} for a given value of δ. A simplified equation can be obtained if it the resistance of the network is considered to be so small that it can be neglected. In this case γ and P_c become zero, giving rise to equation (3.6), this simplified version of the power-angle equation will be used in the following sections to demonstrate the principle of the equal area criterion.

$$P_1 = P_e = \frac{E_1 E_2}{X_{12}}\sin\delta \tag{3.6}$$

If equation (3.6) is plotted for different values of delta the power-angle curve is obtained, Figure 3-3. A similar curve could be plotted if equation (3.5) was used instead of equation (3.6). It can be observed that the output electric power follows a sinusoid waveform having its maximum at 90 degrees. In real power systems the voltage magnitude throughout the network stays very close to 1 p.u., making the equivalent

reactance X_{12} an important factor in the power transfer capability of the system. A lower value of reactance meaning a higher power transfer capability.

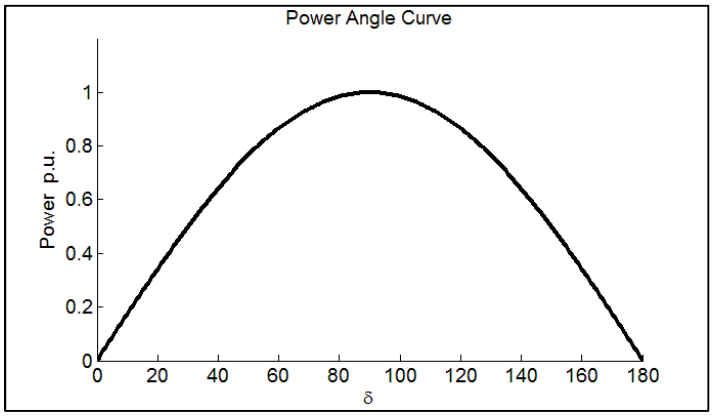

Figure 3-3. Power-Angle Curve

3.3 Equal Area Criterion (EAC)

The equal area criterion provides a graphical representation of the transient stability problem. This method portrays the accelerating energy, also called kinetic energy, the rotor gains when the system has been perturbed. It also depicts the decelerating (potential) energy the system has available to overcome the acceleration effect. If the former is larger than the latter, the machine will pull out of synchronism.

This elegant concept is used to assess the stability of a single machine against an infinite bus. An infinite bus is supposed to represent a system whose inertia is so large that it never deviates from synchronous speed, its voltage magnitude is always 1 p.u. and its voltage angle is fixed at zero degrees, refer to Figure 3-4. Stability assessments for larger power systems, either two-machine or multi-machine systems, can also be carried out using the EAC. The process involves making an equivalent One Machine Infinite Bus (OMIB) system from the larger system using network reduction techniques. The reduction from a two-machine system is straight forward whereas the reduction from a larger system engages more complicated steps. This will be analyzed in the next section where Extended Equal Area Criterion is discussed.

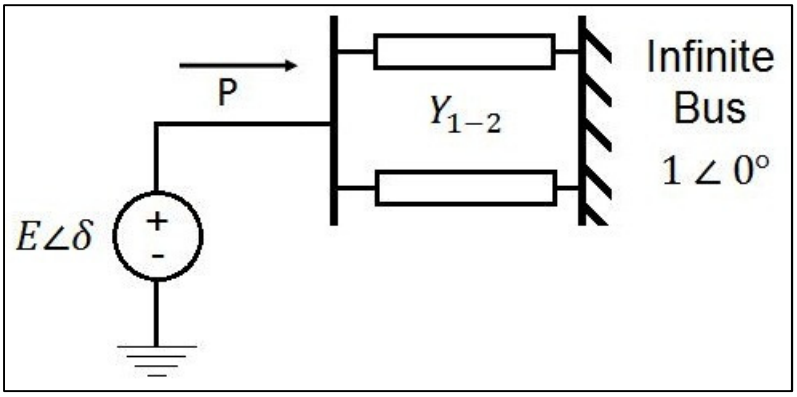

Figure 3-4. One Machine Infinite Bus System

The following assumptions are made regarding the use of the equal area criterion:

- The machine will either lose synchronism or remain at synchronous speed after the first swing (or oscillation).
- Damping is negligible.
- Input Mechanical Power is held constant throughout the transient period.

The swing equation for a single machine was developed in section 3.1, this is also the equation of motion for a single machine connected to an infinite bus. In this case delta is measured with respect to the infinite bus, which has a phase angle of zero degrees.

With some mathematical manipulation, it is proved in [35] that equation (3.3) can be rewritten in the following form:

$$\left(\frac{d\delta}{dt}\right) = (\omega - \omega_0) = \sqrt{\frac{180 f}{H} \int_{\delta_0}^{\delta_m} P_a d\delta} \tag{3.7}$$

In which ω_0 is the synchronous speed and the term $(\omega - \omega_0)$ is the speed deviation from this rotating reference. In order to achieve a stable operating condition, after a system perturbation, this term has to be equal to zero. Meaning that after the transient period is over the machine will return to operate at synchronous speed. This leads to the following equation:

$$\int_{\delta_0}^{\delta_m} P_a d\delta = \int_{\delta_0}^{\delta_m} (P_m - P_e) d\delta = 0 \tag{3.8}$$

Equation (3.8) is in fact the equal area criterion; it states that after a disturbance the area enclosed by the net accelerating power and delta, in the power-angle curve, has to be equal to zero for the system to be stable. This concept can be better explained using Figure 3-5.

Under steady state conditions the input mechanical power is equal to the output electrical power, point a in Figure 3-5. The machine is operating at δ_0 delivering power to the infinite bus and it will stay in this condition as long as the system does not suffer any modification. The net accelerating power acting on the rotor is zero.

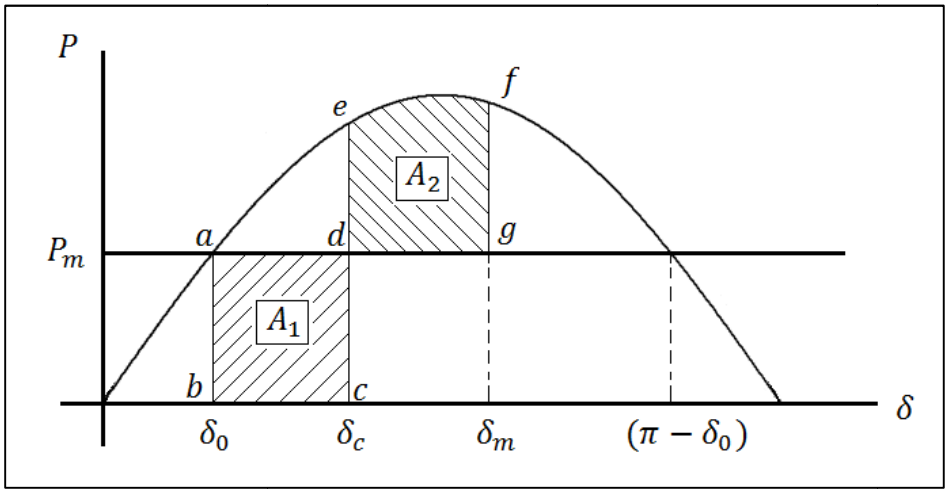

Figure 3-5. Equal Area Criterion

If a three-phase short circuit occurs at the machine terminals, the electrical power delivered by the machine will instantaneously drop to zero; since the power being transferred to the infinite bus will be suddenly interrupted. The input mechanical power will remain constant during the fault period resulting in an accelerating power equal to P_m. The rotor will gain speed and it will deviate from synchronous speed, hence the rotor angle will start moving from its steady state operating point δ_0 to a different

position. At the moment the fault is cleared the rotor will have advanced to position δ_c, at this same instant of time the power transfer capability of the system is restored making the output electric power take the value corresponding to point e in the power-angle curve. This means that the output electric power will be larger than the input mechanical power. The rotor now will experience a deceleration, but due to its inertia and the previous applied accelerating power it will still continue to move forward until it reaches a maximum value at δ_m. After this, the rotor angle will stop for an instant of time and will move backwards to continue an oscillatory movement between the origin and δ_m in the power-angle curve locus.

The accelerating energy, the rotor gained during the fault period, is represented by Area one (A_1) in Figure 3-5. While the total decelerating energy applied to the rotor, in this case, is equal to Area two (A_2). The equal area criterion states that the machine will stay in synchronism if Area two is equal to Area one. Further analysis of the equal area criterion can prove that both areas do not have to be equal, the general first swing stability requirement is that Area two has to be larger than Area one, equation (3.9).

$$A_{acc} < A_{dec} \tag{3.9}$$

The accelerating area, in some occasions, can be larger than the decelerating area, creating an unstable case as shown in Figure 3-6. This might happen if the fault is not cleared fast enough. In this situation, the rotor will reach position $(\pi - \delta_0)$ still moving forward, since the accelerating energy has not been completely balanced out with the decelerating energy. Once the rotor moves beyond this point an accelerating power will be acting on the rotor again, pushing the rotor further away from synchronous speed. In this case the machine will not recover its synchronous operation and its separation from the infinite bus is unavoidable.

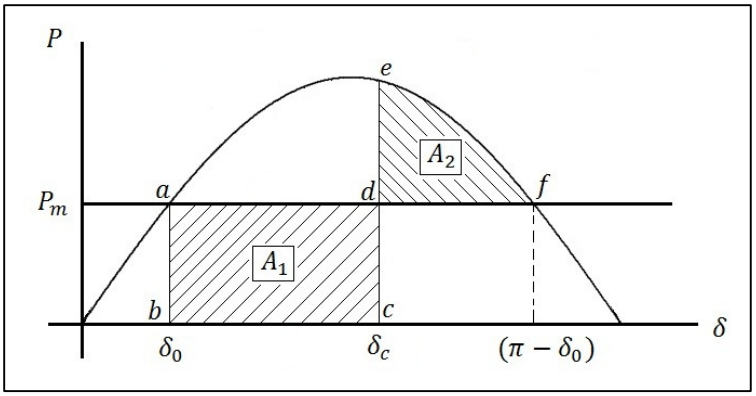

Figure 3-6. EAC-Unstable Case

The stability margin η defined as how close the system is from instability for a given disturbance, can also be expressed using the areas in Figure 3-5 and Figure 3-6.

$$\eta = \frac{A_{acc}}{A_{dec}} \tag{3.10}$$

Obviously for cases in which η is larger than 1 an unstable case is declared. For stable perturbations in the system, the stability margin will take values lower than one. The severity of these disturbances can be ranked accordingly with this stability measure as well.

3.4 Extended Equal Area Criterion (EEAC)

The equal area criterion applied to the one machine infinite bus system is a great theoretical concept that helps understand the key points of the transient stability phenomenon. Nevertheless, it cannot be applied directly to a real system which is composed, generally speaking, of hundreds of machines interconnected through transmission lines. The Extended Equal Area Criterion provides the means to handle a larger power system; it is basically an extension of the EAC for a multi-machine system.

This concept was first introduced in the late eighties [36] and it has proved to be robust and flexible for the assessment of transient stability. The Extended Equal Area Criterion

makes the assumption that the large multi-machine power system can be reduced into a two-machine equivalent, one representing a critical group of machines and the second one formed by the remaining generators in the system. This two-machine system can be transformed, in a subsequent step, into an OMIB system. The basic EAC principles, discussed in the previous sections, are then used in order to assess the stability of the large power system. Figure 3-7 illustrates the main steps of the EEAC method.

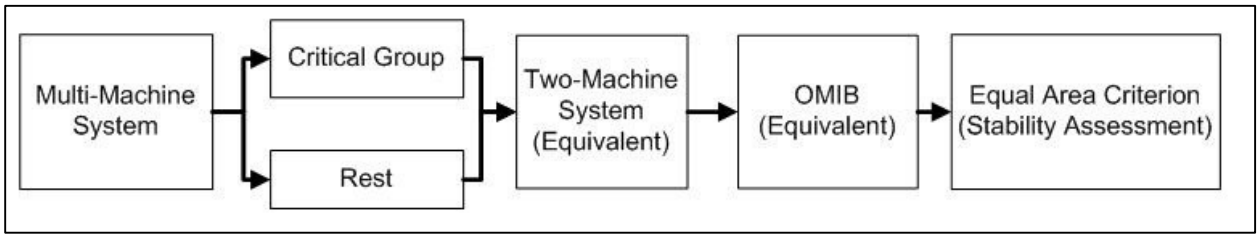

Figure 3-7. EEAC Principle

One of the main assumptions in the EEAC approach is that the loss of synchronism is caused by the separation of the network into two groups. Separation of the system into more than two groups, at the same instant of time, is considered impossible to occur in this method. Another assumption made in this process is that the equivalent rotor angles of the generators, in the two-machine equivalent, can be represented by their respective center of angles.

The identification of the critical group of machines is an important step in this method. Equivalents are affected if additional generators are included or some are disregarded in the machine clusters, giving rise to inaccurate results. The critical group of machines is the one that is expected to lose synchronism after a system disturbance. It is understood that for different event locations and perturbation types the machines composing the critical groups might be different. The procedure to identify these critical machines, for a given disturbance, is described in detail in references [35-37]. It involves the use of Taylor series expansions and the algebraic calculation of the critical clearing angle, with its respective critical clearing time, for that disturbance. The critical

clearing angle is the value of δ_c, in Figure 3-5, that makes the accelerating and decelerating areas equal to each other. The candidate machines are then ranked according to their critical clearing time and the critical cluster is the one with the lowest critical clearing time.

The selection of the critical machines can be obtained with step-by-step simulations as well. In this case, dynamic simulations are run in the system under study and rotor angles are plotted against time for a given disturbance. The critical group is then detected analyzing the plots, the first group that goes unstable is considered to be the critical cluster. This approach is the one used in this dissertation.

Once the critical group of machines has been identified the following step, as illustrated in Figure 3-7, is to make an equivalent of the critical group and the remaining system. The following equations will show how this is accomplished.

Setting the notation for the set of critical machines as C, its equivalent machine as c, the cluster of remaining machines as R and its equivalent representation as r, the following expressions are defined:

$$M_c = \sum_{i \in C} M_i \quad ; \quad \delta_c = \sum_{i \in C} M_i \delta_i \Big/ M_c \tag{3.11}$$

$$M_r = \sum_{j \in R} M_j \quad ; \quad \delta_r = \sum_{j \in R} M_j \delta_j \Big/ M_r \tag{3.12}$$

The swing equations, for the two equivalents, are given by,

$$M_c \ddot{\delta}_c = \sum_{i \in C} P_{m,i} - P_{e,i} \tag{3.13}$$

$$M_r \ddot{\delta}_r = \sum_{j \in R} P_{m,j} - P_{e,j} \tag{3.14}$$

where

M_i Inertia Constant of Machine i, $M_i = 2H_i/\omega_s$

H_i Inertia constant of Machine i in seconds

ω_s Synchronous Speed in radians per second

Once the equivalent two-machine system has been created; the next phase in the Extended Equal Area Criterion is to obtain a OMIB equivalent from the already reduced model. Equations (3.13) and (3.14) can be reduced to a single equation if the difference of the two equivalent rotor angles is computed. Denoting by 1 the critical group of machines and by 2 the remaining set, the following equations are obtained.

$$\delta_{12} = \delta_1 - \delta_2 \tag{3.15}$$

$$\frac{d^2\delta_1}{dt^2} - \frac{d^2\delta_2}{dt^2} = \frac{\omega_s}{2}\left(\frac{P_{m1} - P_{e1}}{H_1} - \frac{P_{m2} - P_{e2}}{H_2}\right) \tag{3.16}$$

Defining H_{12} as:

$$H_{12} = \frac{H_1 H_2}{H_1 + H_2} \tag{3.17}$$

The next expression is obtained if both sides of equation (3.16) are multiplied by H_{12}.

$$\frac{2}{\omega_s}\left(\frac{H_1 H_2}{H_1 + H_2}\right)\frac{d^2(\delta_1 - \delta_2)}{dt^2} = \left(\frac{P_{m1}H_2 - P_{m2}H_1}{H_1 + H_2} - \frac{P_{e1}H_2 - P_{e2}H_1}{H_1 + H_2}\right) \tag{3.18}$$

Making some arrangements to the previous expression, the swing equation (3.19) for an OMIB system is obtained.

$$\frac{2H_{12}}{\omega_s}\frac{d^2\delta_{12}}{dt^2} = P_{m12} - P_{e12} \tag{3.19}$$

where

$$P_{m12} = \frac{P_{m1}H_2 - P_{m2}H_1}{H_1 + H_2} \qquad and \qquad P_{e12} = \frac{P_{e1}H_2 - P_{e2}H_1}{H_1 + H_2}$$

Once the OMIB equivalent has been created, the EAC stability assessment can be carried out in order to identify stable and unstable cases in the multi-machine system.

3.5 Power-Angle Curves

When a real power system is subjected to a fault the power transfer capability of the system is reduced, but the system is still able to deliver some power to the load centers through the non-faulted network. The assumption made in section 3.3 that a three-phase fault would make the electric power in the system drop to zero is only valid for a fault at the generator's terminal of an OMIB system.

In order to clear the fault the faulted portion of the network has to be disconnected from the system, weakening the power transfer capability of the remaining network. The fault and subsequent switching of the power system elements make the power-angle curves of the steady-state, faulted, and post-disturbance condition different. This discrepancy has to be taken into consideration in the Equal Area Criterion assessment for transient stability. Figure 3-8 shows the three different curves for a fault case.

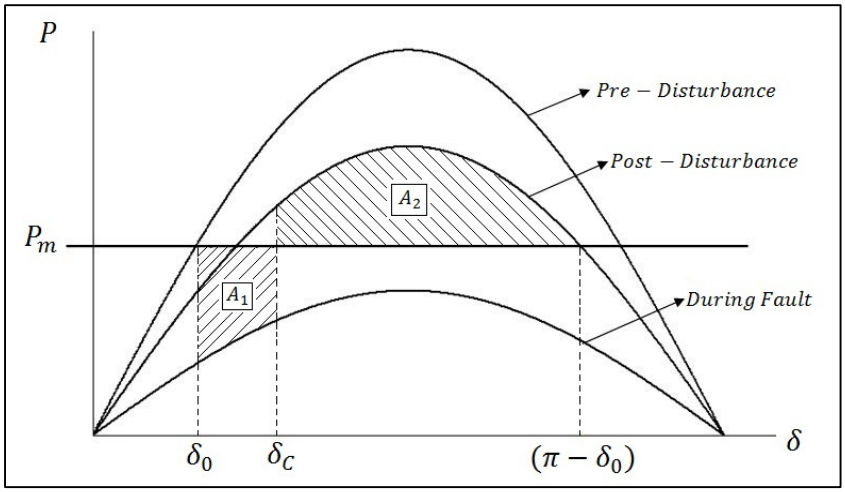

Figure 3-8. Power-Angle Curves

Chapter 4 Forecasting and Time Series Analysis

The concepts of time series analysis and forecasting will be discussed in this Chapter. Just as the Extended Equal Area Criterion method is used to assess transient stability for severe system events, the use of time series in this dissertation attempts to provide an alternative new approach in the evaluation of the same power system phenomenon. A brief summary of the different time series models and their parameter estimation will be discussed; the later will play an important role in the performance of the proposed protection scheme in this dissertation. In the following Chapters the implementation and simulations results of time series forecasting in an Out-of-Step relay will be presented.

4.1 Forecasting

Forecasting is a widely applied tool in the power system industry. Energy prices and growth of power demand are usually predicted for the next day, moths and years to come. Based on the outcome of these predictions, construction of new power infrastructure can be programmed, and in a deregulated power market bids for the best existing and economic power can be placed. In recent years, environmental constrains in the industry have made the forecasting of wind and solar power availability also important. With these predictions, the proper amount of renewable energy can be programmed for a given a period of time [38], leaving the rest of the generation to conventional fossil fuel technologies.

Power system stability is highly influenced by these predictions; accurate estimations of power demand and renewable energy have to be acquired in order to schedule the generating units that would dispatch the required power. Failure to do this would jeopardize stability in the system with the possible outcome of energy outages in some portions of the network. One example of this kind of contingencies is the event that took place in Texas in 2008 when inaccurate predictions of wind power availability and energy demand made the system reach low frequency values. This undesired condition

forced the reliability operator ERCOT to implement load curtailment in parts of the network so stability could be guaranteed in the rest of the system [39].

Forecasting of Geomagnetically Induced Currents (GIC's), in transmission power systems, has become an important topic in recent years. These currents are caused by severe magnetic solar storms which occur in periods of approximately eleven years. When the planet suffers a solar disturbance, a potential difference is created at the earth's surface causing a quasi-DC current to enter and leave the transmission power network through grounded points, mainly transmission power transformers. After they enter the power system, GIC's flow through transmission lines to a different grounded point in the grid and go back to the earth's surface. Power transformers with grounded neutrals are the most affected by such currents. GIC's saturate the transformer core causing an increase in the reactive power consumption by the transformer; these devices also become a source of harmonics in the presence of GIC's. An example of the importance of forecasting these currents is the event that occurred in the Hydro-Quebec system in 1989 which was triggered by a solar storm. The system experienced a sudden increase in reactive power consumption, by transformers, which produced voltage stability problems in the network, this led to a system collapse which lasted for several hours [40]. The prediction of the geomagnetic induced currents in the system involves the forecasting of the electric filed, magnitude and direction, at the earth's surface. With this information, the computation of the currents flowing through the transformers and transmission lines can be carried out. A detailed explanation of the procedure to follow is found in [41]. With an accurate GIC prediction, reactive reserves can be placed in the system in order to offset the effect of transformer saturation.

The events mentioned in this section try to highlight the importance of forecasting in the power system industry, especially its effect on the network stability. The idea of knowing what will happen in the future is surely interesting and frightening at the same time. But the fact is that future cannot be known beforehand, only approximations or estimations can be attempted. This is one of the reasons why time series analysis has become an important tool in many disciplines, and power systems is not an exception.

4.2 Time Series

A time series is a collection of measurements or data points throughout time, it represents the chronological behavior of a given variable. There are two types of time series, continuous and discrete. Continuous series are those in which the variable being monitored is defined at every moment in time, temperature and velocity are examples of such type of variables. Discrete time series, on the other hand, are those in which the values of the variable being recorded are accessible only at certain instants of time. Usually, and for the purpose of this dissertation, these observations are taken at equally spaced time intervals. An example, of a discrete time series, can be the voltage magnitude of a particular bus in the power grid being reordered every 33.33 milliseconds, as illustrated by Figure 4-1.

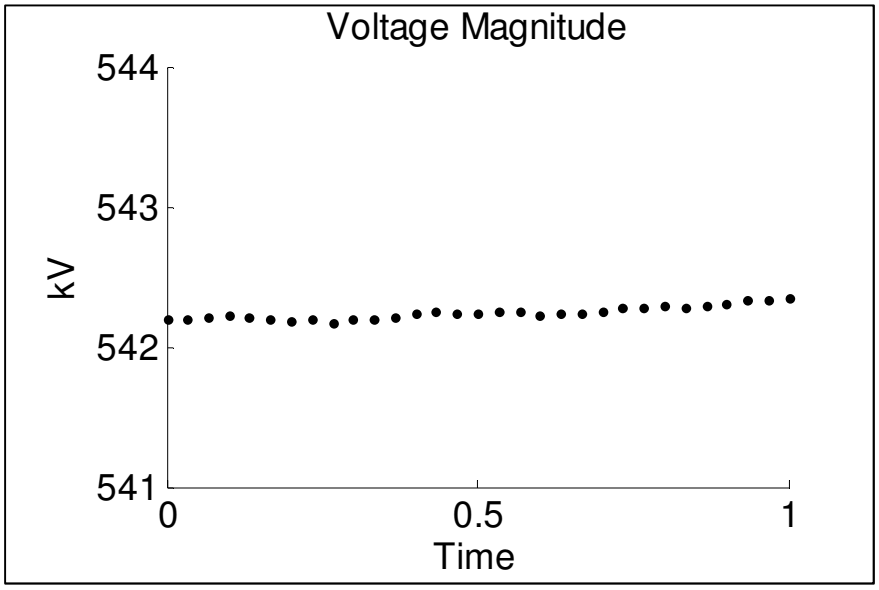

Figure 4-1. Equally Spaced Voltage Measurements

Besides their capacity to describe the evolution in time of a given variable, time series analysis can also be used to forecast the future trend and punctual values of the same variable. Equations, also called Time Series models, can be constructed to estimate or approximate this behavior. After a model has been chosen, different performance

evaluations can be done on the prediction outcome in order to verify the accuracy of such model. The model which gives the best forecasts is the one selected as the predictive mechanism.

Even though there exists a great number of time series models in the literature, the models introduced by Box and Jenkins are the most commonly used. These forecasting methods, which were first presented in 1970 [42], have become the standard for variable predictions in basically every possible research field, from economics to power systems. Their ability to describe the observed variables and the simple means these mechanisms use to forecast future points are the main advantages they have over other time series models. In the following sections a description of the different Box-Jenkins time series models is presented.

4.2.1 Autoregressive Models (AR)

The autoregressive model is the most basic forecasting instrument. This model assumes that the future values, of the time series, are proportional only to the past values of the variable being recorded.

$$\theta_t = \phi_1 \theta_{t-1} + e_t \tag{4.1}$$

In equation (4.1), ϕ_1 is called autoregressive parameter of order one; the term θ_{t-1} represents the immediate past value of the time series and element e_t is the random error associated to the data point at the time period equal to t. This error accounts for the uncertainty of predicting the future and represents the difference of the estimated value, which is calculated, and the true future value of the series which is unknown.

Equation (4.1) actually describes an autoregressive model order one AR(1). In this model the value of the variable at the time period t, in the future, is proportional to the value of the variable in the previous time period $t-1$. It is also possible to relate the future value of the variable to more than one past value. For example equation (4.2)

describes the general autoregressive model of order p AR(p), in this case the future value of the time series is proportional to the p past values plus a random error.

$$\theta_t = \phi_1\theta_{t-1} + \phi_2\theta_{t-2} + \ldots + \phi_3\theta_{t-p} + e_t \tag{4.2}$$

4.2.2 Moving-Average Models (MA)

Moving-average models are very similar to the autoregressive models presented in the previous section. The only difference is that in these models the future values of the series are proportional to the past random errors and not to the past values of the series. A moving-average model of order one, MA(1), can be expressed as follows:

$$\theta_t = \beta_1 e_{t-1} + e_t \tag{4.3}$$

In equation (4.3) the term β_1 is the moving-average parameter of order one, e_{t-1} is the random error associated to the previous data point θ_{t-1} and e_t is the random error of the variable at the time period equal to t.

In the same way as that autoregressive models can be expanded to cover up to p previous data points, the moving-average models can take into consideration more than one previous random error. This leads to the construction of the moving-average model of order q, MA(q).

$$\theta_t = \beta_1 e_{t-1} + \beta_2 e_{t-2} + \ldots + \beta_q e_{t-q} + e_t \tag{4.4}$$

4.2.3 Autoregressive Moving-Average Models (ARMA)

Autoregressive Moving-Average Models come from the combination of autoregressive and moving-average parameters into the same predictive algorithm. Just as the previous models, this combination can take into account up to the last p previous values and up to the q previous random errors, forming an autoregressive moving-average model or order p and q, ARMA(p ,q). The order of the autoregressive and

moving average parameters can be, and usually are, different. Equation (4.5) is the expression of the general ARMA model.

$$\theta_t = \left(\phi_1\theta_{t-1} + \phi_2\theta_{t-2} + \ldots + \phi_p\theta_{t-p}\right) + \left(\beta_1 e_{t-1} + \beta_2 e_{t-2} + \ldots + \beta_q e_{t-q}\right) + e_t \quad (4.5)$$

4.2.4 Differentiation and Stationarity

Autoregressive and moving-average models are used in the forecasting of stationary series. A time series is said to be stationary if the variable, being recorded, fluctuates around a mean value and does not deviate largely from it. However if the series is continuously increasing/decreasing over time or follows an overall trend, among other behaviors, the time series is declared as non-stationary. In order to predict the future points of a non-stationary time series, the use of a differentiation method is needed.

Differentiation is a variable transformation that has to be carried out in a non-stationary series in order to make it stationary. A new variable z could be defined as:

$$z_t = \theta_t - \theta_{t-1} \quad (4.6)$$

Equation (4.6) represents a differentiation process of order one being performed over the time series θ_t, in this case z takes the value of the difference of two immediate successive points. Usually this is enough to achieve stationarity in a non-stationary time series, as depicted in Figure 4-2. Nevertheless, a differentiation order two might be needed in some special occasions. In this case a successive differentiation of order one is performed over z, creating the variable $y_t = z_t - z_{t-1}$.

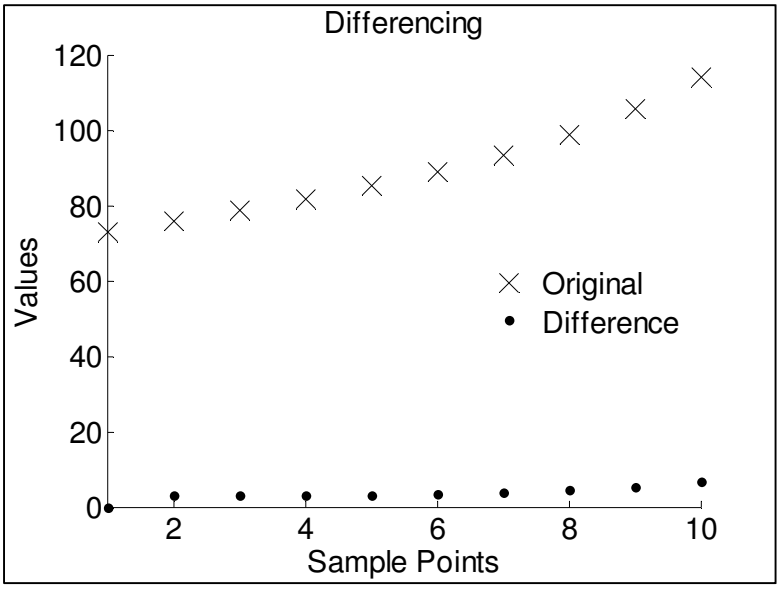

Figure 4-2. Difference Order 1 for a Non-Stationary Series

4.2.5 Integrated Models

Once stationarity in a non-stationary time series has been reached with the help of a differentiation method, an ARMA model can be used in order to forecast future points of the series. The procedure is the same as the ones described in previous sections, equation (4.7) is an ARMA model order p and q for the variable z.

$$z_t = \left(\phi_1 z_{t-1} + \phi_2 z_{t-2} + \ldots + \phi_p z_{t-p}\right) + \left(\beta_1 e_{t-1} + \beta_2 e_{t-2} + \ldots + \beta_q e_{t-q}\right) + e_t \quad (4.7)$$

The points created by equation (4.7) will be future values of the transformed, not original, time series. These futures points, after they have been computed, have to be transformed back to the original series. An integration method, which has the opposite effect than the differentiation process, is then performed over the forecasted values of the variable z. Equation (4.8) shows how the integration, or addition, is executed.

$$\theta_t = z_t + \theta_{t-1} \quad (4.8)$$

The process of applying differentiation and integration methods to a non-stationary time series, for forecasting, creates another set of time series models which are called integrated models. These models are the Autoregressive Integrated ARI(p,d), Integrated Moving-Average IMA(d,q) and Autoregressive Integrated-Moving Average ARIMA(p,d,q), where d stands for the order of the differentiation process used to accomplish the stationarity of the time series.

4.2.6 Model Selection

The selection of the time series model which best describes the behavior of the collection of data points is not a trivial task to complete. Usually the method involves the use of computer programs to obtain the best fitted model, however this procedure does not provide the theoretical understanding needed to comprehend the steps behind the model selection.

Other techniques can be employed to find the type and order of the time series model to be used in the prediction of future values. They consist of the computation of the autocorrelation and partial-autocorrelation factors of the of data points. These statistical indexes provide information regarding patterns in the time series. They are able to portray, in their respective correlograms, the relationship that exists between the most recent points and the previous data of the series. The way in which autocorrelations and partial-autocorrelations are related to Autoregressive and Moving-Average models can be found in [43]. Just as an example, Figure 4-3 shows the autocorrelation factors of a given time series; at position (or lag) one the graph shows a peak that is not present at any other lag. This means that the time series under study can be represented just by a Moving-Average model of order one. A similar conclusion could be established for an Autoregressive model if Figure 4-3 was a partial-autocorrelation plot instead.

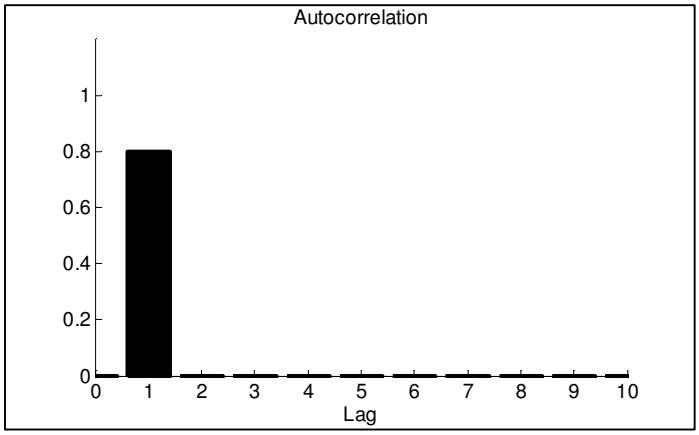

Figure 4-3. Moving-Average Model Identification

The identification of the time series model becomes more complicated when these kind of graphs follow odd patterns difficult to recognize. Computer programs become then the ideal tool to analyze time series for model identification. It is important to mention that over-specification of the time series model is highly undesirable. This means, for example, using a time series model of order four when the data points can be modeled with an order two. Over-specification of the model brings unnecessary burden to all the computations involving the time series analysis, as in parameter estimation and in the calculation of future points.

4.3 Parameter Estimation

Once the appropriate model and its order have been selected, or identified, the next step is to estimate the value of the model parameters; $\phi's$ for autoregressive models and $\beta's$ for moving-average models. The mathematical method that is most frequently used in parameter estimation is the least squares estimator. In this method, which is well known in different branches of science and engineering, the estimated parameters try to minimize the sum of the squared random errors e_t in equation (4.5). In this section the parameter estimation of an autoregressive model will presented. The expression for this model, which was discussed in section 4.2.1, is shown again in equation (4.9).

$$\theta_t = \phi_1 \theta_{t-1} + e_t \tag{4.9}$$

Solving for e_t and knowing that the least squares estimator tries to minimize the sum of the squared errors; the following objective function is obtained:

$$\min J(\phi_1) = \sum_{t=1}^{t=T} (e_t)^2 = \sum_{t=1}^{t=T} (\theta_t - \phi_1 \theta_{t-1})^2 \tag{4.10}$$

Taking the first derivative of $J(\phi_1)$ with respect to ϕ_1 and setting it equal to zero,

$$\frac{d(J(\phi_1))}{d(\phi_1)} = \sum_{t=1}^{t=T} 2(\theta_t - \phi_1 \theta_{t-1})\theta_{t-1} = 0 \tag{4.11}$$

Solving for ϕ_1, the following expression is found.

$$\phi_1 = \sum_{t=1}^{t=T} \theta_t \theta_{t-1} \Big/ \sum_{t=1}^{t=T} {\theta_{t-1}}^2 \tag{4.12}$$

Equation (4.12) defines the estimated value of the parameter ϕ_1 for an autoregressive model order one. In order to estimate the parameters of more complicated time series models, the procedure shown in this section needs to be followed.

After a time series model has been selected and its parameters have been properly estimated, the next step is to validate the model. Model validation essentially involves making sure that the time series model really describes the historical behavior of the variable being monitored. Different methods are employed such as residual analysis; in this dissertation a different approach is used and it will be discussed in Chapter 6. Figure 4-4 summarizes the basic process of building a time series model for forecasting purposes.

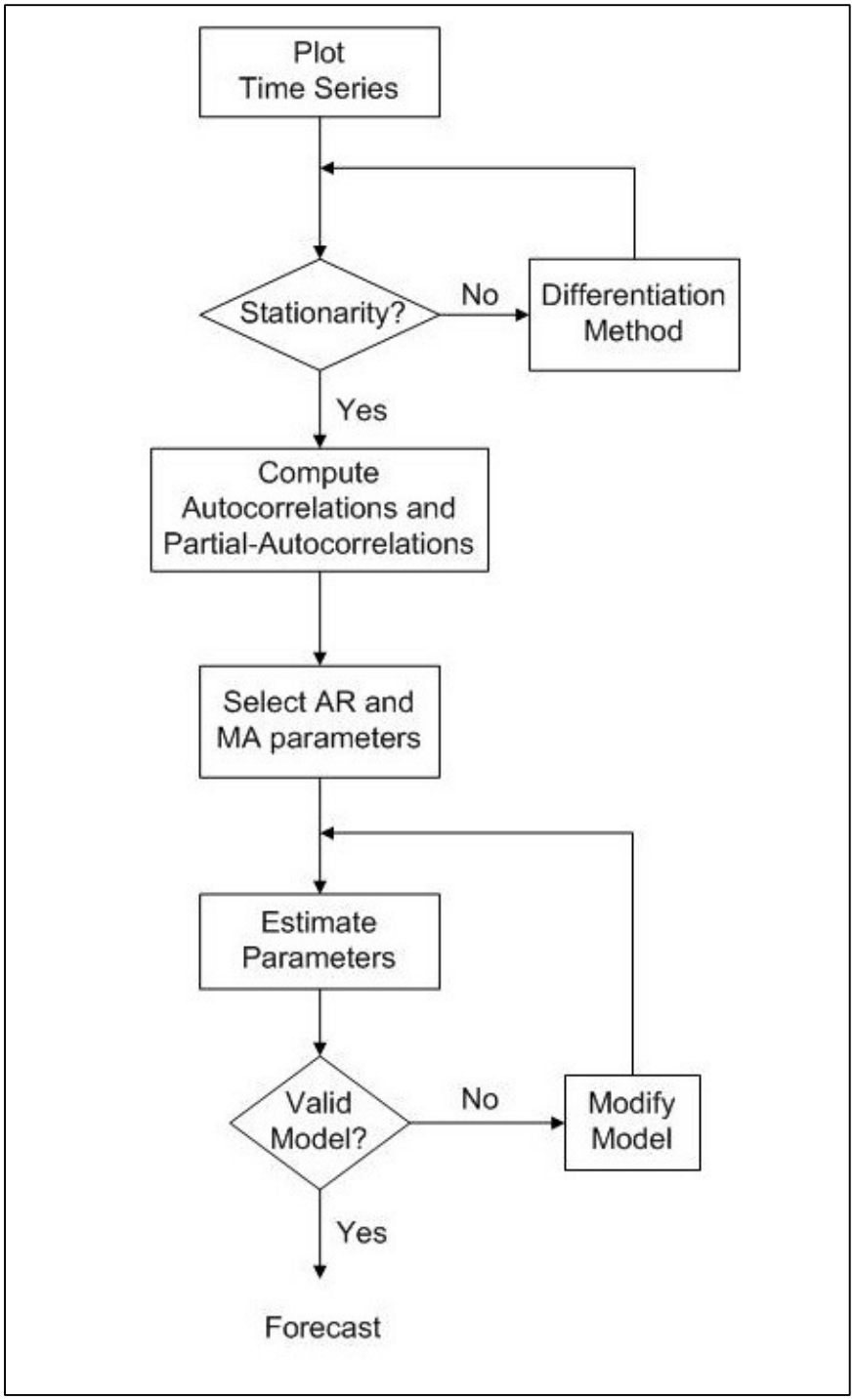

Figure 4-4. Time Series Model Selection

Chapter 5 Proposed Out-of-Step Scheme

In this Chapter the proposed Out-of-Step protection scheme is presented. As mentioned in previous chapters, this new protection philosophy uses Wide Area Measurements to detect transiently unstable power system oscillations. A generic power system model is used in order to show the methodology needed to implement this scheme in a real network. In Chapter 6, the performance of this protection scheme will be tested in several network models; mainly in three different power system models of the state of California. The main ideas behind this protection philosophy are discussed in the following sections.

5.1 Coherent Groups

A power system is composed of different generating units connected through transmission lines. The notion or idea of coherent groups in the power system refers to machines that oscillate together against the rest of the system. In other words, the time response of the rotor angles, of a coherent group of machines, is quite similar for a given system event [44]. This concept is highly related to power system dynamics; in a steady-state condition with no frequency deviation the presence of coherent groups of machines cannot be detected due to the lack of oscillations in the system. It is worth mentioning that machines in a coherent group, in most of the cases, are electrically and geographically close to each other.

One of the main reasons coherency identification plays an important role in the analysis of power systems, is the network reduction that can be accomplished on a large multi-machine system knowing the generators that tend to oscillate together in a coherent group. In this process all the machines in a particular coherent group are aggregated into one equivalent generator, whose rotor dynamics describes the behavior of all the machines in that specific machine set. After this machine reduction is performed, a subsequent reduction in the number of transmission lines can also be carried out. The

resultant equivalent power system has, generally speaking, the same steady-state and dynamic performance as the original large system. Once the equivalent network is obtained, different power flow and dynamic tests can be performed on it in order to verify the accuracy of the reduced model. A decrease in the computation time and the simplification of the analysis of the different power system studies are some of the numerous advantages of using reduced models.

The identification of coherent groups in a given power system can be accomplished mainly through the use of two different techniques. The first one uses a linearized power system represented in a linear state space equation; the coherent groups can be obtained analyzing the coupling among all the machines in the state matrix A [45]. The second approach, which is a more practical method, consists in running multiple dynamic simulations. In this method, different perturbations are applied to the system and the rotor angles of all the machines are plotted against time. Coherent groups of machines are then identified analyzing the time response of the machine rotors, generators that have a similar dynamic behavior are considered to be coherent.

Online coherency identification can also be performed using Wide Area Measurements. Reference [46] proposes a method in which coherent groups can be detected using the rate of change of PMU voltage phase angles gathered in different locations of the power system. Different methods, such as moving and sliding windows, can be utilized in order to obtain a better result in the coherency detection. The rate of change, of the voltage angle, is computed through a linear least-squares fitting of the angle data. This linear approximation takes the form of $\theta = a + bx$, where b is the rate of change of the voltage angle. All b_i are then compared in order to find the coherent groups present in the power system.

The practical approach for coherency identification, mentioned in the previous paragraph, is the technique selected for the implementation of this protection scheme. As previously described, in this method multiple dynamic simulations have to be run in order to detect the coherent groups present in the power system. For the purpose of the

proposed Out-of-Step methodology especial attention has to be paid to the sets of machines that are most likely to lose synchronism under a system disturbance.

A small size power system will be used in order to show how this coherency identification procedure is applied. The network selected for this purpose is the 10 machine 39 bus equivalent system of the New England power grid; which was taken from reference [47]. A detailed description of this model, containing line impedances and generator parameters, is available in Appendix A. The rotor dynamics of the ten generators are represented by classical machine models. Figure 5-1 shows a simplified version of the one-line diagram of the system presented in [31].

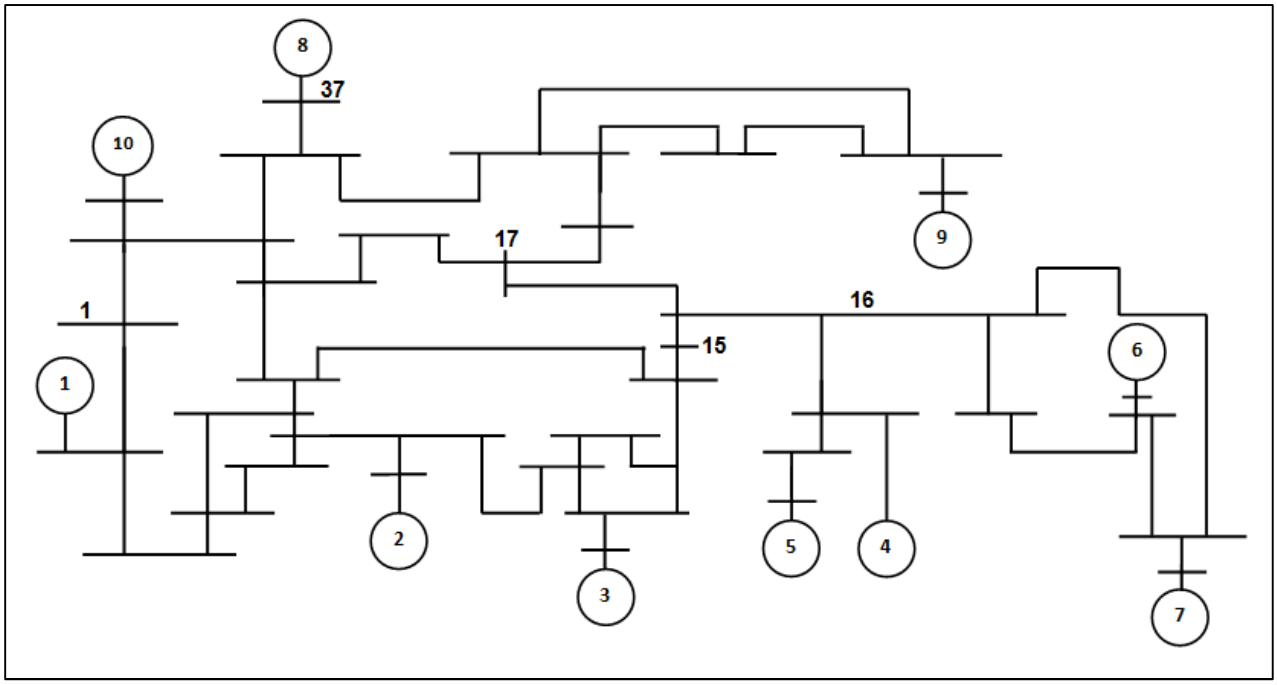

Figure 5-1. New England 10 Machine System

The procedure establishes that a disturbance has to be applied to the power system and the rotor angle response of the machines has to be plotted against time. A perturbation was applied to the system following this guideline, the disturbance consisted in a 10 cycles fault in the transmission line between bus 15 and bus 16; the

fault was cleared by the appropriate tripping of that line. A ten cycles fault is actually a very long fault, in real power systems faults are usually cleared 5 cycles after their inception. But for the intention of explaining the principle of this method a fault span of ten cycles is used. Figure 5-2 shows the outcome of a PSLF dynamic simulation of the aforementioned system event.

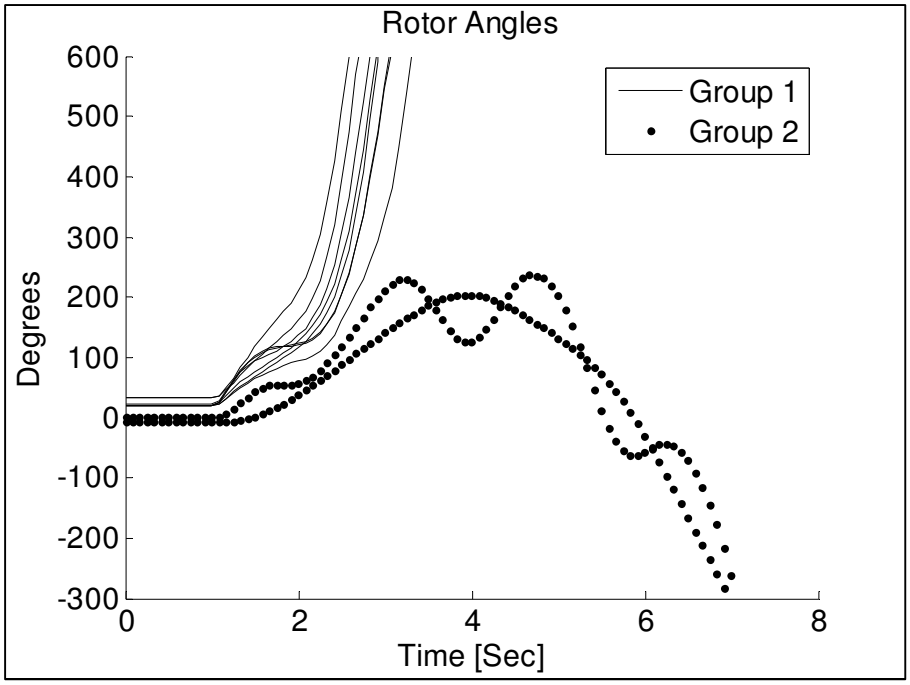

Figure 5-2. 10 Cycles Fault Disturbance

In this picture two coherent groups of machines can be identified, even though the rotor angles of Group 2 are not perfectly similar, these two machines do not separate drastically from each other, feature that makes them a coherent set of generators. Group 2 is composed of machine number one and ten, Group 1 consist of the remaining eight generators in the system.

This is the time response for only one network disturbance, a larger number of simulations with perturbations of different natures have be run in the power system under study, and the same coherency identification technique has to be performed on

each one of the simulation results. Figure 5-3 depicts the outcome of a different system disturbance; in this case a 10 cycles breaker failure fault was applied at bus number seventeen. It can be seen that Group 2 stays unaltered with the same two machines, one and ten. On the other hand Group 1 suffers a modification; machine number eight deviates from this group and it is no longer considered part of this machine set. This machine does not follow the rotor behavior of any of the other two groups; generator eight is then a different coherent group by itself.

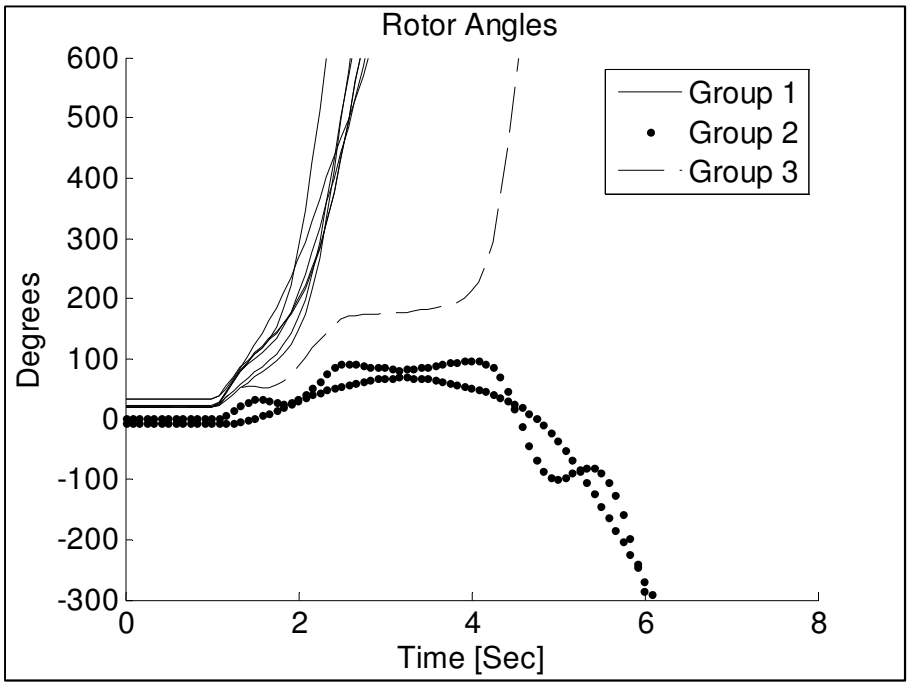

Figure 5-3. Breaker Failure Case

Assuming that several dynamic simulations were run and similar time results were obtained, it can be concluded that 3 coherent groups of machines exist in the equivalent New England system. The machine distribution of these groups is detailed in Table 5-1.

Table 5-1. Coherent Groups

	Machine Number						
Group 1	2	3	4	5	6	7	9
Group 2	1	10					
Group 3	8						

The procedure explained in this section can be applied to any power system for coherency identification and it is used in this dissertation to find the coherent groups of machines in the power system of the state of California.

5.2 Rotor Angles and PMU Voltage Angles

One of the main functional principles of this suggested Out-of-Step protection scheme is its ability to infer rotor angles from measured PMU voltage phase angles in the power system. Even though machine rotor angles provide the best information regarding system stability, there is not a system that can supply a synchronized wide area snapshot of this variable. It is shown, in this section, that PMU voltage angles at selected locations can be used to infer the behavior of the generator rotor angles. The method of placing PMUs in the power system, so some of its variables can be observed, is called PMU placement. This process has become an important research topic in the power system industry, since having a PMU on every bus of the system is not feasible due to some economical and technological challenges that exist in the field deployment of these units. Depending on the desired application, different approaches can be used in order to find the optimal location of the measurement units. As an example, reference [48] shows how PMUs can be efficiently placed to be used in a power system state estimator.

The PMU placement strategy for this real-time application consists in the selection of one bus in the power system, for each coherent group, located close enough to the set of coherent machines, so voltage swings can be observed. In order to demonstrate that PMU voltage angles can be used to infer machine rotor angles, the time response of

some voltage angles for the breaker failure fault case, discussed in the previous section, is analyzed.

Figure 5-4 illustrates how the voltage angles of three different buses in the New England system can depict the behavior of the rotor angles for the breaker failure event, shown in Figure 5-3. These buses are relatively close to the group of machines that need to be observed, and they can be used to monitor the swings in the power system for the proposed Out-of-Step scheme. Table 5-2 lists the selected buses for this application and their respective group of machines.

Table 5-2. Selected Network Buses

Group	Angle @
1	Bus 16
2	Bus 1
3	Bus 37

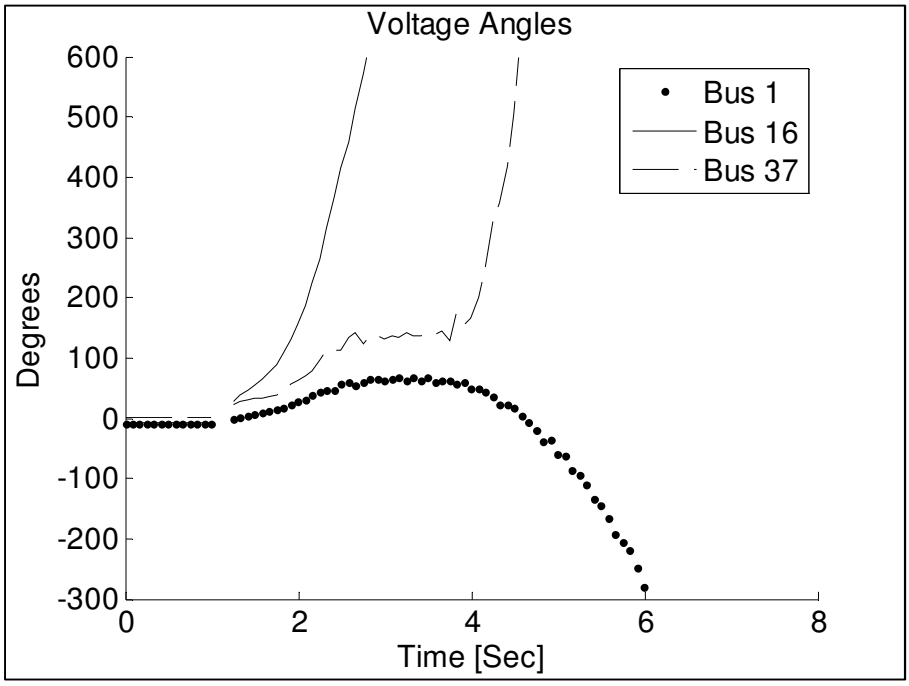

Figure 5-4. Voltages Angles at Selected Locations

5.3 Coherent Groups and PMU Placement

Figure 5-5 summarizes the coherency identification and PMU placement for the New England power system. This figure shows the coherent groups of machines in the system and the buses where PMUs have been located.

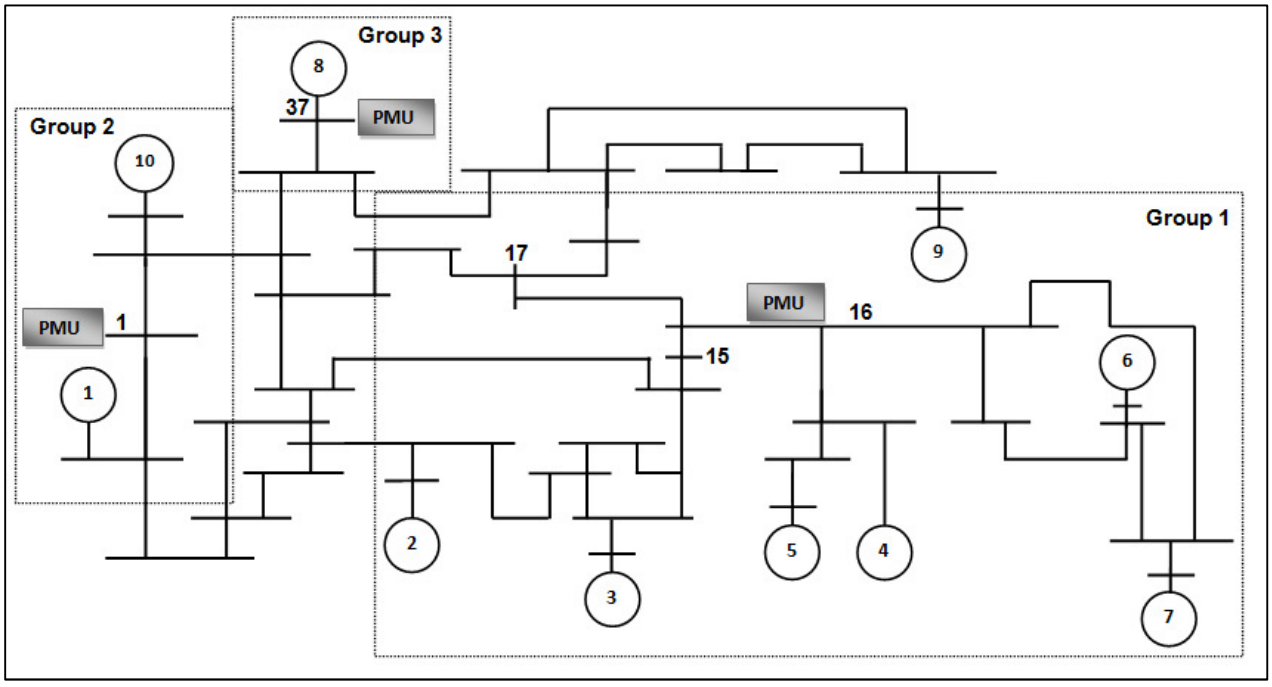

Figure 5-5. Coherent Groups and PMU Placement

5.4 Voltage Angle Unwrapping

In the proposed Out-of-Step protection scheme, voltage angle measurements are used to track power system oscillations in the California system. These measurements are taken at the selected network locations close to the coherent groups of machines, as mentioned in the previous sections. One of the challenges of using voltage angle measurements, obtained from phasor measurement units, is that the phase angle data

is constrained to take values between -180 and 180 degrees. For example, a voltage angle change of -2 degrees from an angle of value of -179 degrees will appear as 179 degrees in the next sample, instead of the expected -181 degrees. This issue makes difficult the detection of constantly increasing, or decreasing, voltage angles. Figure 5-6 shows a set of constantly decreasing voltage angles and the discontinuities that occur when they reach the -180 degrees limit.

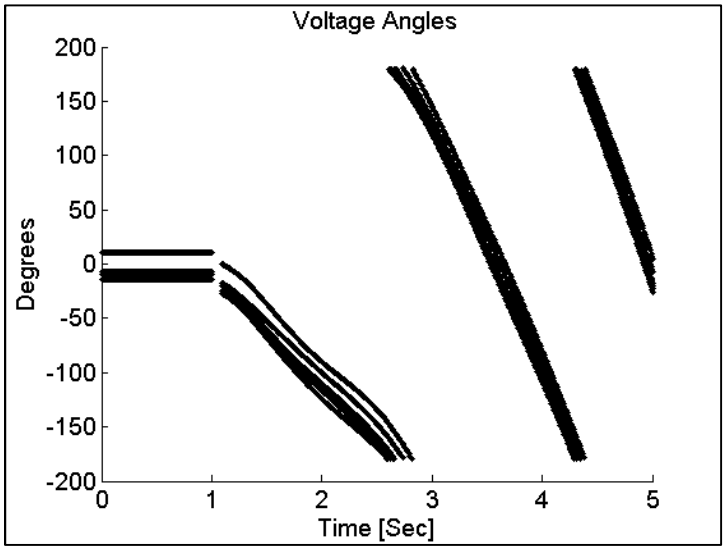

Figure 5-6. PMU Voltage Phase Angles

In order to obtain the correct behavior of the measured voltage angles, a process called voltage angle unwrapping can be employed. In this process the jumps, or discontinuities, in the series of data are eliminated and the real value of the angles is acquired. The voltage angle computed by the phasor measurement unit is replaced by an unwrapped angle; the following equations demonstrate how this process is carried out.

$$Unwrapped\ Angle = Angle + C * 360 \tag{5.1}$$

C in equation (5.1) is called the unwrapping constant and its initial value is equal to zero. This constant changes its value every time a jump occurs between two consecutive voltage angles.

$$If\ \ Angle_n - Angle_{n-1} > 180$$

$$C = C - 1$$

$$If\ \ Angle_n - Angle_{n-1} < -180$$

$$C = C + 1$$

If the change in voltage angle in one time step is greater than 180 degrees, the constant decreases one unit and the algorithm declares that the value of the voltage angle is decreasing; whereas, if the change in voltage angle is smaller than 180 degrees the constant increases one unit and the algorithm declares that the value of the voltage angle is increasing. Figure 5-7 shows how the voltage angles, from Figure 5-6, are converted to their real value using equation (5.1).

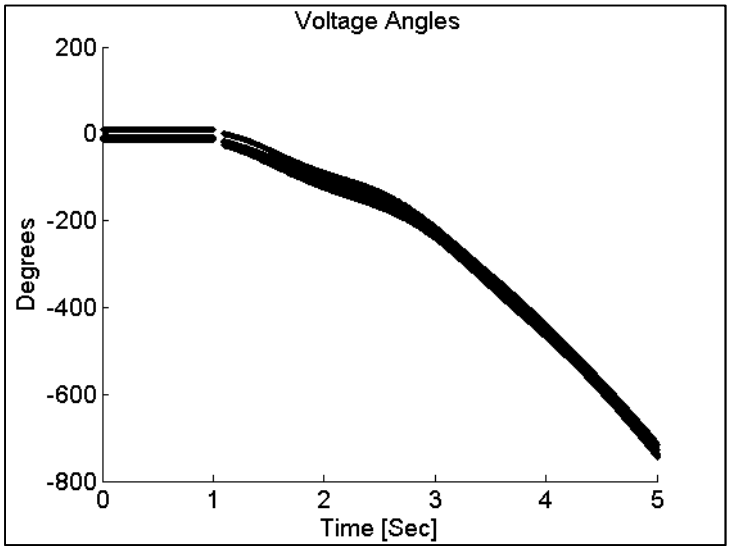

Figure 5-7. Unwrapped Voltage Phase Angle

The unwrapped voltage angles, obtained using this algorithm, can be used for the proposed protection scheme since they depict the real conditions present in the system. In fact the voltages angles shown in Figure 5-4 are unwrapped angles. Unwrapping of angles is a process that is used in many PMU applications; reference [49] explains how unwrapped PMU voltage angles are used to estimate frequency in the power system.

5.5 Scheme Considerations

The suggested protection scheme will predict the evolution of voltage phase angles, measured by PMUs at different buses in the network, in order to assess the stability of the power system. The prediction mechanism used to forecast the future behavior of the voltage angles is time series analysis; in Chapter 6 the time series model selection for this task is presented. In this section, some of the assumptions and decisions made for the proposed Out-of-Step protection scheme are discussed.

In order to apply time series analysis theory along with PMU technology to the Out-of-Step protection scheme, the following considerations should be taken into account:

1. No relay action would take place in the first 20 cycles after the fault has been cleared. In this period of time the parameters, of the selected time series model, are estimated.
2. A rate of 30 messages per second for each PMU is assumed. A higher message rate could improve the performance of this protection scheme. Most of the PMUs in the market have the capability to provide 60 samples per second, and the current trend is to increase this reporting rate even more. However, a rate of 30 samples per second provides a conservative approach to this scheme and it is the highest rate listed in the current synchrophasor standard [50].
3. The relay's algorithm forecasts 10 points (1/3 seconds) in the future using the appropriate time series model; and it is done for each of the voltage angles being monitored.

4. If the tripping decision is met in two consecutive predictions, an unstable swing would be declared and protection action should be initiated. Two consecutive predictions are used, instead of one, in order to verify the accuracy of the estimated values and the forecast outcome.

5. The size of the initial window used to calculate the first model parameters will be 10 points, or 20 cycles assuming a reporting rate of 30 samples per second. After the first prediction is made, the scheme waits for the next set of measurements to arrive and it deletes the first point of the previous sequence of data in every other prediction in order to forecast the following points.

6. Voltage angles referenced to initial values are used; this process removes the steady state difference between all voltage angles, and the real angle deviation between them, due to a disturbance, can be computed.

7. No attempt is made to change power system parameters, such as settings of power system stabilizers, excitation systems, protection elements, load shedding devices, etc.

8. Isolated machines that pull Out-of-Step individually will not be considered for this protection scheme. Their own local protection element is assumed to take the appropriate control action to separate the machine from the rest of the system.

9. After the two groups of machines that are operating asynchronously are separated, by means of tripping the correct transmission lines, the stability constrain of matching generation and load in each portion of the system is assumed to be fulfilled by a different control system.

As it can be inferred from the last 9 points, the main function of this Out-of-Step protection scheme is the detection/prediction of unstable power swings in the system. No other stability control or protection action will be attempted by this relay.

5.6 Tripping Decision

Tripping decision is the condition detected by the protective relay that initiates an action to protect the power system from an undesired situation; most likely this action results in the tripping of a network element in the system. The tripping decision of this Out-of-Step relay will be centered in the computation of a center of angles; this concept, first introduced in the earlier seventies [51] is an inertia weighted average of the all the machine rotor angles in the system.

In the proposed scheme the center of angles is used in a different way. Voltage phase angles are used instead of rotor angles and only voltages angles measured by the PMUs are considered. Another change in the definition of the center of angles is that machine MVA ratings are used instead of inertia constants, meaning that the center of angles computed in this application is a MVA weighted average.

Each measured voltage angle represents the rotor behavior of a coherent group in the system, as mentioned in section 5.2. As a consequence, each voltage angle is assigned a MVA rating; the value of this variable is the summation of all the machine MVA ratings in the coherent group. The inertia constants J or I could also be used, but for simplicity the machine rating was selected. Equation (5.2) shows the calculation of the modified center of angles for this scheme.

$$COA = \frac{\sum_{i=1}^{n} MVA_i * \theta_i}{MVA_{total}} \tag{5.2}$$

where

$MVA_i = \sum_{j=1}^{m} MVA_j$	MVA rating of the coherent group i
θ_i	PMU Voltage Angle of the coherent group i
MVA_{total}	MVA rating of the whole system
n	Number of coherent groups present in the system
m	Number of machines in the coherent group i

It was mentioned, in section 5.5, that 10 points in the future will be forecasted using the appropriate time series model. The tripping decision for this relay makes use of the tenth forecasted point in order to calculate a future center of angles, as indicated by equation (5.3).

$$COA_{t+10} = \frac{\sum_{i=1}^{n} MVA_i * \theta_{i,t+10}}{MVA_{total}} \tag{5.3}$$

The center of angles in equation (5.3) is calculated every time a new phasor measurement package is received at the respective control center. Each voltage angle $\theta_{i,t+10}$, is then compared against this center of angles. If there exists a difference of 150 degrees between a given voltage angle and the center of angles in two consecutive predictions the algorithm declares an unstable swing and the respective group should be disconnected from the system. The disconnected group is then disregarded in the following center of angles calculation. Figure 5-8 illustrates the tripping decision algorithm for this Out-of-Step protection scheme.

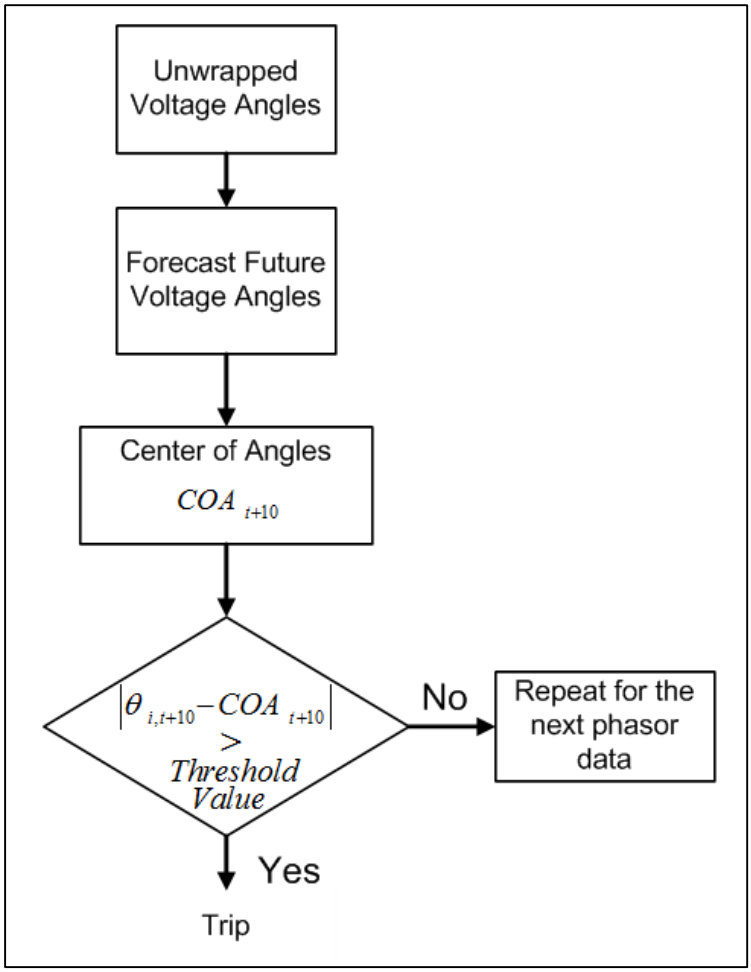

Figure 5-8. Tripping Decision

5.7 PMU Message Rate

As mentioned in section 5.5, there are several output message rate options that can selected in the current commercial Phasor Measurement Units. IEEE standard C37.118 [50] defines how the synchrophasor transmission has to be carried out between the different levels in the PMU architecture. This document is an important tool used by PMU vendors to design their products and it also helps to guarantee a proper interoperability between different PMU devices. This standard establishes that the PMUs should report their measurements at submultiples of the power system

frequency; higher reporting rates are also encouraged by the standard making 60 PMU messages per second also available in most of the devices. The upgrade to higher PMU reporting rates can be expected in the near future; reference [52] mentions the possibility to include 120 messages per seconds in the next synchrophasor standard. Table 5-3 lists the reporting rates a PMU has to have available in order to comply with the current standard.

Table 5-3. C37.118 PMU Reporting Rates

PMU Message Rates	
@ 50 Hz	@ 60 Hz
10	10
25	12
	15
	20
	30

The synchrophasor reporting rate plays an important role in the proposed protection scheme, since two of its main algorithms are highly dependent on this PMU feature, voltage angle unwrapping and time series voltage angle forecasting. These functions perform better at higher message rates; for example more precise predictions can be achieved if more points are available for a given period of time in the time series analysis portion. High sampling rates are not always feasible in practice due to limitations in communication bandwidth and in storage requirements which make the use of high sampling rates an issue for some applications. As previously discussed, a message rate of 30 samples per second is assumed for this PMU application.

As stated in section 5.4, in order to perform the voltage angle unwrapping a change in the voltage phase angle of ± 180 degrees has to be detected by the Out-of-Step relay. In cases where the rate of change of the voltage angle is high and the PMU message rate is low, the algorithm may fail to detect such discontinuities or jumps in the voltage angle data. It will be impossible for the relay to accurately establish if a voltage angle is

increasing or decreasing in magnitude. To show how the voltage angle unwrapping is affected by the PMU reporting rate an example is presented. Figure 5-9 shows the oscillation of a particular voltage angle after a system disturbance. The PMU reporting rate is assumed to be 240 messages per second and the unwrapping mechanism is not being implemented.

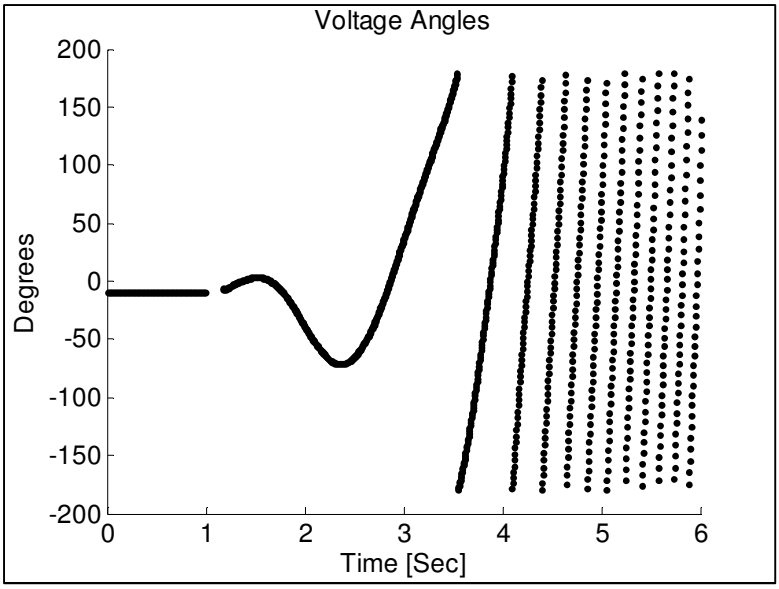

Figure 5-9. Ideal Case: 240 Samples per Second

Assuming real PMU message rates of 12 and 30 samples per second, the voltage angle data shown in the previous figure is downsampled and the voltage angle unwrapping algorithm is implemented to try to obtain the real behavior of the voltage angle. Figure 5-10 shows how the unwrapping mechanism at a reporting rate of 12 samples per seconds fails to describe the correct trend of the voltage angle data. On the other hand at a higher reporting rate, 30 samples per seconds, the unwrapping algorithm succeeds in describing the real voltage angle data behavior. This PMU issue might be considered as an aliasing problem.

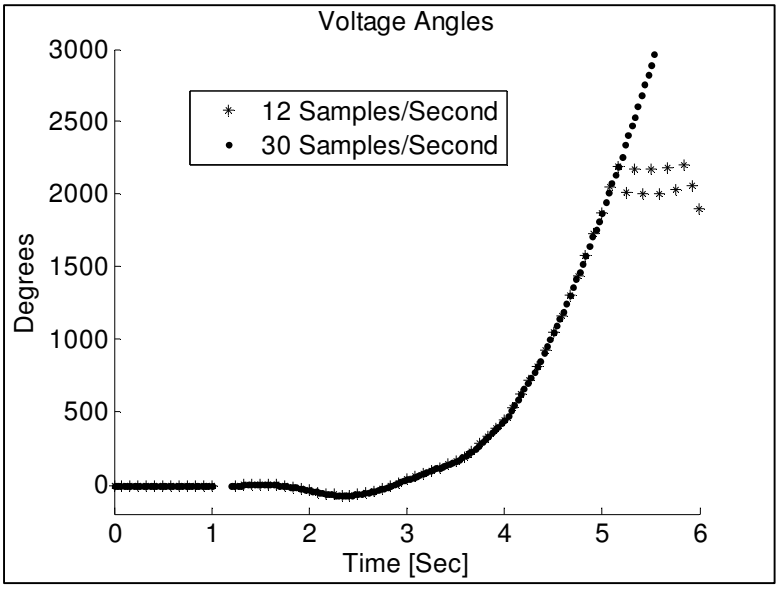

Figure 5-10. Angle Unwrapping Performance

The preferred solution to this problem is to set the PMU reporting rate as high as possible, taking into consideration the aforementioned limitations in the deployment of these devices.

5.8 PMU Architecture

Figure 5-11 illustrates a conceptual diagram of the suggested Out-of-Step protection scheme. Phasor Measurement Units are placed at strategic locations in the power system; there are as many units as coherent groups of machines in the network. Voltage angle measurements, along with other time-stamped data, are sent to a Phasor Data Concentrator (PDC) assumed to be placed at the system operator's control center. This device collects and time-aligns the information from the different PMU's and sends a single PMU packet to a computer. This computer runs the time series predictive mechanism to forecast 10 points in the future for each of the voltage angles. With this prediction, a center of angles is computed and the tripping decision is evaluated to assess the nature of each voltage swing. If instability is determined, a signal is sent to the Out-of-Step relay so it can initiate tripping of selected transmission lines. On the

other hand, if the voltage angle is found to be stable a blocking signal is sent to avoid the unnecessary tripping of these power lines.

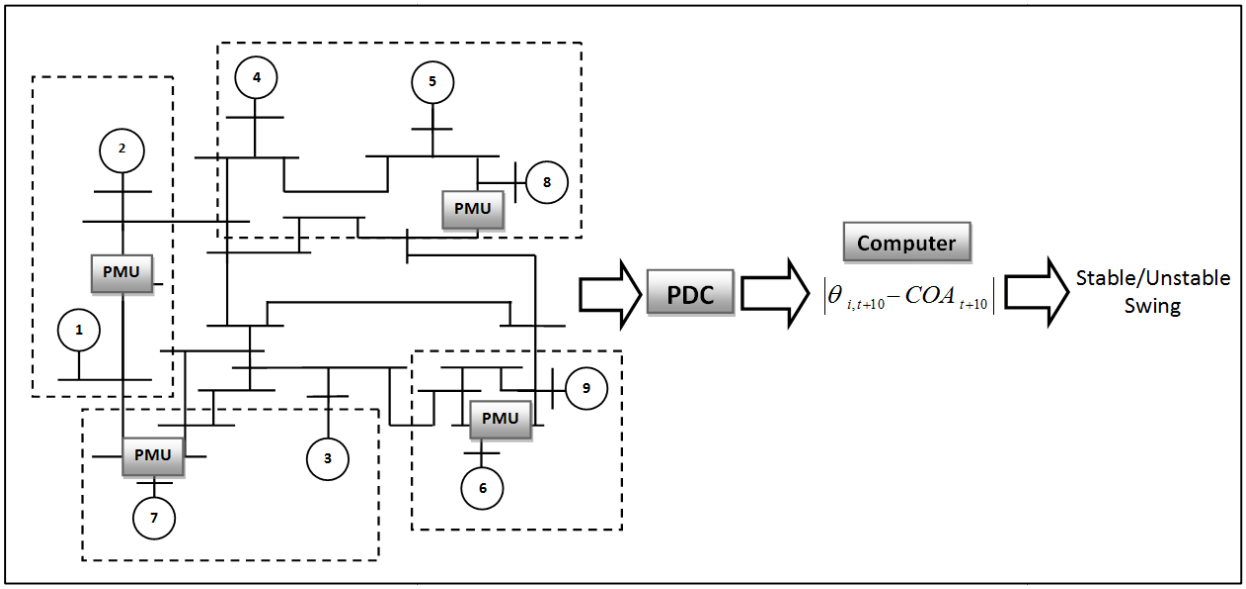

Figure 5-11. Out-of-Step Protection Scheme

Chapter 6 Simulation Results

In this research project several transient stability studies were carried out with the intent to indentify network disturbances that create large power swings, and that might eventually lead to loss of synchronism between groups of machines in the networks. The events which triggered Out-of-Step cases were then analyzed in order to identify the coherent groups of machines in the system models. These unstable cases and some other critically stable cases were used to test the proposed Out-of-Step protection philosophy discussed in the previous Chapter. The Extended Equal Area Criterion presented in Chapter 3 is mentioned in some cases and a comparison showing the advantages and disadvantages of the two methods are provided in the following Chapter of this document.

Breaking the network into different synchronous groups with realistic power system disturbances is a very difficult task to achieve. Most of the power systems in the world are designed and tested to survive the occurrence of one large system disturbance. Most of the Out-of-Step events that occur in power grids are the result of a combination of different system perturbations that are difficult to predict. In order to obtain sufficient Out-of-Step cases, for this research effort, extreme system events such as breaker failure faults were applied to the power systems under test.

The different power system models analyzed in this Chapter are: a One Machine Infinite Bus system, the IEEE 17 Generator System and three power system models of the state of California. A one-line diagram and a brief description of each model are given in the following sections. The performance of the protection scheme in the prediction of instability, in the 3 California models, is also presented at the end of this Chapter.

6.1 One Machine Infinite Bus System

The OMIB power system model was taken from [2] and it is a very simple model used to describe the principles and ideas behind the proposed Out-of-Step protection scheme.

The identification of coherent groups in this system is a trivial step since there is only one machine in the network with rotor dynamics. The dynamic model selected for this generator is a classical machine model, whose parameters are listed in Table 6-1. A one-line diagram of the system is presented in Figure 6-1.

Table 6-1. Classical Machine Model

H	X'd
3.5	0.3

Base: 2220 MVA

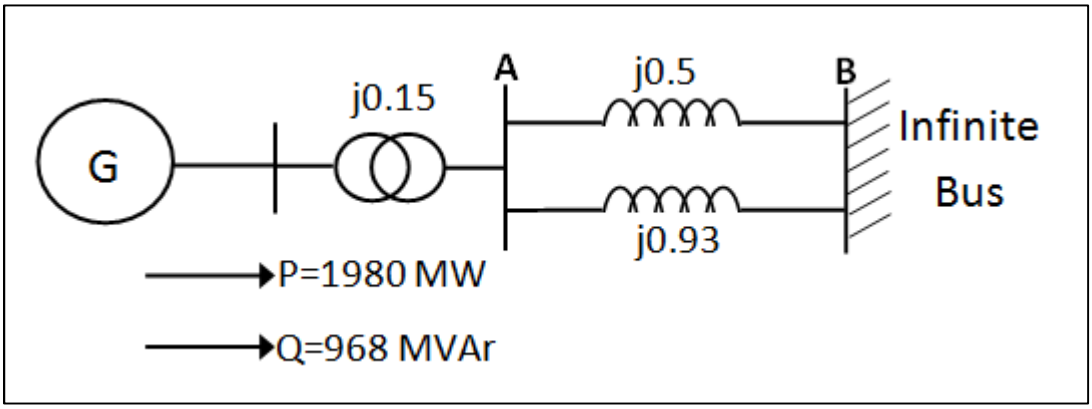

Figure 6-1. OMIB System

A transient stability study was carried out in this power system in order to analyze its dynamic behavior. The disturbances selected for this study were three phase faults, of different durations, applied to the transmission line with an impedance of 0.93 Ohms. The disturbances were initiated at the first second of each simulation. The faults were cleared by the appropriate tripping of the faulted line. In the first case the fault was cleared 3 cycles after its inception and in the second case the fault was applied for 5 cycles. The outcome of the former is a stable case whereas the latter yields to an unstable case. Figure 6-2 shows the rotor angle response for each one of the simulated disturbances.

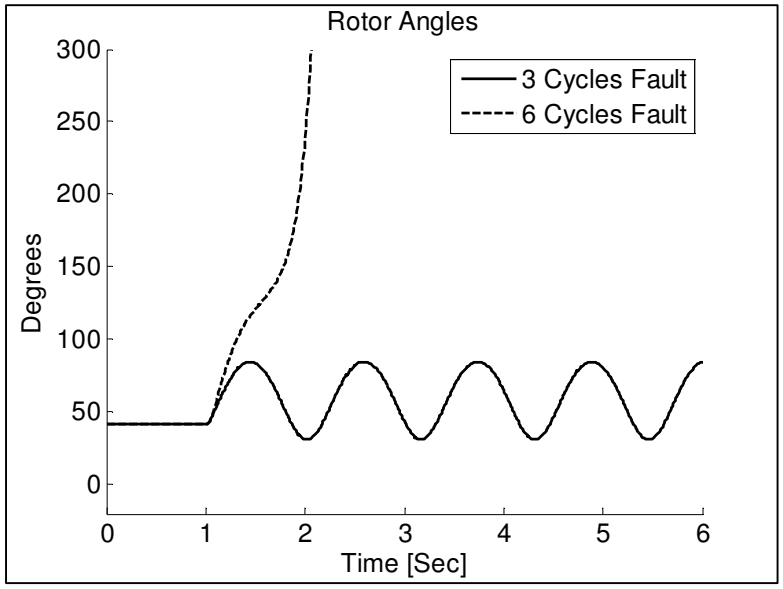

Figure 6-2. Rotor Angle Response for 3 and 6 Cycles Fault

The selected buses to be monitored for this small power system are bus B, which acts as a PMU reference, and the bus located at the machine terminals, which describes the behavior of the machine rotor angle. Voltages angles are assumed to be measured by PMUs at these two buses with a reporting rate of 30 messages per second. The voltage angle unwrapping mechanism is activated to eliminate any discontinuity in the voltage angle data. Voltage angles referenced to initial values are computed and used in the prediction mechanism.

The tripping decision for this single-machine power system does not need the calculation of a center of angles, since this concept only exists for a multi-machine power system. The direct comparison of the predicted voltages angles is used for the tripping decision. If the tenth forecasted voltage angle exceeds a threshold value, which in this case is 150 degrees, the Out-of-Step relay declares the evolving voltage swing as unstable

With the definition of the tripping decision and with the acquirement of one stable and one unstable case for this system, the next step is to test the suggested protection scheme under these two scenarios. The time series models used for the prediction

algorithm are Autoregressive models of different orders. A differentiation process of order one is also applied to the collection of data points in some of the cases.

Figure 6-3 and Figure 6-4 show the first prediction of the protection scheme using an AR(1) model. The time series that shows an oscillatory behavior corresponds to the voltage angle data of the bus at the machine terminals; and the one that stays at zero degrees is the infinite bus voltage angle, which in this case is the system reference. The asterisk points symbolize the 20 cycles window of data used to estimate the time series model parameters. The squared points are the ten forecasted values for each of the voltage angles.

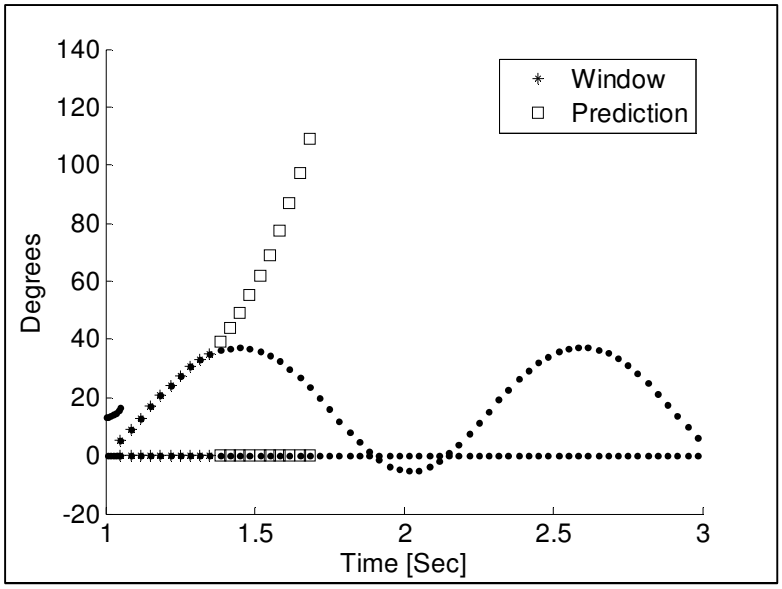

Figure 6-3. AR(1) Stable Case

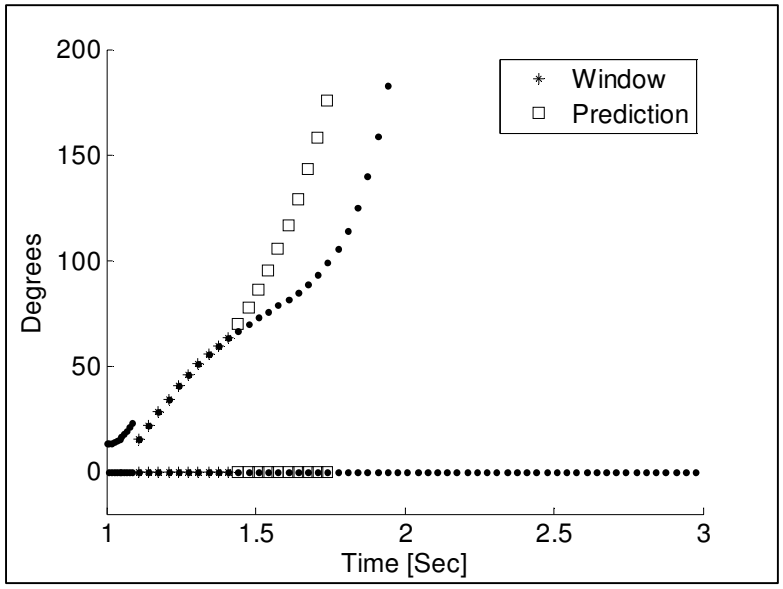

Figure 6-4. AR(1) Unstable Case

Figure 6-5 and Figure 6-6 illustrate the outcome of the first prediction using an Autoregressive model of order one with a differentiation process of order one ARI(1,1).

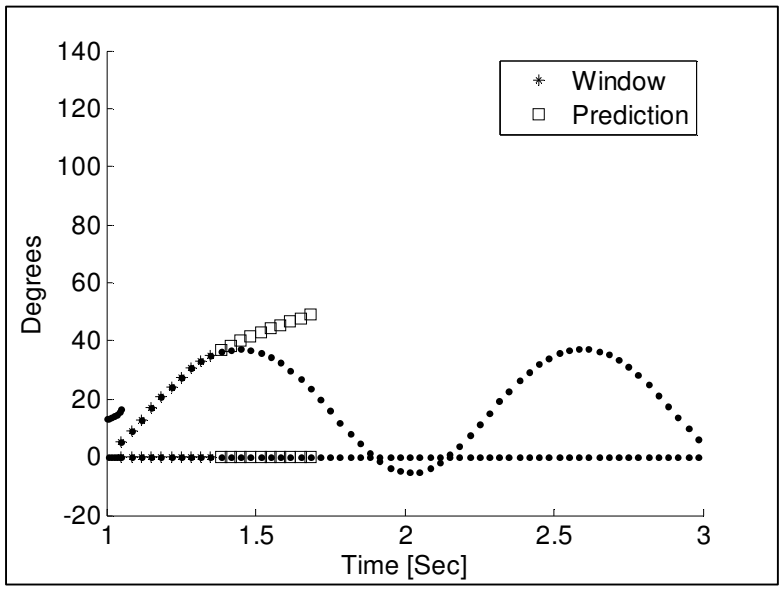

Figure 6-5. ARI(1,1) Stable Case

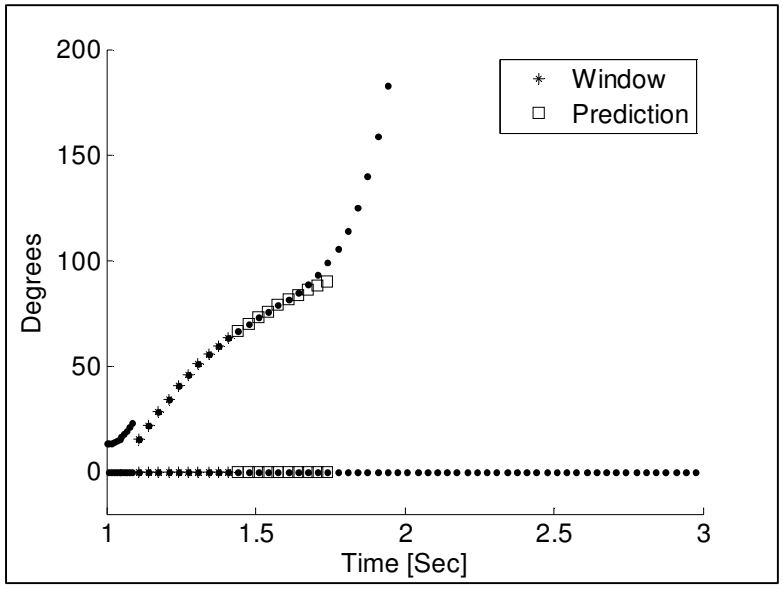

Figure 6-6. ARI(1,1) Unstable Case

Figure 6-7 and Figure 6-8 illustrate the outcome of the first prediction using an Autoregressive model of order two with a differentiation process of order one ARI(2,1).

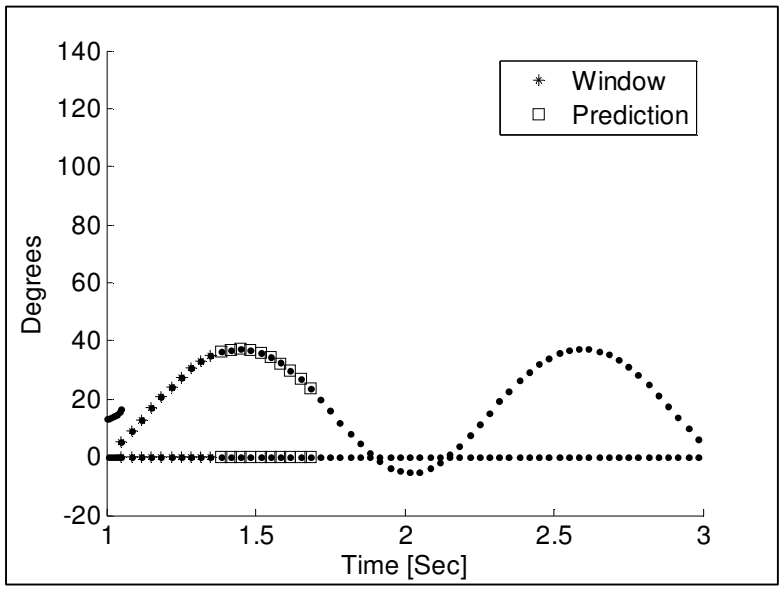

Figure 6-7. ARI(2,1) Stable Case

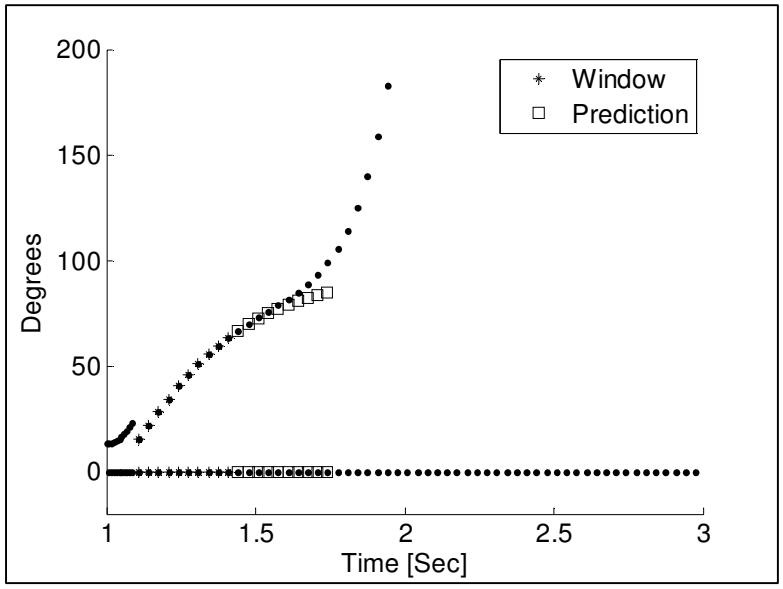

Figure 6-8. ARI(2,1) Unstable Case

Figure 6-9 and Figure 6-10 illustrate the outcome of the first prediction using an Autoregressive model of order three with a differentiation process of order one ARI(3,1).

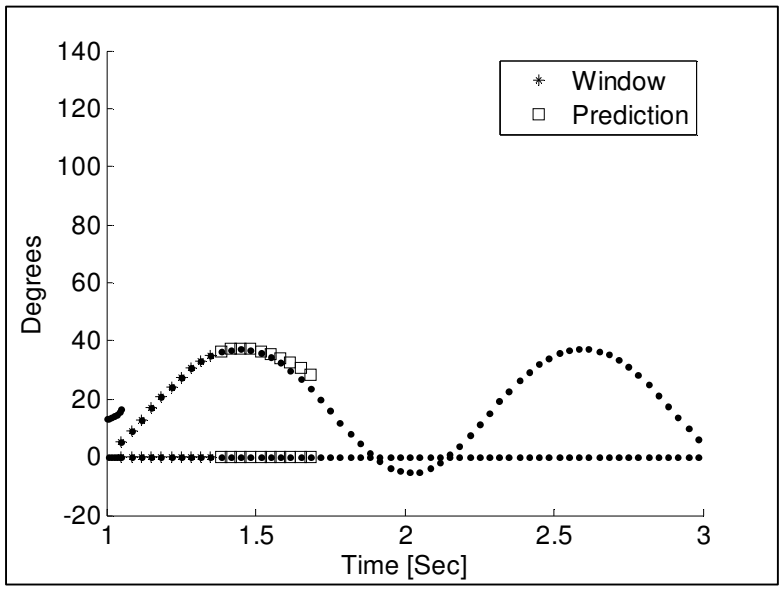

Figure 6-9. ARI(3,1) Stable Case

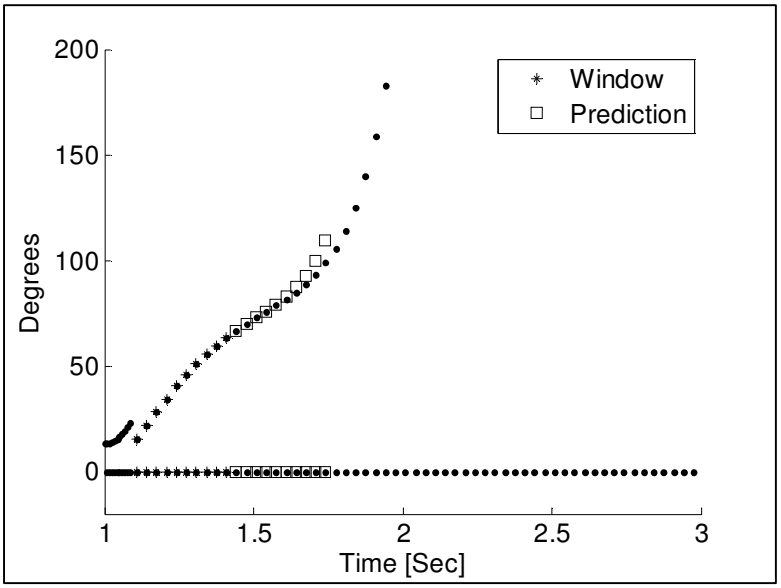

Figure 6-10. ARI(3,1) Unstable Case

As it can be seen in the previous figures the simplest time series model AR(1) does not provide a good first prediction for the voltage angle data. The inclusion of a differentiation process of order one seems to improve the forecasting outcome considerably, making the prediction of the Autoregressive Integrated model ARI(1,1) more accurate than the previous one. The Autoregressive model of order 2 with a differentiation process of order one ARI(2,1) appears to have the best performance in describing the future behavior of the angle data.

Assuming the first prediction is the only one needed for this protection scheme, the time series model selection part could be completed using an ARI(2,1) model. A more sophisticated model, an ARI(3,1), was tested and its results are also shown in the previous set of figures. It can be seen that the prediction outcome is not substantially improved by this model; making the ARI(2,1) model the best predictive mechanism for this power system. The use of an over-specified time series model, such as an ARI(3,1) model for this power system, should be avoided since its parameter estimation is more complex and it does not provide a real improvement to the forecasting results.

In the proposed protection scheme more than one voltage angle prediction has to be computed. A more comprehensive analysis of the different time series models has to be carried out involving the first and subsequent voltage angle predictions. The simplest model that best describes the voltage angles is the one that has to be selected.

Even though a good performance in the prediction of voltage angles is an essential requirement for the proposed Out-of-Step relay, the most important task this device has to achieve is the correct transient stability assessment of the system dynamics. In other words, the objective of this protection scheme is to predict instability in the system; a good performance in the voltage angle forecasting is only the means to accomplish this goal.

The time series models previously mentioned, plus another two, were tested to determine their stability assessment outcome for the 3 and 5 cycles fault cases. Table 6-2 provides a summary of the results for the different time series models. The table shows at which angle of separation, and at which time in the simulation, the voltage swing was declared as unstable by the proposed Out-of-Step relay.

Table 6-2. Time Series Models Results

	3 Cycles Fault Case		**5 Cycles Fault Case**	
AR Order	No Differentiation	Differentiation	No Differentiation	Differentiation
1	-	-	66.65^0 @ 1.442 s	105.6^0 @ 1.775 s
2	-	-	105.6^0 @ 1.775 s	85.12^0 @ 1.642 s
3	-	-	88.93^0 @1.675 s	85.12^0 @ 1.642 s

Most of the time series models yielded different results, but two interesting results have to be highlighted. The first one is that the relay, using any of the time series models, did not misoperate for the stable case. The second one is that no improvement in the detection of instability was accomplish by the ARI(3,1) model when compared to the ARI(2,1) model. Another good reason to use the ARI(2,1) model for this power system.

Figure 6-11 shows the prediction outcome of the protection scheme for the stable 3 cycles fault case. The tripping decision was never met and the relay did not operate.

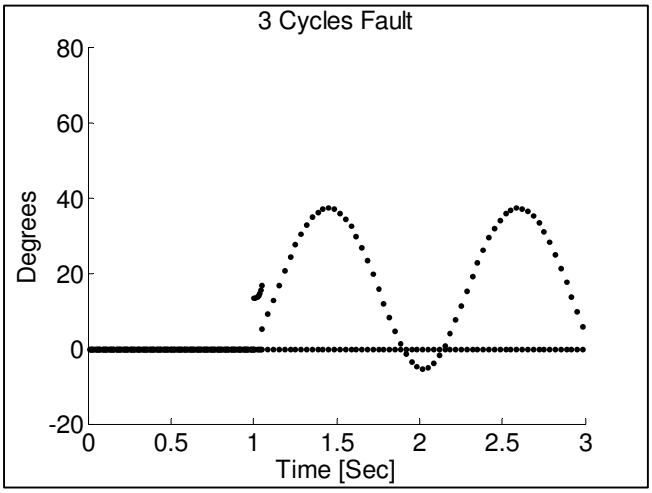

Figure 6-11. Scheme Output for Stable Cases

Figure 6-12 shows the prediction outcome for the 5 cycles fault case using an AR(1) model, which proved to be the fastest in forecasting instability. The squared point in this picture indicates the moment when the scheme declares instability.

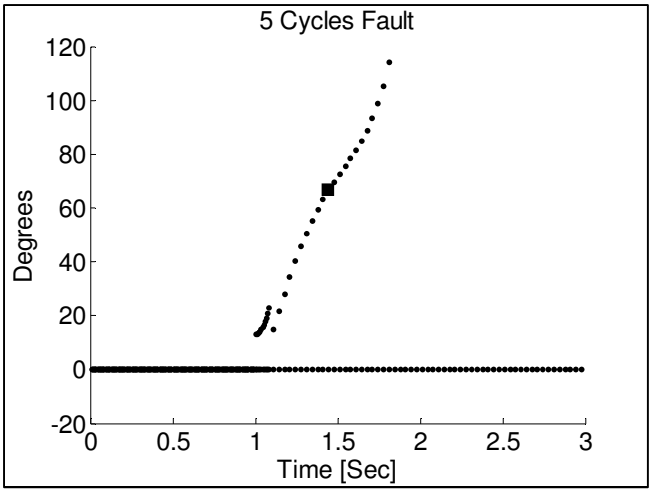

Figure 6-12. Scheme Output - AR(1)

The concepts and ideas behind this protection scheme were explained with the help of this small power system. Similar analysis of the power system and time series models has to be performed for larger multi-machine networks. In the following sections more complex models are presented and discussed.

6.2 IEEE 17 Machine System

This network is an equivalent model of the high voltage power system of the state of Iowa. It consists of 17 generating units, whose rotor dynamics are described by classical machine models, 162 buses and 284 transmission lines. A simplified one-line diagram is shown in Figure 6-13. The machine model parameters and a more detailed diagram can be found in reference [5]. The network information, such as transmission line parameters and generation levels, was acquired from reference [53]. Appendix B provides all this information for convenience of the reader.

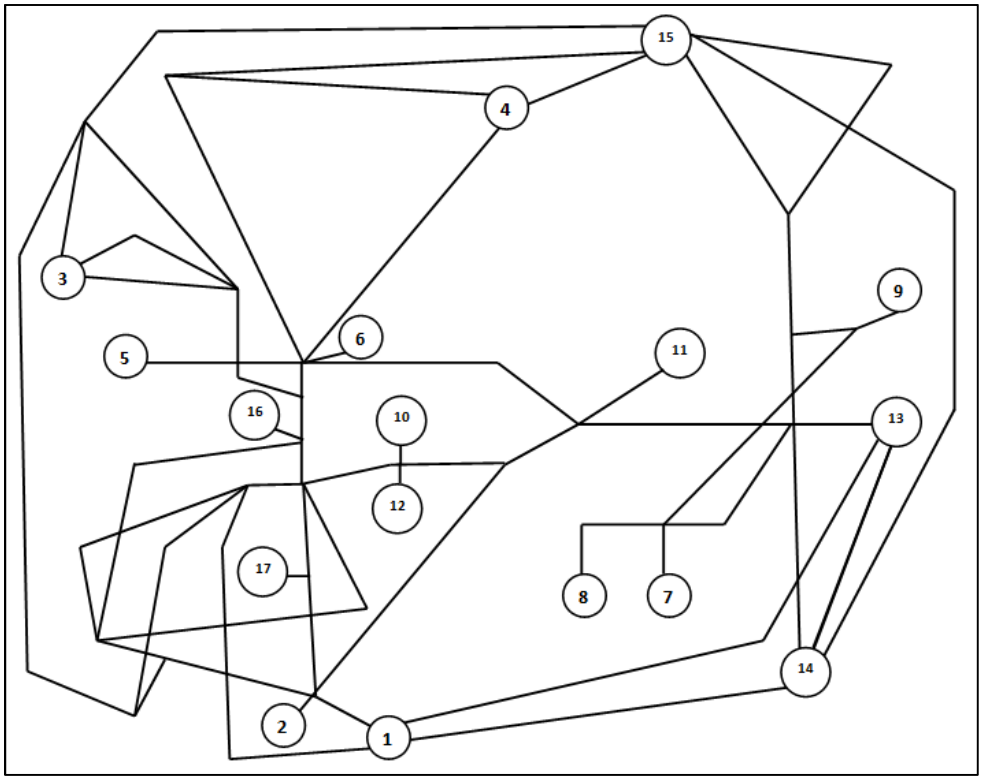

Figure 6-13. IEEE 17 Machine System

A similar transient stability study, as the one for the OMIB network, was performed in this power system. The disturbances applied for this study were breaker failure faults; since the system proved to withstand perturbations of smaller magnitude with no major problems.

The events which take place in a breaker failure fault are explained using Figure 6-14.

1 A fault develops between G and H close to bus number 1.

2 Breaker G, which usually would operate 3 cycles after the inception of the fault, fails to trip.

3 Breaker H successfully trips 5 cycles after the event was initiated. But the fault is still being fed, by system, since breaker G did not trip.

4 Breakers B, F and C, which are operated by back up relays, trip 10 cycles after the inception of the event to finally clear the fault.

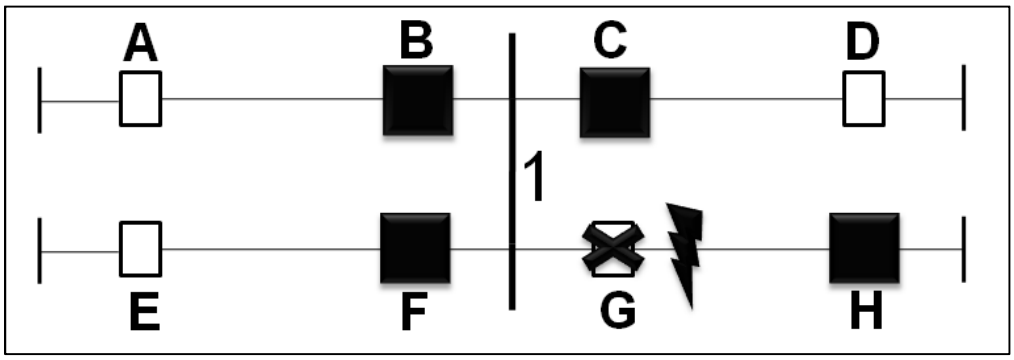

Figure 6-14. Breaker Failure Fault Event

The final result of a breaker failure fault is the isolation of bus number one in Figure 6-14. To simplify computer simulations of this type of events, the fault can be applied directly to the Bus and no to the power line. This modified disturbance was run for each of the 162 buses of the 17 machine system. The time span of the fault was slightly stretched to 12 cycles for additional stress to the system.

Out of the 162 cases that were simulated in this power system 30 of them resulted in unstable system events. The other 132 breaker failure faults produced stable cases. Figure 6-15 shows the rotor angle response of the system when the disturbance was applied at bus 128, this is a stable case. Figure 6-16 portrays the unstable behavior of one rotor angle when a breaker failure fault is applied to bus 52.

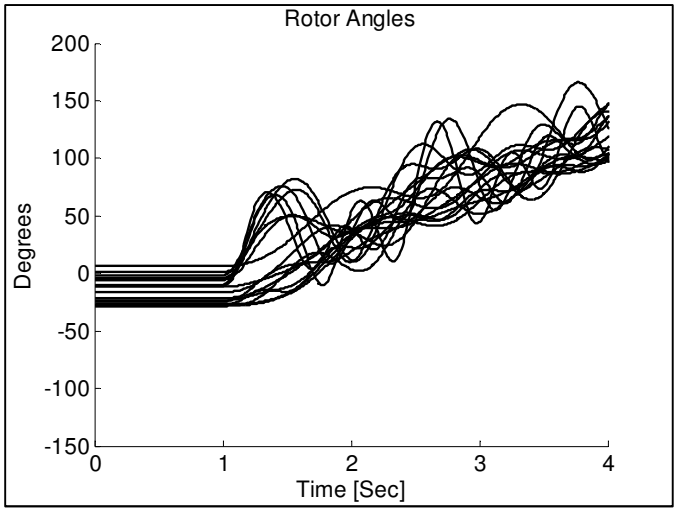

Figure 6-15. Breaker Failure Fault at Bus 128

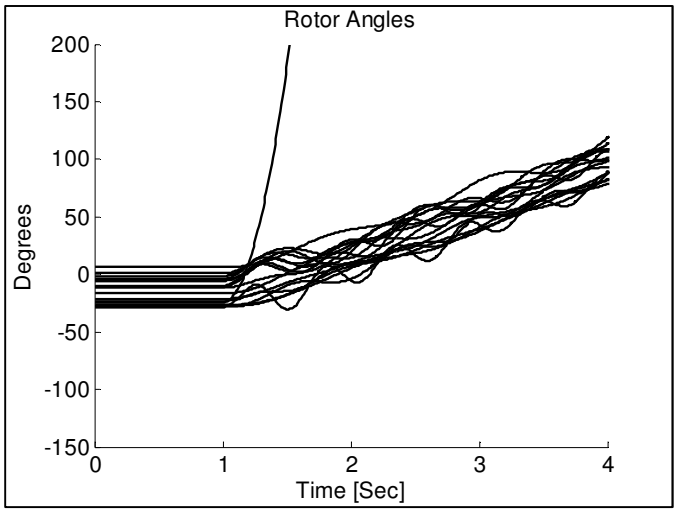

Figure 6-16. Breaker Failure Fault at Bus 52

Even though the result of the disturbance at bus 52 is an unstable case, these kinds of cases are trivial to this proposed Out-of-Step protection scheme. As mentioned in the Scheme Considerations section of the previous Chapter, machines that individually pull out of synchronism will not be considered by this relay. In this case machine number 11 is the only one separates from the rest of the system. Cases like this one are very frequent and they tend to occur because of faults that are applied close or at the terminals of such machines.

Out of the 30 unstable cases found in this power system, 28 of them follow the same pattern as the breaker failure event in bus 52. In the other two unstable cases, coherent groups of machines can actually be recognized. These groups of generating units can be identified when a breaker failure fault is applied to bus 1 and bus 120; Figure 6-17 and Figure 6-18 show the rotor angle response for these cases and the clusters of coherent generators for this multi-machine unstable swing. Machine number 3 is regarded as a coherent group in these plots, but it will be disregarded in the protection scheme since this group consists of only one generating unit. Table 6-3 shows the machine distribution for each coherent set.

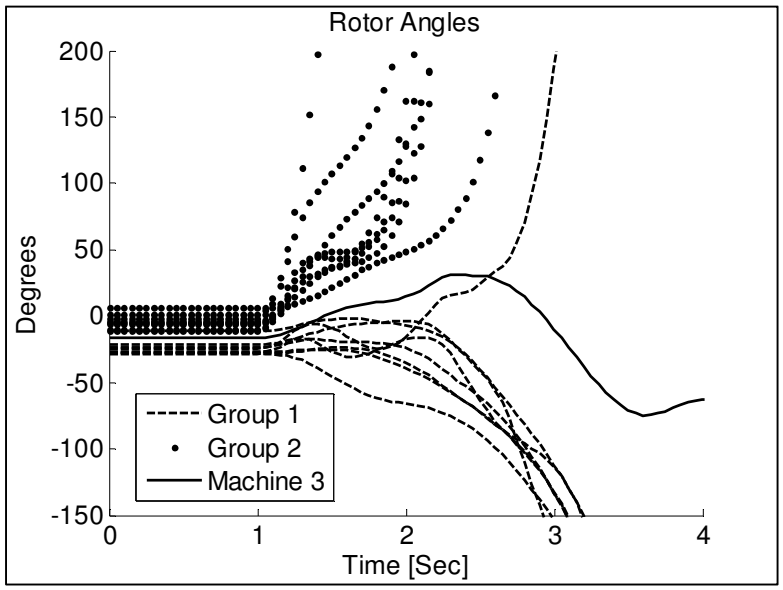

Figure 6-17. Breaker Failure Fault at Bus 1

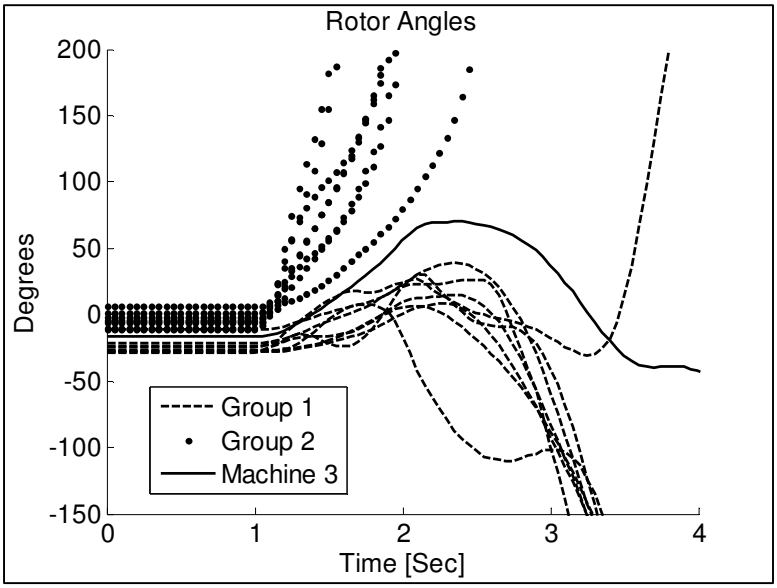

Figure 6-18. Breaker Failure Fault at Bus 120

Table 6-3. 17 Machine System - Coherent Groups

	Machine Number							
Group 1	1	7	8	9	11	13	14	15
Group 2	2	4	5	6	10	12	16	17

An analysis of the voltage angles for the two unstable cases, previously mentioned, was carried out in order to identify the buses that best described the rotor angle response of the coherent groups. Bus 109 was selected for Group 1 and acts as a PMU reference for this power system. Bus 112 was chosen for Group number 2.

Figure 6-19 illustrates the system location of the coherent groups of machines and the buses where PMUs have to be placed, so the rotor angles can be inferred. The buses where a breaker failure fault produced the two meaningful unstable cases, are also indicated in this figure.

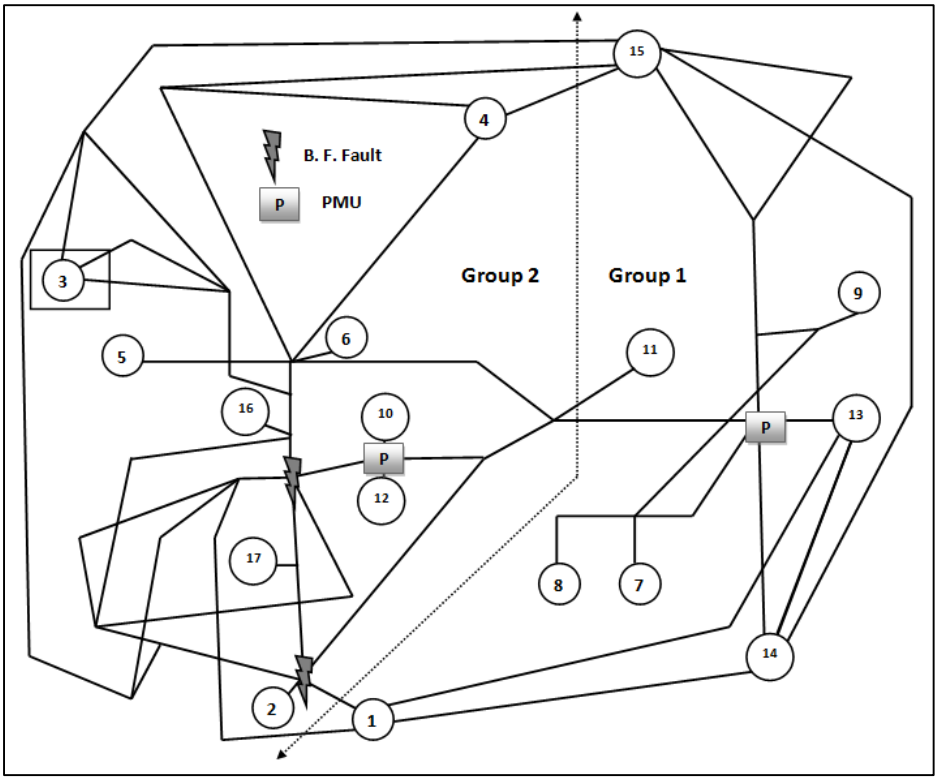

Figure 6-19. IEEE 17 - PMU Placement

With the voltages angles from these buses the performance of the time series models in the prediction of future points and the accuracy of the protection scheme in forecasting instability can be tested. The cases that were used to examine this protection scheme were the breaker failure faults at buses 1, 120 and 128. Autoregressive models with and without a differentiation process of order one were assessed.

The tripping decision chosen for this power system is the same one as for the OMIB system. Even though this is a multi-machine power system, there are only two coherent groups of machines, and the direct comparison of the forecasted angles can be used. The threshold value selected is again 150 degrees.

Table 6-4 and Table 6-5 show the results of the suggested protection scheme when tested for the aforementioned cases. The scheme did not misoperate for the stable case, an attribute that is desired in protection relays. For the breaker failure case at bus

one, most of the autoregressive models yielded different results, the fastest in the prediction of instability was the ARI(3,1) model. For the breaker failure fault at bus 120, the majority of the models had the same performance in the prediction of instability. Four of the five models predicted instability as fast as possible, since the second set of PMU measurements was assumed to arrive at 1.542 seconds.

Table 6-4. 17 Machine System - Stable Case

	128	
AR Order	No Differentiation	Differentiation
1	-	-
2	-	-
3	-	-

Table 6-5. 17 Machine System - Unstable Cases

	1		120	
AR Order	No Differentiation	Differentiation	No Differentiation	Differentiation
1	82.93^0 @ 1.842 s	55.39^0 @ 1.742 s	239.4^0 @ 1.542 s	239.4^0 @ 1.542 s
2	55.39^0 @ 1.742 s	45.02^0 @ 1.675 s	297.6^0 @ 1.608 s	239.4^0 @ 1.542 s
3	55.39^0 @ 1.742 s	38.76^0 @ 1.608 s	239.4^0 @ 1.542 s	239.4^0 @ 1.542 s

Figure 6-20, Figure 6-21 and Figure 6-22 illustrate the moment when the tripping decision is met in the previous cases, for the unstable cases the fastest model to react is shown.

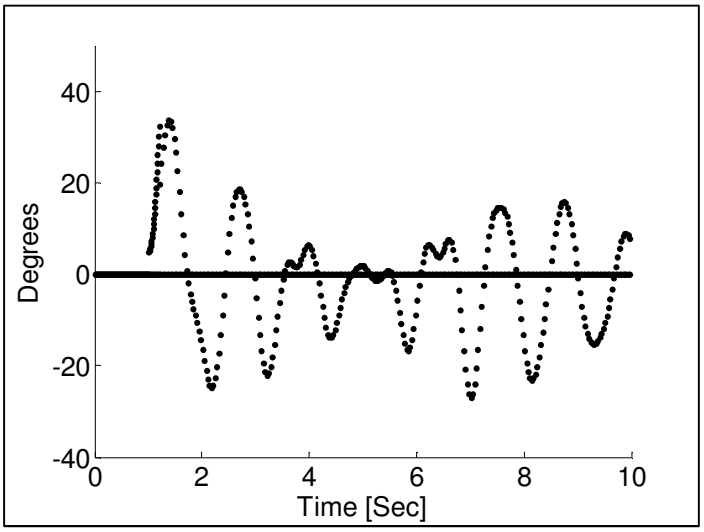

Figure 6-20. Protection Scheme Output for Case 128

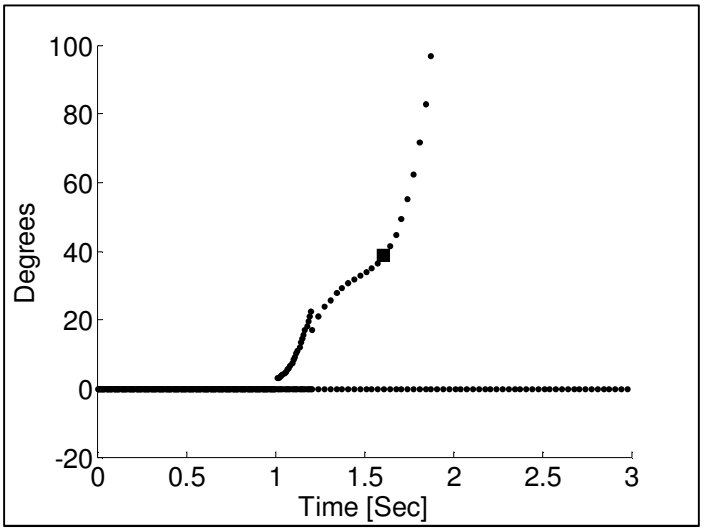

Figure 6-21. Protection Scheme Output for Case 1

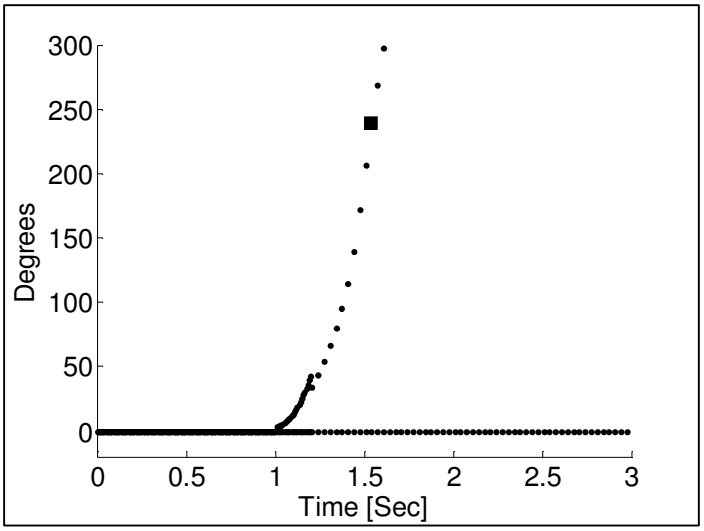

Figure 6-22. Protection Scheme Output for Case 120

EEAC Assessment

The Extended Equal Area Criterion discussed in Chapter 3 is used in this section to assess the transient stability of the three cases analyzed for the 17 machine system. For this assessment, coherent group number one was selected as the critical cluster of machines and coherent group number two as the remaining set of generating units. The inertia values of the machine rotors can be found in Appendix B. The two-machine and OMIB equivalents were created as discussed in Chapter 3.

The Equal Area Criterion in the time domain as the one mentioned in reference [24] is used in this section. Using this approach, for the stability assessment of power systems, the electric power of the OMIB equivalent is compared against its mechanical power at every instant of time. If the summation of the electric output power of the equivalent is larger than the summation of its mechanical power during the first swing of oscillation, the system is declared to be stable otherwise it is determined that the system will lose synchronism.

Figure 6-23 shows the result for the stable case using this analysis. Area one (A_1) represents the kinetic energy the system gained during the time the fault was present,

and area two (A_2) represents the decelerating energy the system has available to overcome the acceleration effect. For this case $A_1 = 262$ and $A_2 = 464$; EEAC correctly assessed stability for this case.

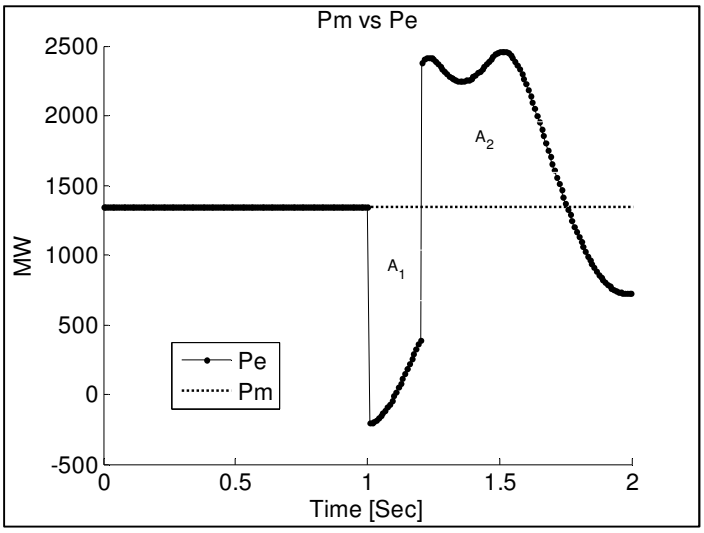

Figure 6-23. EEAC for Case 128

Figure 6-24 and Figure 6-25 show the Extended Equal Area Criterion analysis for the two unstable cases. For case one, $A_1 = 196$ and $A_2 = 70$. For case number 120, $A_1 = 291$ and $A_2 = 95$.

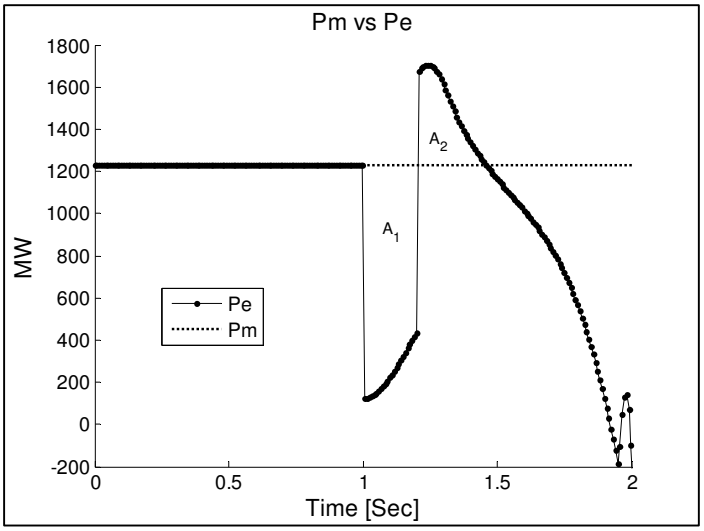

Figure 6-24. EEAC for Case 1

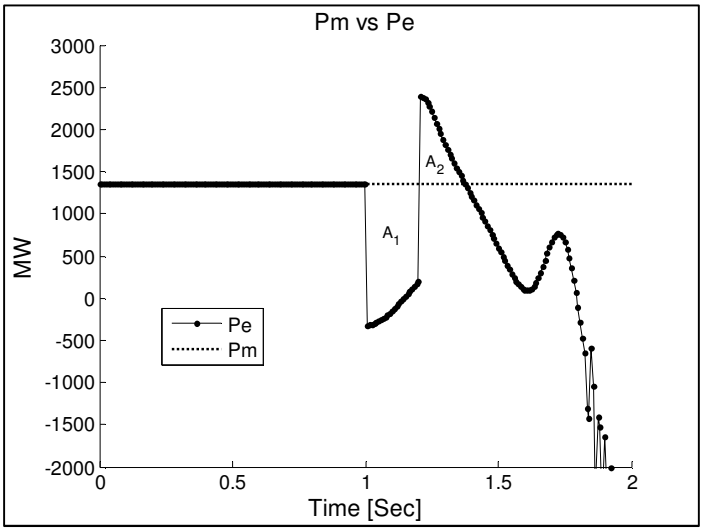

Figure 6-25. EEAC for Case 120

Instability was correctly assessed for both of the unstable cases using the Extended Equal Area Criterion. Both of the unstable cases followed a first swing instability behavior, characteristic that makes possible the use of this method.

6.3 California System

The State of California power network is part of the Western Electricity Coordinating Council (WECC) interconnection system. WECC is a larger power system that covers most of western states of U.S.A. and spans in parts of Mexico and Canada as well. The power system models for the state of California used in this dissertation were derived from a larger WECC power system model. The network reduction techniques mentioned in Chapter 5 were employed to obtain a reduced equivalent system. In the reduction process two equivalent machines were inserted at the borders of the state of California, one in the north and the other one in the east. These machines represent the portions of WECC network outside the state of California. Power flow simulations and dynamic tests were run in order to verify the accuracy of the reduced model and its accordance to the larger system.

The network models used in this section describe the Californian power grid in great detail. Each one of the three system models is composed of more than 4,000 buses and 400 generators; whose dynamic response is described by different machine models. Different control systems such as excitation, governor and power system stabilizers are also present in the dynamic modeling of the network.

A simplified one-line diagram of the 500 kV transmission system of the state of California is shown in Figure 6-26. As it can be seen in this picture, the power system has a longitudinal topology which runs from north to south. Even though the main two power utilities, PG&E and SCE, provide most of the power in the state, different neighbor utilities have to export an important amount of energy to California in order to compensate for its deficit of power. A more comprehensive description of the California power system can be found in [54]; in this reference an adaptive protection scheme, which uses PMU measurements to determine the level of stress of the power system, was developed with the help of a data mining process. Knowing the stress level of the system a relay could be biased towards a secure or dependable operation characteristic.

The methodology provided in this dissertation and the tests performed on the different small power systems have the objective of developing an Out-of-Step protection scheme for the power system of the state of California. The main results obtained in this research project, funded by the California Institute for Energy and Environment, are presented in the following sections.

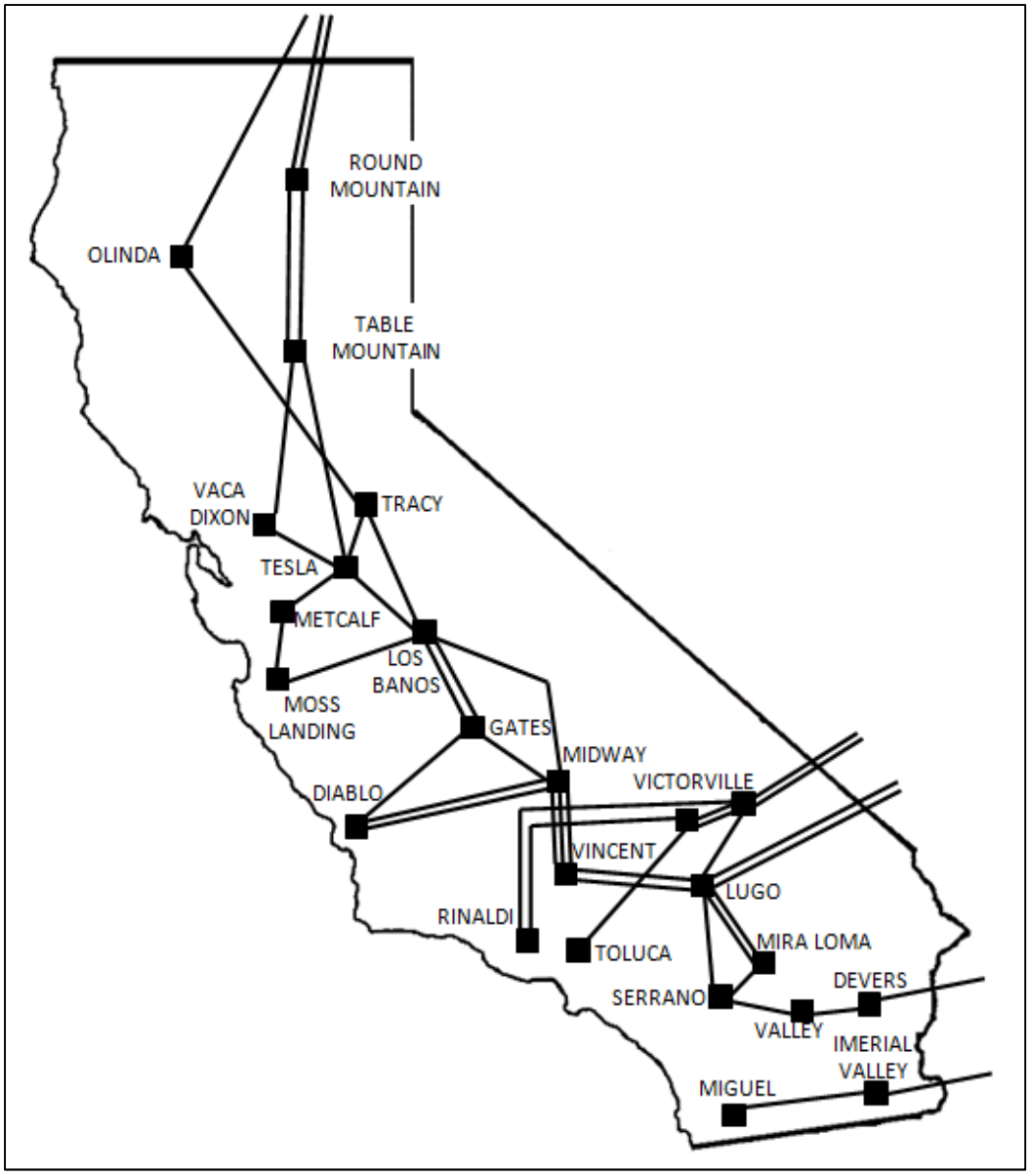

Figure 6-26. California Transmission System

Heavy Winter, Heavy Summer and Light Summer cases are the three different power system models analyzed for the state of California; each of them describes different seasonal operating conditions for this power grid. Heavy Summer being the more stressed model and the one with more stability issues. These three models have basically the same power system components in terms transmission lines, loads and generation stations; the main difference between them is the loading condition of the system and the amount of generating units that are in service.

Different perturbations were applied to these models in order to obtain stable and unstable dynamic behaviors of the generators in grid. Reference [54] also discusses some of the faults that were simulated in order to find the appropriate location of the adaptable relay. In this case different N-3 contingencies involving transmission line trippings were applied to the system, a total of 501 different disturbances were run for every model with a surprising result of only two important unstable cases. These events involve the removal of the three transmission lines connecting the Midway and Vincent 500 kV buses.

Breaker failure faults, in this part of the project, were also simulated in order to find more unstable cases in the California power system. The buses selected to apply this perturbation were all the 500 and 230 kV buses present in the network. A total of 1500 simulations were run in the three different power system models; only in seven of these cases coherent groups of machines could be recognized.

Table 6-6 provides a summary of the unstable cases that were found in the system and that were used to test the proposed Out-of-Step protection scheme. Some stable cases with important power oscillations were also analyzed and they are presented in the performance evaluation section.

Table 6-6. California - Unstable Cases

Model	Case Number	Disturbance
Heavy Winter	1	Breaker Failure @ Lugo 500 kV
	2	Breaker Failure @ Vincent 500 kV
	3	1 Fault and 2 Hidden Failures @ Midway - Vincent 500 kV
Light Summer	4	Breaker Failure @ Lugo 500 kV
Heavy Summer	5	Breaker Failure @ Midway 500 kV
	6	Breaker Failure @ Lugo 500 kV
	7	Breaker Failure @ Vincent 500 kV
	8	Breaker Failure @ Market Place 500 kV
	9	1 Fault and 2 Hidden Failures @ Midway - Vincent 500 kV

Tripping Decisions and PMU Placement

Figure 6-27 shows the rotor angle response for a breaker failure fault of 10 cycles at the Lugo 500 kV bus in the Heavy Winter model, case number one in Table 6-6. The first paramount conclusion that can be made, analyzing this plot, is that the northern and southern parts of the California system appear to behave as two different coherent groups. These two sets of machines are geographically separated by the three transmission lines that connect the Vincent and Midway 500 kV buses.

It can also be noted that the southern portion of the system experiences unstable power oscillations inside its own fraction of the network. In other words, the southern part of the California system can be divided into more coherent groups of machines. In Figure 6-27, more than 5 coherent set of generating units can be identified in this portion of the network. The northern part of the system, on the other hand, does not suffer any unstable oscillation inside its own network. Similar results in terms of rotor angle behavior, in the southern and northern portions of the network, are obtained for the rest of the unstable cases.

Out-of-Step relays are usually design to handle just one network separation, meaning that they attempt to protect systems that behave as a two-machine equivalent. As seen in this figure the California power grid has a multi-machine system behavior, since more than 2 unstable coherent groups of machines can be recognized in Figure 6-27. One of the main contributions of this research project, to the Out-of-Step relaying theory, is the protection of a network that has more than one system separation, or that behaves as a multi-machine equivalent.

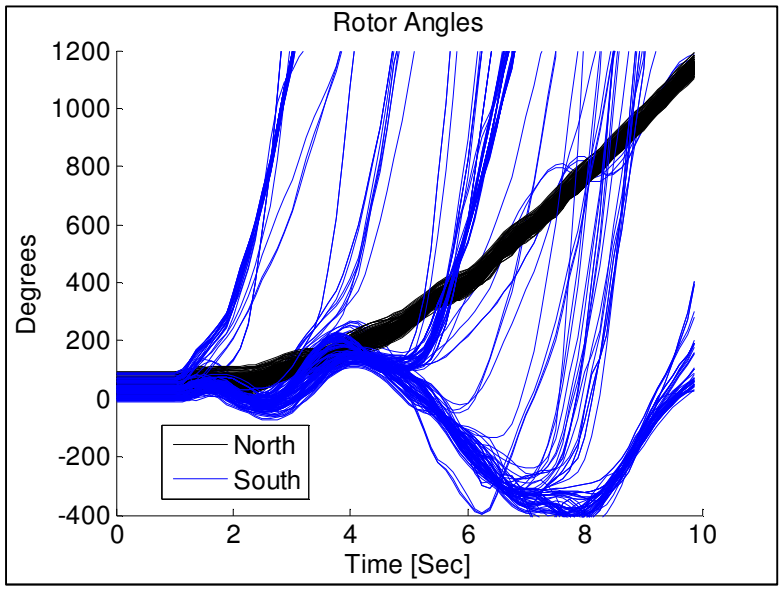

Figure 6-27. Rotor Angle Response for Case 1

The previous illustration does not show the correct behavior of the rotor angles for that given disturbance, case number one. The unstable machines were never disconnected from the system; something that will actually occur in a real system event. The simulation does not depict the real conditions of the system after the first group of generators loses synchronism; this group has to be disconnected so the remaining of the simulation can be valid.

In order to test the Out-of-Step protection scheme proposed in this dissertation, the different groups of coherent machines in the system were identified following the next procedure.

1. The simulation was run until the first unstable group of machines was detected.
2. The proposed protection scheme was used in order to determine the time instant the relay predicted instability.
3. The unstable group of machines was disconnected from the system at this instant of time by the appropriate removal of transmission lines.
4. The simulation was run again until the following unstable group of machines was detected.

For the California power system two different tripping decisions were implemented in the Out-of-Step protection scheme; one for inter-area system separation and a different one for area separation, both of them use the concept of a center of angles to predict instability. The predictive mechanism that was chosen, for the three power system models, was an Autoregressive Integrated Model, an ARI(3,1). This time series model gave a good estimation of the future voltage angle data and a good stability assessment of the power system. The parameter estimation for this time series model is presented in Appendix C.

The inter-area tripping decision was used to detect instability between the northern and southern portions of the network; meanwhile the area tripping decision was employed to detect machine instability inside these parts of the system. Denoting the set of voltage angles and machines in the northern part of the system as P and the ones in the southern part as C, the following center of angles can be defined.

$$COA_{P,t+10} = \frac{\sum_{i=1}^{N} S_i * \theta_{i,t+10}}{\sum_{i=1}^{N} S_i} \tag{6.1}$$

$$COA_{C,t+10} = \frac{\sum_{i=1}^{N} S_i * \theta_{i,t+10}}{\sum_{i=1}^{N} S_i} \tag{6.2}$$

where

N	Number of coherent groups in each part of the network
θ_i	PMU Voltage Angle of the coherent group i
S_i	MVA rating of the coherent group i

Using the previous definitions of center of angles for the northern and southern parts of the system, the following tripping decisions can be defined for the California system.

Northern area of the system:

$$if \quad \left|\theta_{i,t+10} - COA_{P,t+10}\right| > Threshold\ Value \tag{6.3}$$

Southern area of the network:

$$if \quad \left|\theta_{i,t+10} - COA_{C,t+10}\right| > Threshold\ Value \tag{6.4}$$

For inter-area separation:

$$if \quad \left|COA_{C,t+10}\right| > Threshold\ Value \tag{6.5}$$

As it can be inferred from the previous equations, each voltage angle (coherent group) is compared against its respective center of angles in the area tripping decision. The northern center of angles is not used in the inter-area tripping decision since the PMU that will act as a reference, Los Banos 500 kV, is located in this part of the system; and for most of the cases it will have a value equal to zero. The threshold value selected for these tripping decisions is 150 degrees.

If any of the tripping decisions described by these equations are met in two consecutive predictions, an Out-of-Step condition is declared and separation of the system should be attempted. Two consecutive predictions are used in order to verify the accuracy of the voltage angle forecasting. Another method was also implemented in this network to assure that valid predictions are being used by the protection relay. These methods evaluate the absolute value of the 10^{th} forecasted point, for each voltage angle, and the absolute value of both center of angles. If these values exceed 2000 degrees, the prediction for that angle and/or center of angles is disregarded.

The nine unstable cases, found in the California system, were analyzed using the coherency identification method and tripping decisions described before. The outcome of this analysis was the correct identification of the different coherent groups in the system and the proper location of the PMU's in the network. The PMU devices needed for this system are listed in Table 6-7. Figure 6-28 shows the location of the PMU's in the power grid, the first three PMUs are located in the northern portion of the network; the rest are placed in the southern part of California.

Table 6-7. PMU Placement and MVA Rating

Heavy Winter		
BUS		MVA
Los Banos	500 kV	15800
Morrobay	230 kV	1450
Diablo	500 kV	2640
Imp. Valley	230 kV	14000
Magunden	230 kV	2069
Kramer	230 kV	1707
Mnt. View	230 kV	1224
Haynes	230 kV	984
Vulcan 1	92 kV	470

Light Summer		
BUS		MVA
Los Banos	500 kV	19500
Morrobay	230 kV	1900
Diablo	500 kV	2640
Imp. Valley	230 kV	12400
Magunden	230 kV	1000
Kramer	230 kV	2104
Mnt. View	230 kV	1224
Haynes	230 kV	1634
Vulcan 1	92 kV	470

Heavy Summer		
BUS		MVA
Los Banos	500 kV	26000
Morrobay	230 kV	5700
Diablo	500 kV	2640
Magunden	230 kV	2070
Kramer	230 kV	3270
Mnt. View	230 kV	1224
Haynes	230 kV	1364
Vulcan 1	92 kV	470
Litehipe	230 kV	24400

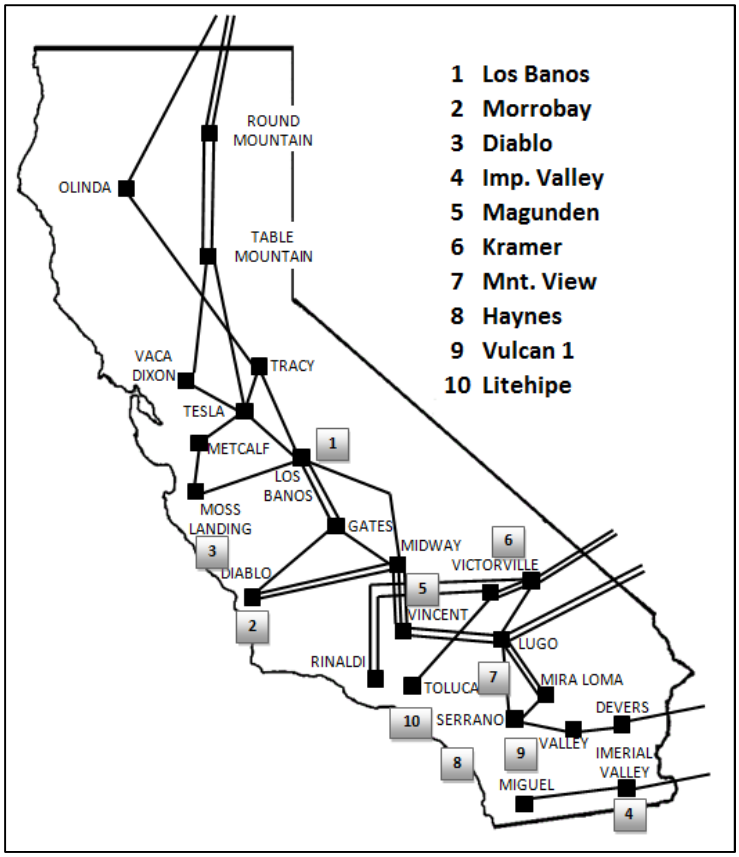

Figure 6-28. California - PMU Placement

There are 8 fixed PMU's used in the three power system models. Imperial Valley 230 kV and Litehipe 230 kV will have to be interchanged depending on the current season of the year; this gives a total number of 10 PMU's in the network of California. Each of the voltage angles has a MVA rating assigned to it; this rating is equal to the summation of all the machine MVA ratings present in each of the coherent groups. This rating is used to compute the different center of angles.

In the next sections the coherency identification and the Out-of-Step protection scheme implemented for this power system are described. The first set of cases to be investigated is the one corresponding to the Heavy Winter model.

6.3.1 Heavy Winter Model

Case 1

Figure 6-29 shows the rotor angle response for case number one. The first group of machines that goes out of synchronism with respect to the rest of the system is highlighted in blue. Table 6-8 list some of the machines that belong to this group, Kramer 230 kV is the bus selected to monitor this set of generators.

As sated earlier, this group of unstable machines has to be disconnected from the power grid so the rest of the simulation can be valid. The proposed OOS protection scheme was implemented in order to predicted instability for this case. Figure 6-30 shows the instant of time the relay declared instability for this group. All the tripping times for all unstable cases are presented in the performance evaluation section.

Table 6-8. Group 1 - Kramer 230 kV

Kramer 230 kV	
MC GEN	ALTA42GT
LUZ8 G	MOGEN G
LUZ9 G	KERRMGEE
ALTA41GT	OXBOW G1

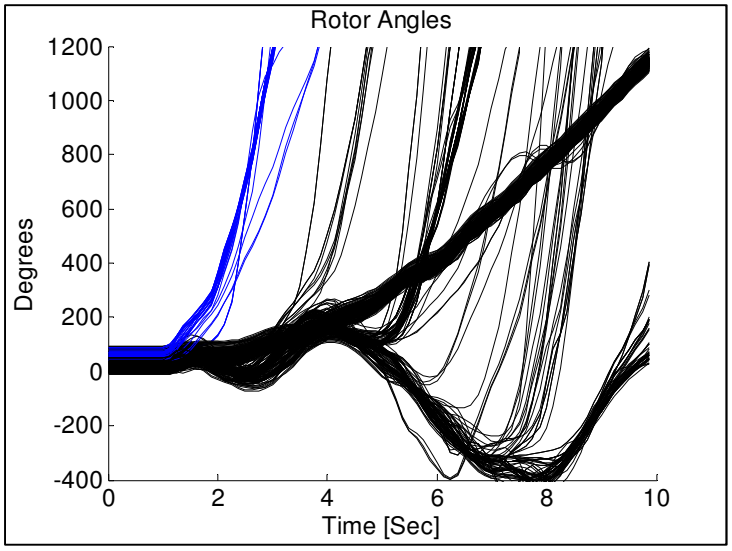

Figure 6-29. First Unstable Group

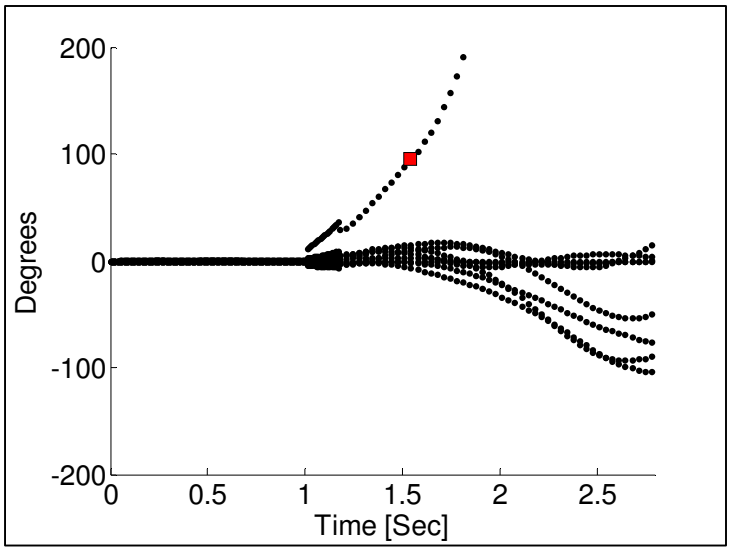

Figure 6-30. OOS Prediction - Kramer 230 kV

After the first unstable group of machines was disconnected from the system, the simulation was run again until the second group of unstable machines was found. Figure 6-31 shows the rotor angle response for this case. Appendix D provides a list of

the transmission lines that have to be tripped to isolate the different coherent groups of machines in the California System.

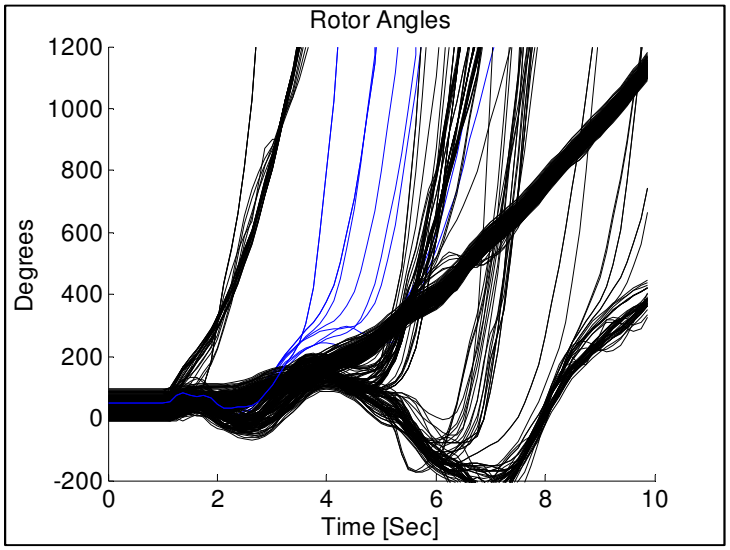

Figure 6-31. Second Unstable Group

Figure 6-32 shows the instant of time the second group of machines was declared as unstable by the Out-of-Step relay. The machines that compose this group are listed in Table 6-9. Isolated machines were also disconnected in this part of the simulation.

Table 6-9. Group 2 - Haynes 230 kV

Haynes 230 kV
HAYNES1G
HAYNES8G
HAYNES9G
HAYNS10G

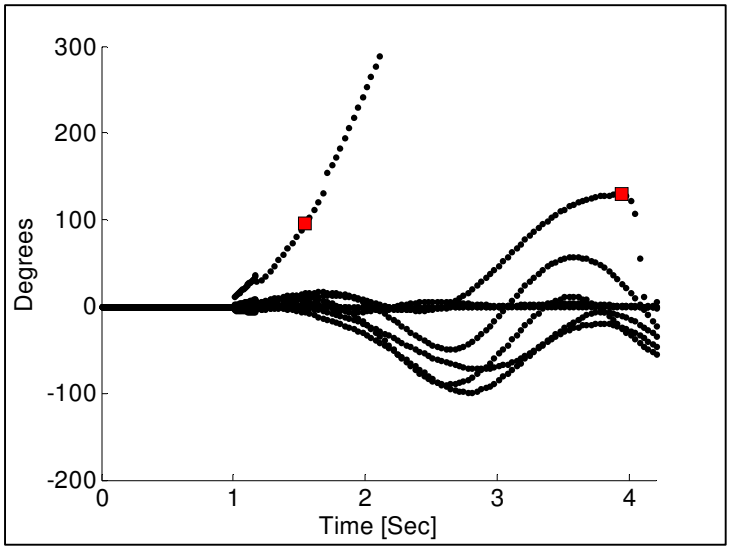

Figure 6-32. OOS Prediction - Haynes 230 kV

The simulation was run again until the third system separation was detected. In this occasion the inter-area tripping decision was met two consecutive times and the three lines that connect the northern and southern portions of the networks were disconnected. The simulation was run again in order to find the fourth unstable group.

Figure 6-33 depicts the rotor angle response after the northern and southern areas were separated. The fourth unstable group of machine is again highlighted in blue and Table 6-10 lists some of the machines that belong to this set.

Table 6-10. Group 4 - Vulcan1 92 kV

Vulcan 1 230 kV	
DELRANCH	LEATHERS
DPWR#3	SALTSEA4
EENERGY	SIGC
JJELMORE	VULCAN1

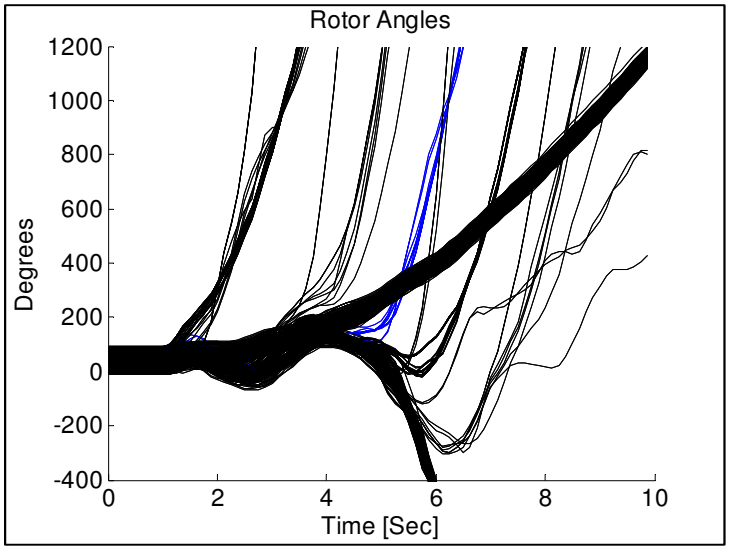

Figure 6-33. Fourth Unstable Group

Figure 6-34 shows the instant of time the fourth group of machines is declared as unstable by the Out-of-Step relay.

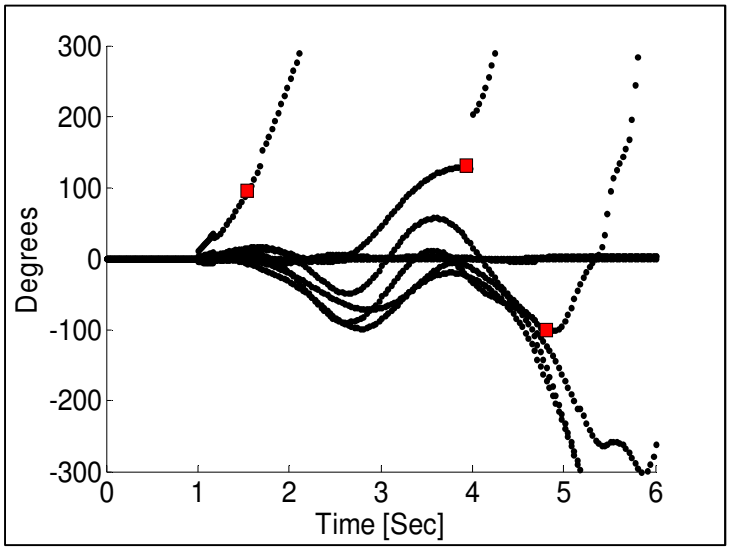

Figure 6-34. OOS - Vulcan1 92kV

Figure 6-35 illustrates the rotor angle response of the system after the fourth unstable group was disconnected from the network. A fifth unstable group can be recognized in this plot.

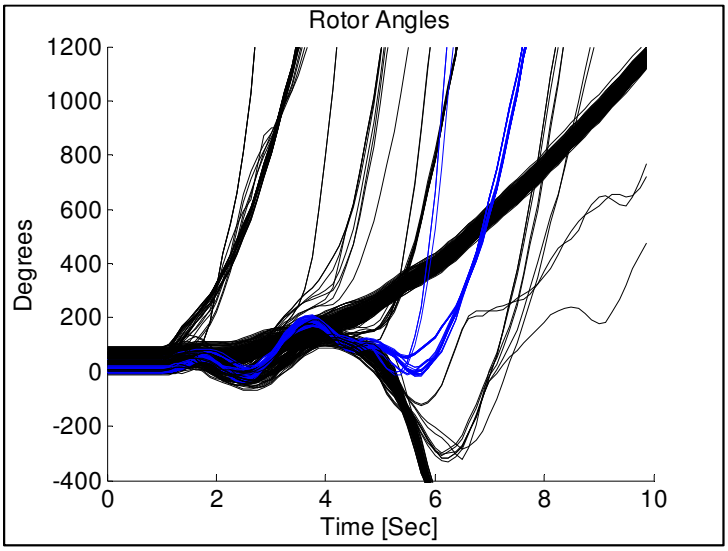

Figure 6-35. Fifth Unstable Group

Table 6-11 lists some of the machines that belong to this group.

Table 6-11. Group 5 - Magunden 230 kV

Magunden 230 kV	
MAMOTH1G	EASTWOOD
MAMOTH2G	ULTRAGEN
OMAR 1G	WARNE1
SYCCYN1G	B CRK 4

Figure 6-36 shows the outcome of the protection scheme for the fifth unstable group of machines.

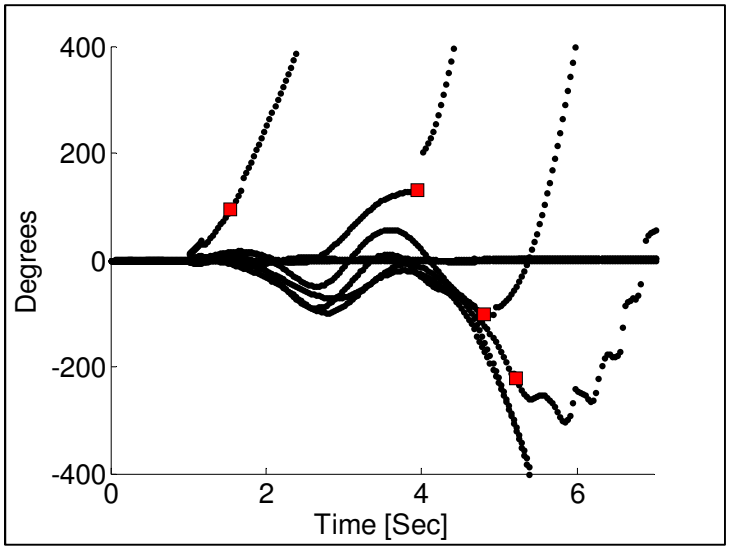

Figure 6-36. OOS - Magunden 230 kV

Figure 6-37 depicts the rotor angle response of the system after the fifth unstable group was disconnected. The highlighted machines are isolated generators that are disregarded for this protection scheme. No further unstable machines were found after this set of generators was disconnected from the system.

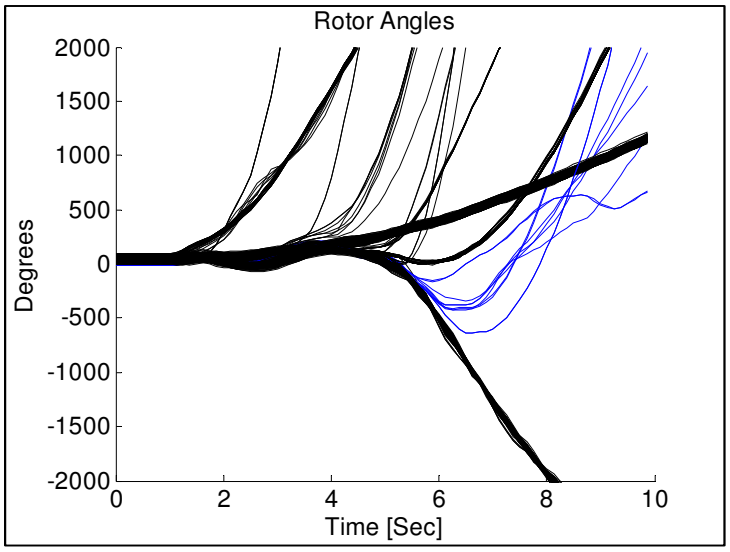

Figure 6-37. Sixth Unstable Group

The process of how the simulations were run was presented and fully described for this case. A similar procedure was followed for the remaining unstable cases listed in Table 6-6. In the following sections only the final result for each one of these system events is presented.

Case 2

Figure 6-38, Breaker Failure Vincent 500 kV.

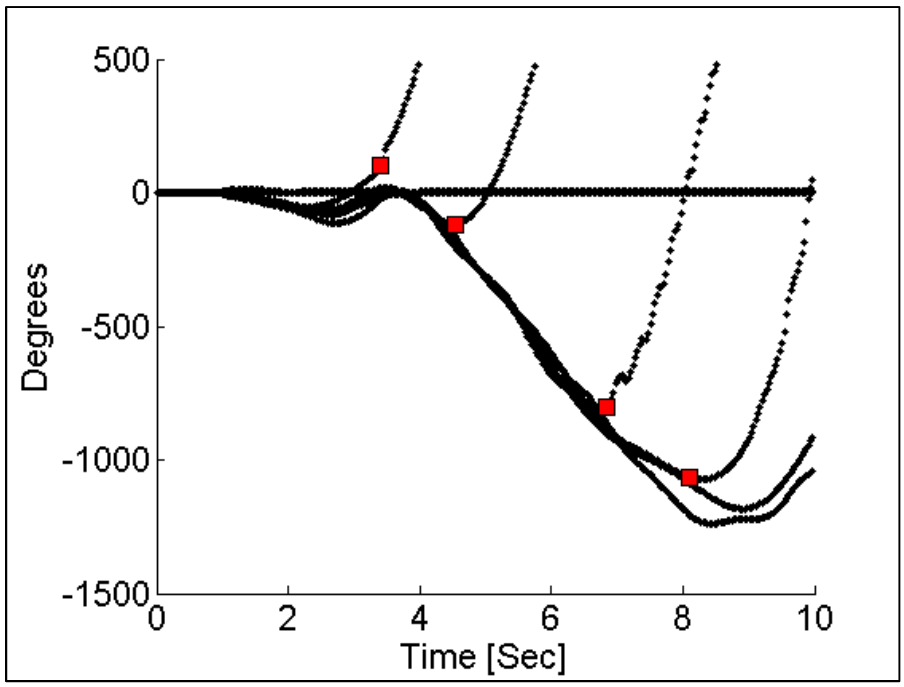

Figure 6-38. OOS Prediction - Case 2

Case 3

Figure 6-39, 1 Fault and 2 Hidden Failures between Midway and Vincent 500 kV.

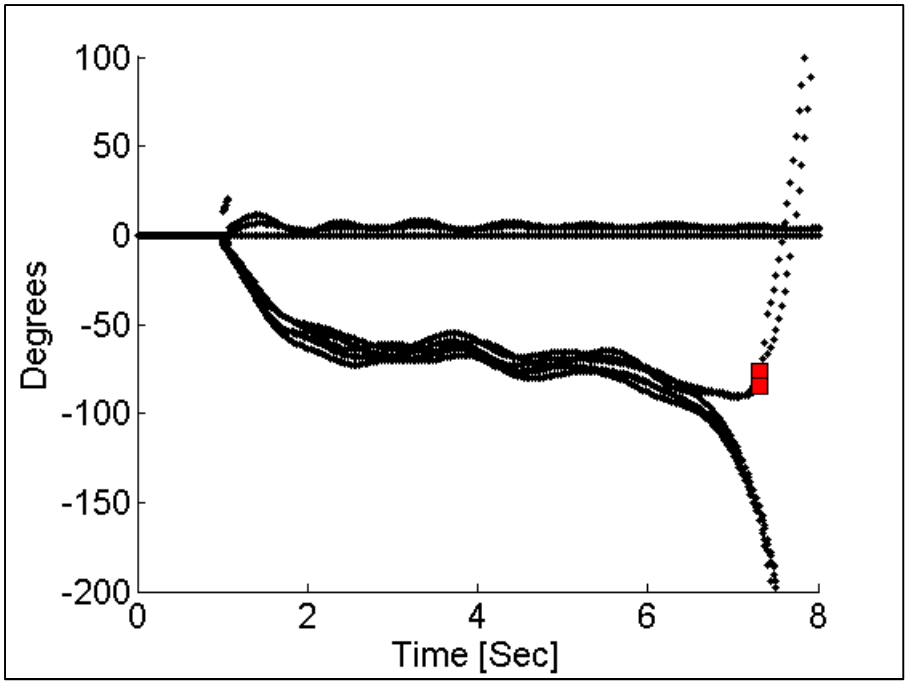

Figure 6-39. OOS Prediction - Case 3

6.3.2 Light Summer Model

Case 4

Figure 6-40, Breaker Failure Fault Lugo 500 kV.

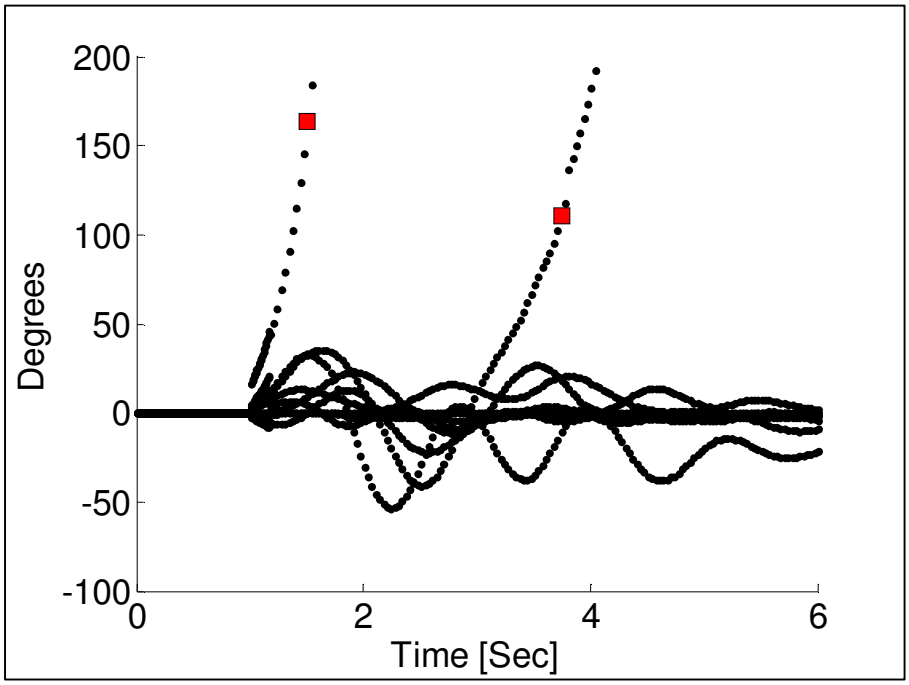

Figure 6-40. OOS Prediction - Case 4

6.3.3 Heavy Summer Model

Case 5

Figure 6-41, Breaker Failure Fault Midway 500 kV.

This case was the only system event in which unstable oscillations were present inside the northern part of the California network.

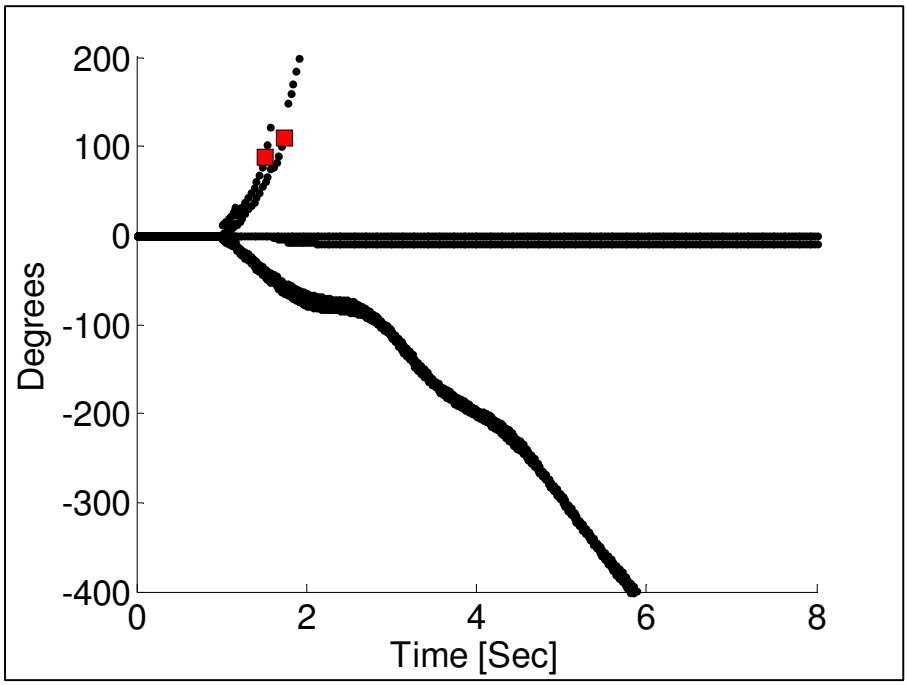

Figure 6-41. OOS Prediction - Case 5

Case 6

Figure 6-42, Breaker Failure Fault Lugo 500 kV.

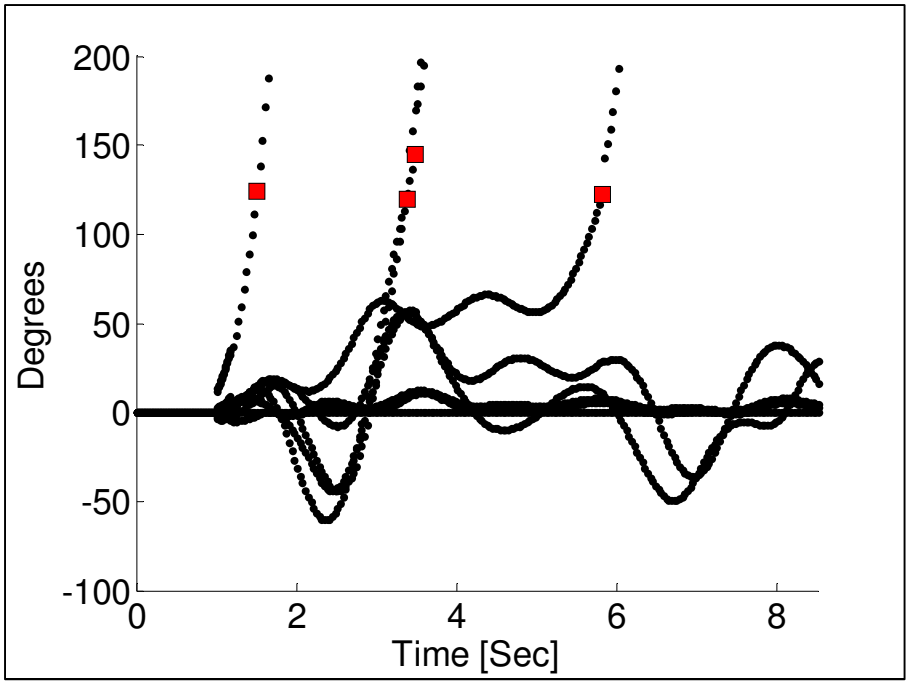

Figure 6-42. OOS Prediction - Case 6

Case 7

Figure 6-43, Breaker Failure Fault Vincent 500 kV.

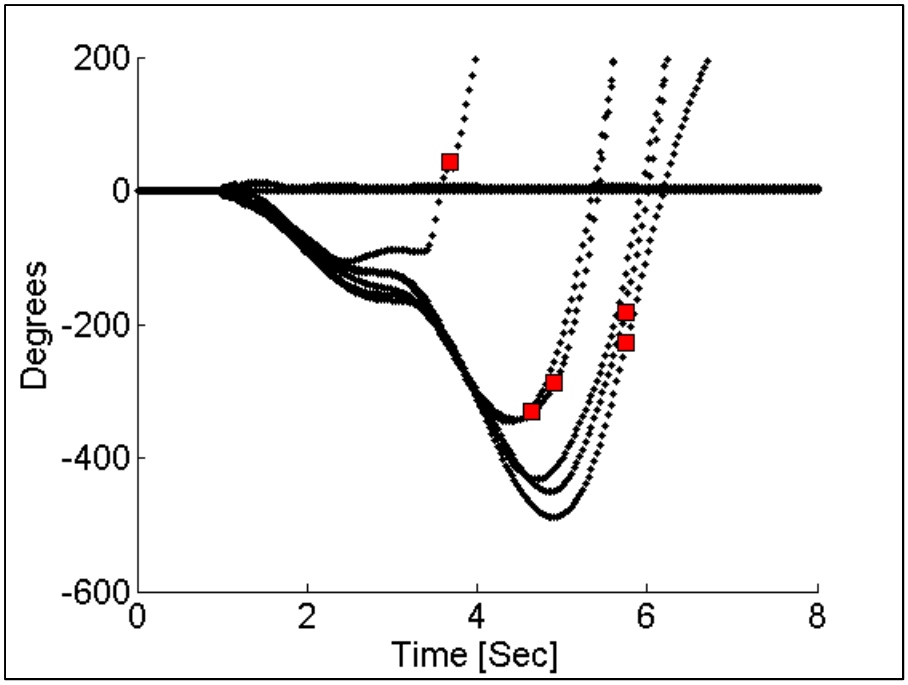

Figure 6-43. OOS Prediction - Case 7

Case 8

Figure 6-44, Breaker Failure Fault Market Place 500 kV.

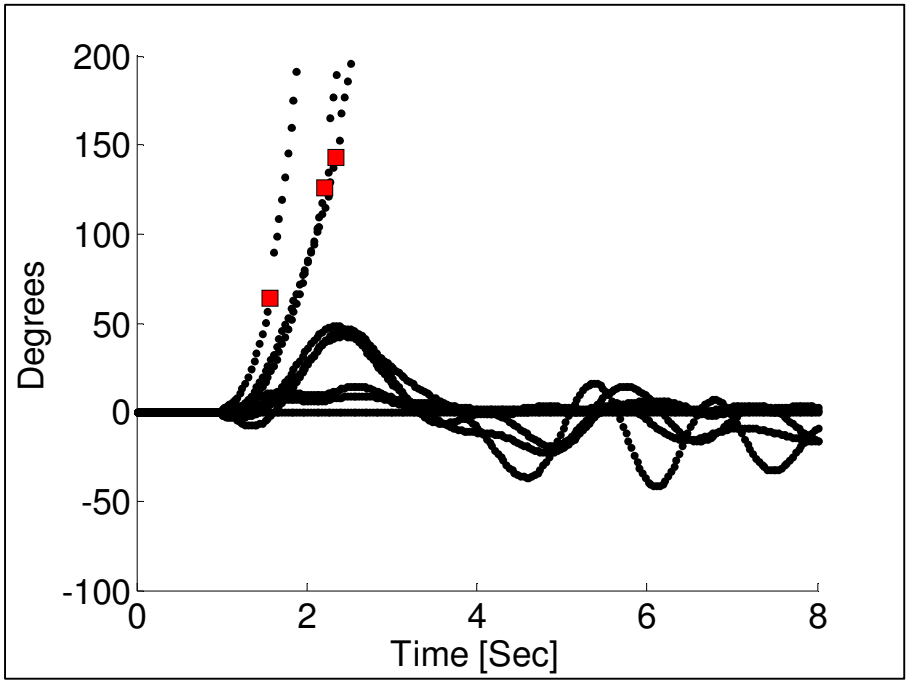

Figure 6-44. OOS Prediction - Case 8

Case 9

Figure 6-45, shows the OOS prediction for the case of one Fault and two Hidden Failures between Midway and Vincent 500 kV.

No protection action is needed in this case; the three lines that connect the two systems are already out of service.

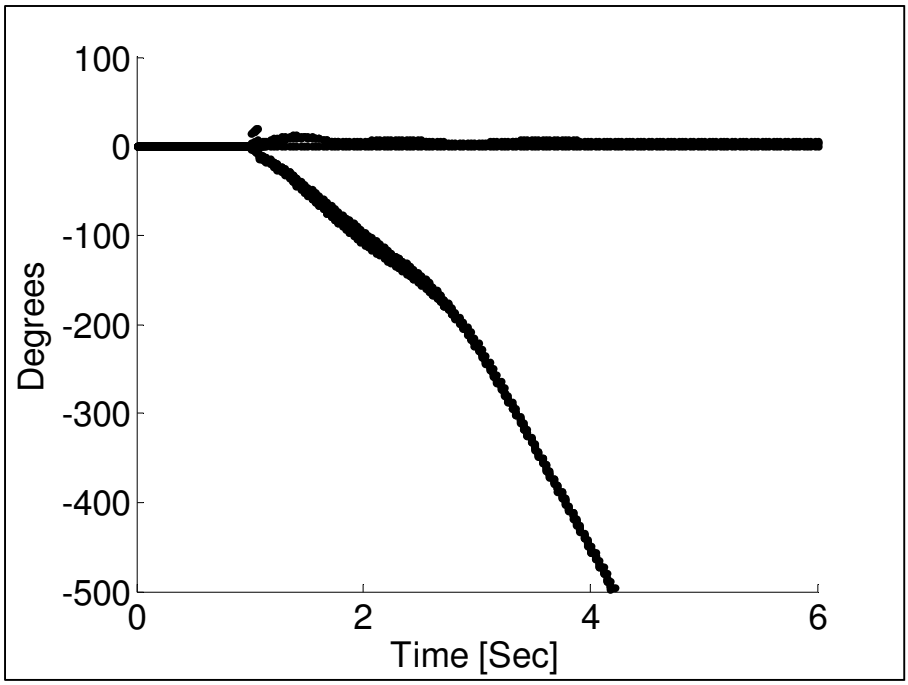

Figure 6-45. OOS Prediction - Case 9

Performance Evaluation

It was shown in the previous figures that the Out-of-Step protection scheme properly identified all stable and unstable oscillations as such; the relay's algorithm did not operate for any stable oscillation. The protection scheme was also tested using four critically stable cases, which are events that presented large stable oscillations; Table 6-12 lists these cases.

Table 6-12. California - Stable Cases

Model	Case Number	Disturbance
Heavy Winter	10	Breaker Failure @ Imperial Valley 500 kV
	11	Breaker Failure @ Miraloma 500 kV
Heavy Summer	12	8 cycles Fualt @ Coachella Valley 230 kV
	13	7 Cycles Fault @ Mountain View 230 kV

Figure 6-46 depicts the outcome of the Out-of-Step protection scheme for case number 10. In this figure the voltage angle corresponding to Imperial Valley 230 kV presents a large stable oscillation. The protection scheme did not operate for this case.

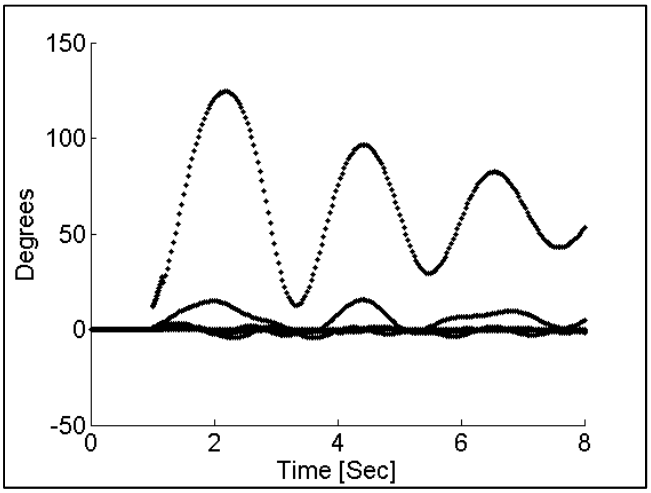

Figure 6-46. OOS Prediction - Case 10

Figure 6-47 illustrates the output for case number 11. It can be seen that even though the system has large oscillations, the device algorithm did not identify any swing as unstable. Similar results are obtained from the other 2 critically stable cases.

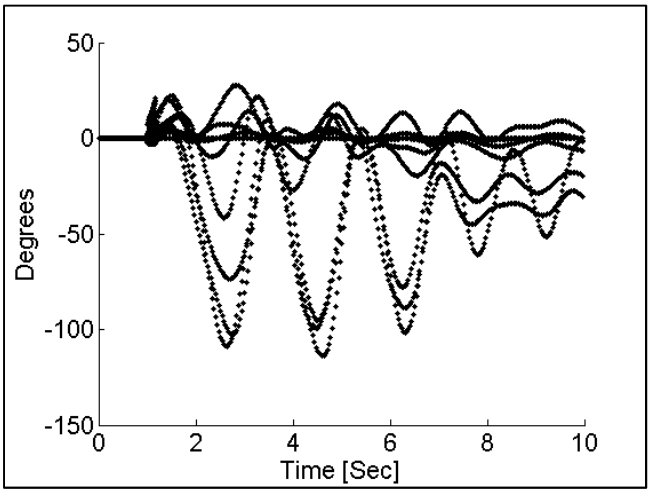

Figure 6-47. OOS Prediction - Case 11

After analyzing all the 13 unstable and critically stable system events in the power system of the state of California, it can be concluded that the Out-of-Step protection scheme correctly assessed all voltage angle oscillations as stable or unstable. Correct tripping and/or blocking signals can be sent to the relays in the field using this approach.

Another aspect that has to be evaluated for this protection scheme is how rapid it declares instability for unstable swings. An Out-of-Step condition is declared when the terminal voltage of a machine or group of machines suffers a deviation of 180 degrees with respect to the rest of the power system. In other to evaluate if the proposed protection scheme declares instability before the actual Out-of-Step condition occurs, the concept of center of angles is used again.

$$COA = \frac{\sum_{i=1}^{i=m} Rotor\ Angle_i * S_i}{S_{total}} \tag{6.6}$$

where:

m	Number of machines in the Group
$Rotor\ Angle_i$	Rotor angle of machine i
S_i	MVA rating of machine i
S_{total}	MVA rating of the whole group

One center of angles was calculated for the unstable group of machines and a second one for the remaining set of machines in the system. In the following tables, Table 6-13 and Table 6-14, the time instant when the Out-of-Step protection scheme detected instability for each unstable oscillation is listed. The instant of times when a difference of 100, 120, 150 and 180 degrees occurred between the center of angles of the unstable group of machines and the rest of the system is also presented.

Communication time delays have to be taken into account for this protection scheme. The first table assumes no delay in the communication of phasors in the different levels of the PMU architecture. The second table assumes a communication time delay of 30 milliseconds. The highlighted times in the following tables represent a failure of the protection scheme to detect instability before the two groups of machines reach the specific angle separation.

Analyzing these tables in can be concluded that the protection scheme has a poor performance in the detection of instability at small angle separations, but in most of the cases it can predict instability before the systems reach 180 degrees of angle separation; that is to say, before the Out-of-Step condition occurs.

Table 6-13. Performance - No Time Delay

Case	Group	Prediction	100°	120°	150°	180°
1	Kramer	1.542	1.450	1.550	1.683	1.775
	Haynes	3.942	2.880	3.108	3.800	3.983
	North-South	4.608	4.450	4.592	4.775	4.925
	Vulcan 1	4.808	5.125	5.167	5.217	5.292
	Magunden	5.208	5.225	5.317	5.425	5.508
2	Kramer	3.408	2.925	3.100	3.317	3.450
	Vulcan 1	4.542	4.625	4.700	4.775	4.842
	Mnt. View	6.842	6.670	6.758	6.867	6.950
	Haynes	8.108	7.767	8.108	8.608	8.783
3	Kramer	7.308	7.233	7.333	7.433	7.500
	Vulcan 1	7.308	7.358	7.442	7.542	7.608
4	Kramer	1.508	1.358	1.417	1.500	1.567
	Vulcan 1	3.742	3.492	3.708	3.908	4.033
5	Diablo	1.508	1.375	1.458	1.567	1.650
	Morrobay	1.742	1.558	1.667	1.800	1.892
6	Kramer	1.508	1.375	1.442	1.542	1.617
	Vulcan 1	3.375	3.467	3.558	3.700	3.808
	Mnt. View	3.475	3.500	3.583	3.683	3.750
	Haynes	5.808	5.758	5.867	5.992	6.083
7	Kramer	3.675	2.975	3.158	3.317	3.400
	Vulcan 1	4.642	6.475	6.517	6.575	6.625
	Mnt. View	4.908	4.758	4.900	5.125	5.283
	Haynes	5.742	5.892	5.992	6.200	6.342
	Magunden	5.742	4.867	5.008	5.250	5.942
8	Kramer	1.575	1.567	1.658	1.775	1.850
	Mnt. View	2.208	2.242	2.333	2.425	2.500
	Vulcan 1	2.342	2.283	2.400	2.525	2.608

Table 6-14. Performance - 30 ms Delay

Case	Group	Prediction	100°	120°	150°	180°
1	Kramer	1.542	1.450	1.550	1.683	1.775
	Haynes	3.942	2.880	3.108	3.800	3.983
	North-South	4.608	4.450	4.592	4.775	4.925
	Vulcan 1	4.808	5.125	5.167	5.217	5.292
	Magunden	5.208	5.225	5.317	5.425	5.508
2	Kramer	3.408	2.925	3.100	3.317	3.450
	Vulcan 1	4.542	4.625	4.700	4.775	4.842
	Mnt. View	6.842	6.670	6.758	6.867	6.950
	Haynes	8.108	7.767	8.108	8.608	8.783
3	Kramer	7.308	7.233	7.333	7.433	7.500
	Vulcan 1	7.308	7.358	7.442	7.542	7.608
4	Kramer	1.508	1.358	1.417	1.500	1.567
	Vulcan 1	3.742	3.492	3.708	3.908	4.033
5	Diablo	1.508	1.375	1.458	1.567	1.650
	Morrobay	1.742	1.558	1.667	1.800	1.892
6	Kramer	1.508	1.375	1.442	1.542	1.617
	Vulcan 1	3.375	3.467	3.558	3.700	3.808
	Mnt. View	3.475	3.500	3.583	3.683	3.750
	Haynes	5.808	5.758	5.867	5.992	6.083
7	Kramer	3.675	2.975	3.158	3.317	3.400
	Vulcan 1	4.642	6.475	6.517	6.575	6.625
	Mnt. View	4.908	4.758	4.900	5.125	5.283
	Haynes	5.742	5.892	5.992	6.200	6.342
	Magunden	5.742	4.867	5.008	5.250	5.942
8	Kramer	1.575	1.567	1.658	1.775	1.850
	Mnt. View	2.208	2.242	2.333	2.425	2.500
	Vulcan 1	2.342	2.283	2.400	2.525	2.608

Assuming a 30 millisecond delay and establishing as satisfactory if the relay predicted instability before the groups of machines reached a separation of 150 degrees; the relay reacted properly in 21 out of 27 unstable power swings; this is a 77.78 percent efficiency.

EEAC in the California System

The Extended Equal Area Criterion in the time domain approach was also investigated for the California System. For this assessment, the first unstable group for each case was selected as the critical cluster of machines and the rest of the system as the remaining set of generating units. The two-machine and OMIB equivalents were created as discussed in Chapter 3.

Figure 6-48 shows the equivalent delta for the OMIB system for case number one. It can be seen that the system follows a first swing instability.

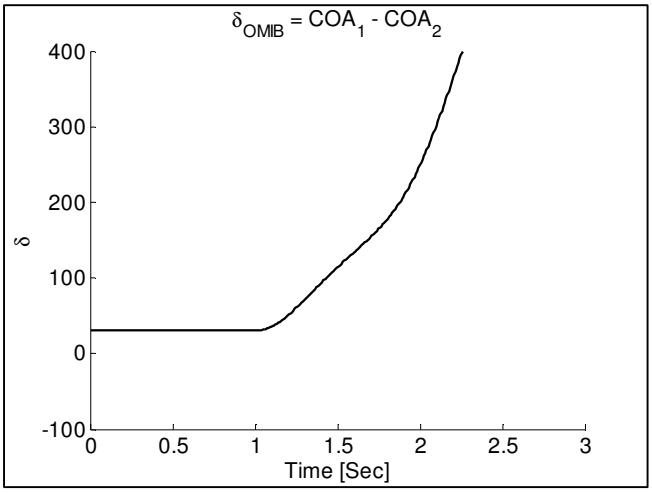

Figure 6-48. Delta Case 1

Figure 6-49 illustrates the accelerating and decelerating areas for this case. The accelerating area was divided into two sub-areas, A_1 and A_2. The former corresponding to the kinetic energy gained during the fault and the latter equal to the kinetic energy gained due to the change of topology in the system when the fault was extinguished. In this case $A_1 = 262$, $A_2 = 50$ and $A_3 = 50$. The total accelerating energy is equal to 312 and the total decelerating energy is 50. The EEAC correctly assessed the stability for this case.

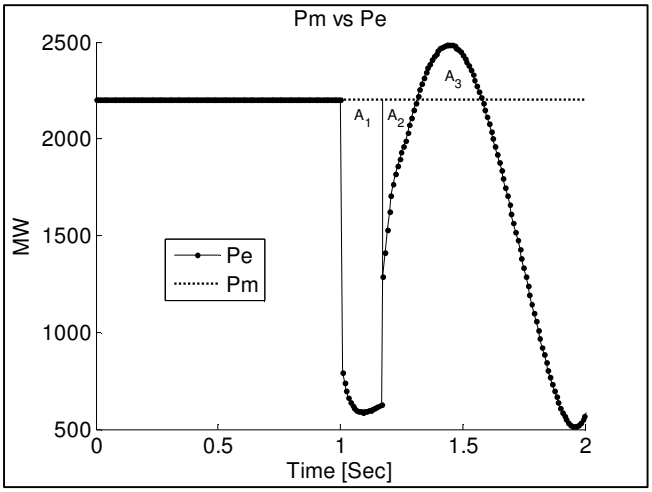

Figure 6-49. EEAC Assessment - Case 1

Figure 6-50 shows the equivalent delta for the OMIB system for the case number two. It can be seen that the system follows a third swing instability behavior. The EEAC method was also tested under this case in order to find out if it correctly identifies this event as unstable.

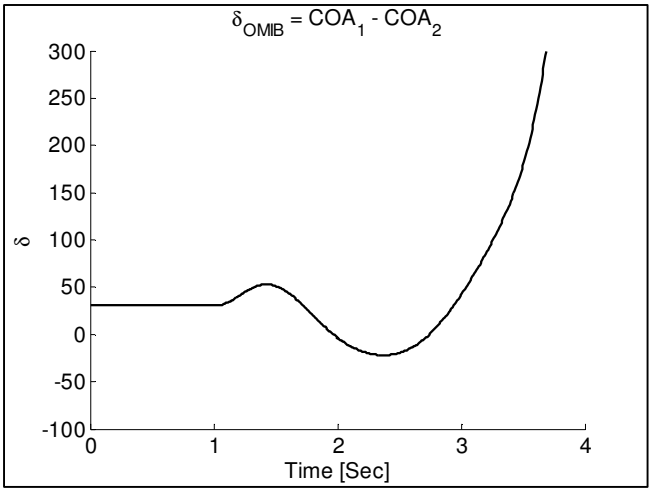

Figure 6-50. Delta Case 2

Figure 6-51 illustrates the accelerating and decelerating areas for this case. Area two has a much larger value than area one; $A_1 = 142$ and $A_2 = 284$. EEAC fails to assess this case correctly as unstable. The reason why the EEAC does not provide a correct assessment is because this method can only handle events in which generators go unstable at the first swing of oscillation; as mentioned in Chapter 3. The third swing instability behavior in this event makes EEAC unsuccessful.

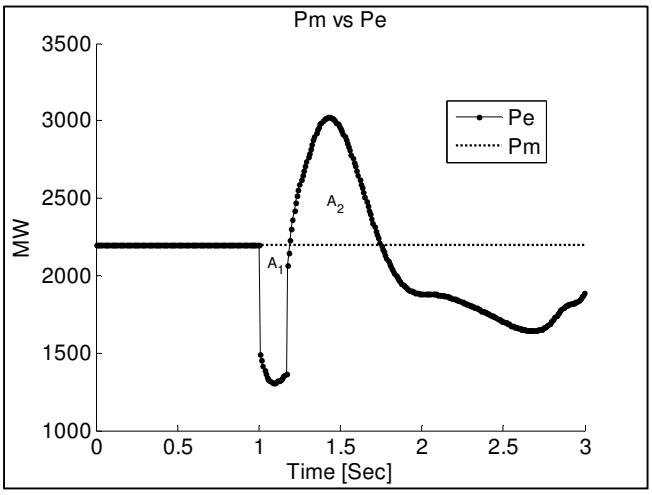

Figure 6-51. EEAC Assessment - Case 2

Even though EEAC provided a good assessment for the first case, its implementation as the one proposed by [33] is not possible since the accelerating energy gained during the fault, neglected in this reference, accounts for the majority of the kinetic energy gained in this system event.

Chapter 7 Conclusions and Future Work

The research work presented in this dissertation attempts to provide an alternative approach to handle transient stability of interconnected power systems. It is known that after the system has been subjected to a large disturbance, its behavior cannot be linearized and it is difficult to predict whether or not it will be able to reach a stable operating point. The reduced amount of time protection and control systems have available to react, makes this kind of stability assessment difficult to accomplish.

The Out-of-Step protection scheme that is presented in this dissertation proved to correctly assess the stability of power systems after large perturbations. This device was tested under different scenarios and did not operate for any of the stable swings or stable cases. It also predicted the behavior of unstable power swings, and it was shown that in 77 percent of the cases the protection scheme was able to forecast pole slipping before this condition actually occurs.

7.1 Conclusions

The main conclusions obtained from this research effort are listed in this section.

1 Proved that voltage angles measurements taken from network buses can provide information regarding the oscillation of rotor angles.

2 Showed that there is no need to place a PMU on every generation bus to correctly assess the transient stability of the whole system; as proposed by many authors.

3 Developed an autoregressive model of order three with a differentiation process of order one ARI(3,1), to predict angle oscillations. This model proved to have the best forecasting performance among all tested models.

4 Demonstrated that a difference of 150 degrees, between each voltage angle and its respective center of angles, in two consecutive predictions is an effective trigger for detecting unstable swings.

5 Developed an Out-of-Step protection scheme that can accurately predict stability of power systems; and in most of the cases it can do it before the system reaches 180 degrees of angle separation.

6 Demonstrated that the proposed protection scheme algorithm is independent of the type of perturbation applied to the power grid. System faults, line trippings and generation drops can be treated equally using this technique.

7.2 Future Work

As mentioned in Chapter 5, a PMU reporting rate of 30 samples per second is assumed. Even though PMU devices can transmit data at higher sampling rates, this option is not fully exploited due to the high communication bandwidth it requires. Most probably, future improvements in the PMU technology will make feasible the use of a higher reporting rate in the transmission of synchrophasors. The accuracy of the time series models, in the prediction of voltage angles, would be highly improved if a reporting rate of 60, or even more, messages per second is assumed. As a consequence of this increment, the detection of unstable swings is expected to be faster as well, improving the performance of the Out-of-Step protection scheme. It is suggested that reporting rates of 60 and 120 messages per second be tested for this technique.

The tripping decision, centered in the computation of center of angles, was set to 150 degrees of separation for this algorithm. A threshold value of 120 degrees was also tested and proved to be faster in some occasions; the downside is that the protection scheme mis-operated for some stable cases. Future research could be carried out, for a giving protection system, using different values for the angle separation threshold. In some cases providing a faster decision will be better than mis-operating for stable cases.

This dissertation assumed that the protection scheme had a continuous input from all PMU units installed in the field. It is well known though, that communication dropouts

occur in the transmission of synchropahsors. A study of the impact of loss of phasors, in this Out-of-Step protection scheme, is encouraged.

7.3 Main Contribution

The main contribution of this research effort to the power systems protection theory, in particular to the Out-of-Step condition, is an effective methodology for identification of multiple unstable swings after a given disturbance. The current protection philosophy for Out-of-Step relays is limited to the identification of two asynchronous groups using a first swing stability assessment approach. The identification of more than two asynchronous groups of machines after the first swing of oscillation is an important contribution to the power systems field.

References

1. Dobson, I., et al. *Examining criticality of blackouts in power system models with cascading events*. in *System Sciences, 2002. HICSS. Proceedings of the 35th Annual Hawaii International Conference on*. 2002.
2. Kundur, P., N.J. Balu, and M.G. Lauby, *Power system stability and control*. 1994, New York: McGraw-Hill. xxiii, 1176.
3. Novosel, D., et al., *IEEE PSRC Report on Performance of Relaying During Wide-Area Stressed Conditions.* Power Delivery, IEEE Transactions on, 2010. **25**(1): p. 3-16.
4. Anderson, P.M., A.A. Fouad, and Institute of Electrical and Electronics Engineers., *Power system control and stability*. 2nd ed. 2003, Piscataway, N.J.: IEEE Press ; Wiley-Interscience. xiv, 658.
5. Fouad, A.A. and V. Vittal, *Power system transient stability analysis using the transient energy function method*. 1992, Englewood Cliffs, N.J.: Prentice Hall. xviii, 357.
6. Horowitz, S.H. and A.G. Phadke, *Power system relaying*. 2nd ed. 1995, Taunton, Somerset, England, New York: Research Studies Press ; Wiley. xiv, 319.
7. IEEE-PSRC, *POWER SWING AND OUT-OF-STEP CONSIDERATIONS ON TRANSMISSION LINES*. 2005.
8. Centeno, V., et al., *Adaptive out-of-step relaying using phasor measurement techniques.* Computer Applications in Power, IEEE, 1993. **6**(4): p. 12-17.
9. Niglye, N., et al. *Considerations for the Application of Synchrophasors to Predict Voltage Instability*. in *Power Systems Conference: Advanced Metering, Protection, Control, Communication, and Distributed Resources, 2006. PS '06*. 2006.
10. Phadke, A.G., J.S. Thorp, and M.G. Adamiak, *A New Measurement Technique for Tracking Voltage Phasors, Local System Frequency, and Rate of Change of Frequency.* Power Apparatus and Systems, IEEE Transactions on, 1983. **PAS-102**(5): p. 1025-1038.
11. NERC, *Real-Time Application of Synchrophasors for Improving Reliability*. 2010.
12. Bhargava, B. and A. Salazar. *Use of Synchronized Phasor Measurement system for monitoring power system stability and system dynamics in real-time*. in *Power and Energy Society General Meeting - Conversion and Delivery of Electrical Energy in the 21st Century, 2008 IEEE*. 2008.

13. Chunyan, L., et al. *An on-line transient stability emergency control strategy based on PMU forecasted trajectory*. in *Power Engineering Conference, 2007. IPEC 2007. International*. 2007.

14. Stanton, S.E., et al., *Application of phasor measurements and partial energy analysis in stabilizing large disturbances.* Power Systems, IEEE Transactions on, 1995. **10**(1): p. 297-306.

15. Yi-Jen, W., et al. *A remedial control scheme protects against transient instabilities based on phasor measurement units (PMUs)-a case study*. in *Power Engineering Society Summer Meeting, 2000. IEEE*. 2000.

16. Blackburn, J.L., *Protective relaying : principles and applications*. 1987, New York: M. Dekker. xiii, 545.

17. Taylor, C.W., et al., *A New Out-of-Step Relay with Rate of Change of Apparent Resistance Augmentation.* Power Apparatus and Systems, IEEE Transactions on, 1983. **PAS-102**(3): p. 631-639.

18. Haner, J.M., T.D. Laughlin, and C.W. Taylor, *Experience with the R-RDOT out-of-Step Relay.* Power Delivery, IEEE Transactions on, 1986. **1**(2): p. 35-39.

19. Ohura, Y., et al., *A predictive out-of-step protection system based on observation of the phase difference between substations.* Power Delivery, IEEE Transactions on, 1990. **5**(4): p. 1695-1704.

20. Centeno, V., A.G. Phadke, and A. Edris. *Adaptive out-of-step relay with phasor measurement*. in *Developments in Power System Protection, Sixth International Conference on (Conf. Publ. No. 434)*. 1997.

21. Centeno, V., et al., *An Adaptive Out-of-Step Relay.* Power Engineering Review, IEEE, 1997. **17**(1): p. 39-40.

22. Kimbark, E.W., *Power system stability*. 1995, New York: IEEE Press.

23. Monchusi, B.B., et al. *PMU based power system stability analysis*. in *TENCON 2008 - 2008 IEEE Region 10 Conference*. 2008.

24. Paudyal, S., G. Ramakrishna, and M.S. Sachdev. *Out-of-step protection using the equal area criterion in time domain - SMIB and 3-machine case studies*. in *TENCON 2008 - 2008 IEEE Region 10 Conference*. 2008.

25. Schweitzer, E., Newton T., Baker, R. *Power Swing Relay Also Records Disturbances*. in *Georgia Tech Protective Relaying Conference*. 1987. Atlanta, Ga.

26. So, K.H., et al., *Out-of-step detection algorithm using frequency deviation of voltage.* Generation, Transmission & Distribution, IET, 2007. **1**(1): p. 119-126.

27. Benmouyal, G., Tziouvaras D., Hou,D. *Zero-Setting Power Swing Blocking Protection*. in *31 Annual Western Protective Relay Conference*. 2003. Spokane, WA.

28. Rovnyak, S., et al., *Decision trees for real-time transient stability prediction.* Power Systems, IEEE Transactions on, 1994. **9**(3): p. 1417-1426.

29. Marpaka, D.R., M.H. Thursby, and S.M. Aghili. *Artificial neural net based stability study of power systems*. in *Southeastcon '91., IEEE Proceedings of*. 1991.

30. Llamas, A. and J. De La Ree. *Stability and the transient energy method for the classroom*. in *System Theory, 1993. Proceedings SSST '93., Twenty-Fifth Southeastern Symposium on*. 1993.

31. Pai, M.A., *Energy function analysis for power system stability*. 1989, Boston: Kluwer Academic Publishers. viii, 240.

32. Llamas, A., et al., *Clarifications of the BCU method for transient stability analysis.* Power Systems, IEEE Transactions on, 1995. **10**(1): p. 210-219.

33. Centeno, V.A., *Adaptive out-of-step relaying with phasor measurement*. 1995, Virginia Polytechnic Institute and State University. p. xv, 205 leaves.

34. Grainger, J.J. and W.D. Stevenson, *Power system analysis*. 1994, New York: McGraw-Hill. xix, 787.

35. Pavella, M. and P.G. Murthy, *Transient stability of power systems : theory and practice*. 1994, Chichester ; New York: Wiley. xvi, 403.

36. Xue, Y., T. Van Cutsem, and M. Ribbens-Pavella, *A simple direct method for fast transient stability assessment of large power systems.* Power Systems, IEEE Transactions on, 1988. **3**(2): p. 400-412.

37. Xue, Y., T. Van Custem, and M. Ribbens-Pavella, *Extended equal area criterion justifications, generalizations, applications.* Power Systems, IEEE Transactions on, 1989. **4**(1): p. 44-52.

38. Botterud, A., et al., *Wind Power Forecasting in U.S. Electricity Markets.* The Electricity Journal, 2010. **23**(3): p. 71-82.

39. ERCOT, *ERCOT OPERATIONS REPORT ON THE EVENT OF FEBRUARY 26, 2008*.

40. NERC, *March 13, 1989 Geomagnetic Disturbance*.

41. Lehtinen, M., and Pirjola, R., *Currents produced in earthed conductor networks by geomagnetically-induced electric fields.* Annales Geophysicae, 1985. **3**: p. 479-484.

42. Box, G.E.P. and G.M. Jenkins, *Time series analysis; forecasting and control*. 1970, San Francisco,: Holden-Day. xix, 553.

43. Hoff, J.C., *A practical guide to Box-Jenkins forecasting*. 1983, Belmont, Calif.: Lifetime Learning Publications. xii, 316.

44. Sung-Kwan, J., et al., *Coherency and aggregation techniques incorporating rotor and voltage dynamics.* Power Systems, IEEE Transactions on, 2004. **19**(2): p. 1068-1075.

45. Wang, L., et al., *Dynamic reduction of large power systems for stability studies.* Power Systems, IEEE Transactions on, 1997. **12**(2): p. 889-895.

46. Fan, D., *Synchronized measurements and applications during power system dynamics*. 2008, Blacksburg, Va.: University Libraries Virginia Polytechnic Institute and State University.

47. Athay, T., R. Podmore, and S. Virmani, *A Practical Method for the Direct Analysis of Transient Stability.* Power Apparatus and Systems, IEEE Transactions on, 1979. **PAS-98**(2): p. 573-584.

48. Phadke, A.G., et al. *Recent developments in state estimation with phasor measurements*. in *Power Systems Conference and Exposition, 2009. PSCE '09. IEEE/PES*. 2009.

49. Phadke, A.G. and J.S. Thorp, *Synchronized phasor measurements and their applications*. 2008, New York: Springer. x, 247.

50. *IEEE Standard for Synchrophasors for Power Systems.* IEEE Std C37.118-2005 (Revision of IEEE Std 1344-1995), 2006: p. 0_1-57.

51. Tavora, C.J. and O.J.M. Smith, *Characterization of Equilibrium and Stability in Power Systems.* Power Apparatus and Systems, IEEE Transactions on, 1972. **PAS-91**(3): p. 1127-1130.

52. FitzPatrick, J., *NIST Interoperability Standards Update Part 2: Testing and Verification of Interoperability*, in *NASPI*. 2010: Arlington, Virginia.

53. University_of_Washington. *17 Generator (with 162 bus power flow case)*. [cited 2010 October 27]; Available from: http://www.ee.washington.edu/research/pstca/.

54. Bernabeu, E.E., *Methodology for a security-dependability adaptive protection scheme based on data mining*. 2009, Blacksburg, Va.: University Libraries Virginia Polytechnic Institute and State University.

Appendix A 10 Machine System

Table A-1lists the machine parameters.

Table A-2 presents the bus data.

Table A-3 lists the branch data.

Table A-1. Machine Model Data

Machine	Bus	H	X'd
10	30	42.0	0.0310
2	31	30.3	0.0697
3	32	35.8	0.0531
4	33	28.6	0.0436
5	34	26.0	0.1320
6	35	34.8	0.0500
7	36	26.4	0.0490
8	37	24.3	0.0570
9	38	34.5	0.0570
1	39	500.0	0.0060

Base= 100 MVA

Table A-2. Bus Data

Bus	Type	Volt P.U.	Volt Angle	Load MW	Load MVAr	Gen MW	Gen MVAr
1	0	1.036	-8.66	-	-	-	-
2	0	1.0193	-5.74	-	-	-	-
3	0	0.9914	-8.72	322	2.4	-	-
4	0	0.9551	-9.76	500	184	-	-
5	0	0.9543	-8.63	-	-	-	-
6	0	0.9555	-7.89	-	-	-	-
7	0	0.9475	-10.31	233.8	84	-	-
8	0	0.9481	-10.86	522	176	-	-
9	0	1.0085	-10.61	-	-	-	-
10	0	0.9621	-5.08	-	-	-	-
11	0	0.9585	-6.03	-	-	-	-
12	0	0.939	-5.99	7.5	88	-	-
13	0	0.9604	-5.84	-	-	-	-
14	0	0.961	-7.6	-	-	-	-
15	0	0.969	-7.74	320	153	-	-
16	0	0.9882	-6.07	329	32.3	-	-
17	0	0.9923	-7.3	-	-	-	-
18	0	0.9905	-8.31	158	30	-	-
19	0	0.9898	-0.27	-	-	-	-
20	0	0.987	-1.26	628	103	-	-
21	0	0.9951	-3.5	274	115	-	-
22	0	1.0215	1.21	-	-	-	-
23	0	1.0202	0.98	247.5	84.6	-	-
24	0	0.9965	-5.95	308.6	-92.2	-	-
25	0	1.0282	-4.25	224	47.2	-	-
26	0	1.0176	-5.45	139	17	-	-
27	0	0.9998	-7.54	281	75.5	-	-
28	0	1.0191	-1.73	206	27.6	-	-
29	0	1.0206	1.19	283.5	26.9	-	-
30	1	1.0475	-3.31	-	-	250	168.5
31	2	0.982	0	9.2	4.6	524.4	144.3
32	1	0.9831	2.82	-	-	650	148.1
33	1	0.9972	4.93	-	-	632	49.4
34	1	1.0123	3.92	-	-	508	139.3
35	1	1.0493	6.18	-	-	650	232.3
36	1	1.0635	9	-	-	560	198.1
37	1	1.0278	2.55	-	-	540	16.2
38	1	1.0265	8.27	-	-	830	47.7
39	1	1.03	-10.35	1104	250	1000	216.7

Type: 0 = P-Q
1 = P-V
2 = Swing

Table A-3. Line Data

From	To	R (p.u.)	X (p.u.)	B (p.u.)
1	2	0.0035	0.0411	0.6987
1	39	0.001	0.025	0.75
2	3	0.0013	0.0151	0.2572
2	25	0.007	0.0086	0.146
2	30	0.0	0.0181	0.0
3	4	0.0013	0.0213	0.2214
3	18	0.0011	0.0133	0.2138
4	5	0.0008	0.0128	0.1342
4	14	0.0008	0.0129	0.1382
5	6	0.0002	0.0026	0.0434
5	8	0.0008	0.0112	0.1476
6	7	0.0006	0.0092	0.113
6	11	0.0007	0.0082	0.1389
6	31	0.0	0.025	0.0
7	8	0.0004	0.0046	0.078
8	9	0.0023	0.0363	0.3804
9	39	0.001	0.025	1.2
10	11	0.0004	0.0043	0.0729
10	13	0.0004	0.0043	0.0729
10	32	0.0	0.02	0.0
12	11	0.0016	0.0435	0.0
12	13	0.0016	0.0435	0.0
13	14	0.0009	0.0101	0.1723
14	15	0.0018	0.0217	0.366
15	16	0.0009	0.0094	0.171
16	17	0.0007	0.0089	0.1342
16	19	0.0016	0.0195	0.304
16	21	0.0008	0.0135	0.2548
16	24	0.0003	0.0059	0.068
17	18	0.0007	0.0082	0.1319
17	27	0.0013	0.0173	0.3216
19	20	0.0007	0.0138	0.0
19	33	0.0007	0.0142	0.0
20	34	0.0009	0.018	0.0
21	22	0.0008	0.014	0.2565
22	23	0.0006	0.0096	0.1846
22	35	0.0	0.0143	0.0
23	24	0.0022	0.035	0.361
23	36	0.0005	0.0272	0.0
25	26	0.0032	0.0323	0.513
25	37	0.0006	0.0232	0.0
26	27	0.0014	0.0147	0.2396
26	28	0.0043	0.0474	0.7802
26	29	0.0057	0.0625	1.029
28	29	0.0014	0.0151	0.249

Appendix B 17 machine System

Table B-1 lists the machine parameters.

Table B-2 and Table B-3 presents the bus information.

Table B-4, Table B-5 and Table B-6 list the branch data.

Table B-1. Machine Model Data

Machine	Bus	H	X'd
1	3	100.00	0.0040
2	6	34.56	0.0437
3	15	80.00	0.0100
4	27	80.00	0.0500
5	73	16.79	0.0507
6	76	32.49	0.0206
7	99	6.65	0.1131
8	101	2.66	0.3115
9	108	29.60	0.0535
10	114	5.00	0.1770
11	118	11.31	0.1049
12	121	19.79	0.0297
13	124	200.00	0.0020
14	125	200.00	0.0020
15	126	100.00	0.0040
16	130	28.60	0.0559
17	131	20.66	0.0544

Base= 100 MVA

Table B-2. Bus Data 1of 2

Bus	Type	Volt P.U.	Volt Angle	Load MW	Load MVAr	Gen MW	Gen MVAr
1	0	1.0244	-25.45	-	-	-	-
2	0	1.0135	-30.22	-	-	-	-
3	1	0.9891	-32.73	2370.00	96.90	2000.00	0.00
4	0	1.0107	-33.96	-	-	-	-
5	0	1.0217	-24.58	-	-	-	-
6	1	1.0000	-19.53	-	-	794.00	-142.30
7	0	1.0089	-30.59	-	-	-	-
8	0	1.0015	-34.21	398.00	19.20	-	-
9	0	1.0126	-27.90	-	-	-	-
10	0	0.9952	-36.14	226.00	-11.50	-	-
11	0	1.0008	-32.26	-	-	-	-
12	0	1.0061	-33.96	193.00	-5.90	-	-
13	0	1.0053	-31.00	204.00	37.30	-	-
14	0	1.0010	-31.32	381.00	56.30	-	-
15	1	1.0165	-24.89	1420.00	0.00	1500.00	0.00
16	0	1.0067	-29.77	-54.20	26.70	-	-
17	0	1.0014	-28.95	-116.50	44.70	-	-
18	0	1.0076	-33.79	34.40	11.67	-	-
19	0	0.9839	-38.28	64.40	3.78	-	-
20	0	1.0015	-32.99	37.90	12.50	-	-
21	0	0.9900	-30.35	-69.80	23.20	-	-
22	0	0.9979	-37.58	17.39	5.27	-	-
23	0	0.9825	-35.21	63.50	21.40	-	-
24	0	0.9997	-33.57	-	-	-	-
25	0	1.0032	-29.66	-	-	-	-
26	0	1.0164	-21.48	-	-	-	-
27	1	1.0008	-30.72	1824.00	57.90	1500.00	0.00
28	0	0.9920	-36.64	38.47	13.17	-	-
29	0	1.0000	-38.49	28.31	9.03	-	-
30	0	0.9986	-40.32	101.20	32.52	-	-
31	0	0.9987	-37.50	72.50	-3.10	-	-
32	0	1.0046	-41.67	52.70	15.06	-	-
33	0	0.9993	-43.68	45.17	15.16	-	-
34	0	0.9888	-43.62	14.18	5.25	-	-
35	0	0.9899	-45.12	54.48	14.63	-	-
36	0	0.9932	-43.78	31.96	8.68	-	-
37	0	1.0178	-30.96	-	-	-	-
38	0	0.9886	-38.24	14.76	4.08	-	-
39	0	1.0120	-33.45	-	-	-	-
40	0	0.9865	-42.58	52.88	17.60	-	-
41	0	0.9872	-40.58	39.20	12.80	-	-
42	0	1.0094	-33.13	-	-	-	-
43	0	0.9980	-35.86	41.50	-17.20	-	-
44	0	0.9920	-36.40	16.32	3.71	-	-
45	0	0.9880	-36.57	20.02	5.41	-	-
46	0	1.0011	-39.49	65.31	22.30	-	-
47	0	0.9940	-42.34	4.82	1.56	-	-
48	0	0.9963	-41.20	33.76	-7.11	-	-
49	0	0.9927	-42.68	6.82	1.78	-	-
50	0	0.9932	-40.05	99.70	-23.40	-	-
51	0	0.9969	-38.96	-	-	-	-
52	0	0.9894	-39.65	218.20	42.80	-	-
53	0	0.9951	-31.10	-	-	-	-
54	0	0.9828	-38.31	70.34	20.57	-	-
55	0	0.9951	-30.80	-	-	-	-
56	0	0.9839	-40.99	25.29	7.26	-	-
57	0	0.9886	-37.96	48.48	-4.39	-	-
58	0	1.0104	-29.10	-	-	-	-
59	0	0.9882	-33.43	84.43	27.05	-	-
60	0	0.9804	-34.35	244.00	26.00	-	-
61	0	0.9912	-31.83	-	-	-	-
62	0	1.0229	-18.83	-865.60	-70.80	-	-
63	0	0.9941	-30.16	59.10	-2.90	-	-
64	0	1.0159	-29.30	-	-	-	-
65	0	0.9968	-25.70	-26.30	116.00	-	-
66	0	1.0015	-31.54	-	-	-	-
67	0	0.9908	-42.27	22.54	7.03	-	-
68	0	0.9957	-40.67	40.42	12.68	-	-
69	0	0.9999	-39.29	-	-	-	-
70	0	1.0077	-23.67	-	-	-	-
71	0	0.9847	-32.32	29.87	11.93	-	-
72	0	0.9991	-31.06	427.00	110.00	-	-
73	1	1.0000	-18.66	-	-	447.00	-19.30
74	0	1.0075	-33.79	-	-	-	-
75	0	1.0130	-25.50	-	-	-	-
76	1	1.0000	-16.60	-	-	1055.00	-155.50
77	0	0.9938	-40.95	26.41	8.88	-	-
78	0	1.0009	-38.56	79.12	0.00	-	-
79	0	1.0065	-36.41	-	-	-	-
80	0	0.9940	-38.74	15.76	5.25	-	-
81	0	1.0223	-47.06	50.88	16.80	-	-
82	0	0.9856	-42.55	62.28	20.26	-	-
83	0	0.9877	-41.59	-	-	-	-
84	0	0.9836	-38.04	37.90	9.49	-	-
85	0	0.9806	-41.93	40.52	11.36	-	-
86	0	0.9861	-45.92	50.73	13.35	-	-
87	0	0.9886	-44.31	16.91	4.23	-	-
88	0	0.9784	-45.52	60.60	4.44	-	-
89	0	0.9939	-47.10	-	-	-	-
90	0	0.9888	-50.39	50.21	16.76	-	-
91	0	0.9869	-36.73	51.24	12.83	-	-
92	0	0.9811	-37.76	36.12	9.05	-	-
93	0	0.9954	-32.61	103.80	34.56	-	-
94	0	1.0021	-37.11	164.00	6.49	-	-
95	0	0.9866	-36.75	117.20	39.01	-	-
96	0	0.9834	-45.88	119.20	0.00	-	-
97	0	0.9852	-37.50	22.84	5.71	-	-
98	0	0.9898	-35.38	151.10	20.35	-	-
99	1	1.0000	-31.54	-	-	130.90	25.50
100	0	0.9818	-46.80	23.21	6.90	-	-

Table B-3. Bus Data 2 of 2

Bus	Type	Volt P.U.	Volt Angle	Load MW	Load MVAr	Gen MW	Gen MVAr
101	1	1.0000	-40.95	-	-	82.00	19.70
102	0	0.9853	-37.27	16.54	4.08	-	-
103	0	1.0024	-34.89	322.00	-45.80	-	-
104	0	0.9845	-45.36	31.52	10.56	-	-
105	0	0.9784	-38.79	24.84	6.23	-	-
106	0	0.9776	-43.64	-	-	-	-
107	0	0.9732	-44.53	35.41	5.41	-	-
108	2	1.0000	-27.69	-	-	553.80	53.50
109	0	1.0101	-33.20	-	-	-	-
110	0	1.0113	-29.75	-	-	-	-
111	0	0.9891	-34.26	65.41	16.72	-	-
112	0	1.0171	-27.15	-	-	-	-
113	0	1.0073	-31.23	32.70	-95.20	-	-
114	1	1.0000	-24.04	-	-	131.00	-8.20
115	0	1.0021	-36.33	17.32	3.34	-	-
116	0	0.9974	-37.53	56.08	11.20	-	-
117	0	0.9930	-38.27	101.90	20.06	-	-
118	1	1.0000	-34.44	-	-	173.00	28.30
119	0	1.0052	-35.49	-	-	-	-
120	0	1.0124	-27.50	-	-	-	-
121	1	1.0000	-20.50	-	-	620.00	-54.00
122	0	0.9731	-46.55	47.28	9.36	-	-
123	0	0.9834	-46.88	165.00	-54.67	-	-
124	1	0.9994	-31.14	2000.00	90.90	2571.00	0.00
125	1	1.0000	-29.37	2000.00	0.00	2388.00	-76.60
126	1	1.0141	-26.93	2000.00	0.00	2467.00	0.00
127	0	1.0049	-29.91	-52.60	65.00	-	-
128	0	1.0098	-27.40	-	-	-	-
129	0	1.0118	-27.63	-	-	-	-
130	1	1.0000	-19.25	-	-	455.00	-36.40
131	1	1.0000	-20.48	-	-	575.00	-149.90
132	0	1.0019	-30.62	159.00	36.10	-	-
133	0	1.0010	-32.45	30.10	6.02	-	-
134	0	1.0066	-31.14	17.46	3.34	-	-
135	0	0.9997	-32.52	20.06	4.01	-	-
136	0	0.9956	-32.84	20.06	4.01	-	-
137	0	0.9981	-32.78	20.06	4.01	-	-
138	0	1.0082	-31.63	-	-	-	-
139	0	0.9999	-32.40	10.10	2.01	-	-
140	0	0.9987	-32.71	13.58	2.68	-	-
141	0	0.9984	-34.47	-	-	-	-
142	0	1.0010	-41.22	27.09	5.35	-	-
143	0	0.9966	-40.39	21.07	4.01	-	-
144	0	1.0008	-36.75	12.37	2.01	-	-
145	0	0.9964	-34.91	10.83	2.21	-	-
146	0	1.0028	-40.83	21.33	4.01	-	-
147	0	0.9869	-39.33	216.40	42.80	-	-
148	0	0.9862	-40.40	120.00	24.00	-	-
149	0	1.0077	-23.85	-	-	-	-
150	0	1.0060	-24.54	4.80	1.60	-	-
151	0	0.9981	-26.94	24.00	8.00	-	-
152	0	1.0053	-26.96	6.00	-2.80	-	-
153	0	1.0141	-25.99	4.00	1.60	-	-
154	0	1.0209	-32.89	28.00	9.60	-	-
155	0	1.0114	-30.84	12.00	4.00	-	-
156	0	1.0180	-32.45	8.00	2.40	-	-
157	0	1.0049	-32.89	32.00	10.40	-	-
158	0	1.0203	-34.23	16.00	5.60	-	-
159	0	1.0264	-34.20	8.00	2.40	-	-
160	0	1.0273	-33.64	14.40	4.80	-	-
161	0	0.9955	-28.40	32.00	10.40	-	-
162	0	0.9944	-29.32	20.00	6.40	-	-

Type: 0 = P-Q
1 = P-V
2 = Swing

Table B-4. Line Data 1 of 3

From	To	R (p.u.)	X (p.u.)	B (p.u.)	From	To	R (p.u.)	X (p.u.)	B (p.u.)
1	2	0.0035	0.0321	0.5438	16	18	0.0297	0.1070	0.0546
1	3	0.0034	0.0326	0.7224	16	27	0.1574	0.8871	0.0000
1	4	0.0064	0.0621	0.9870	16	126	0.1053	0.5132	0.0000
1	5	0.0011	0.0119	0.2012	16	127	0.0958	0.5276	0.0000
1	6	0.0000	0.0133	0.0000	17	18	0.0213	0.1013	0.0642
2	7	0.0014	0.0125	0.2122	17	19	0.2314	0.7678	0.0000
2	13	0.0046	0.0417	0.7058	17	21	0.0471	0.2665	0.0000
3	14	0.2361	1.0122	0.0000	17	127	0.0287	0.2637	0.0000
3	50	0.0389	0.1699	0.0000	18	30	0.0207	0.1088	0.0520
3	103	0.1074	1.8023	0.0000	18	32	0.0234	0.1220	0.0582
3	123	0.2883	1.6719	0.0000	18	37	0.0000	0.0456	0.0000
3	124	0.0140	0.6483	0.0000	19	21	0.3867	1.9005	0.0000
3	125	0.0084	0.1139	0.0000	19	38	0.0239	0.1250	0.0596
4	112	0.0059	0.0568	0.9250	19	43	0.0603	0.2572	0.0000
4	115	0.0000	0.0185	0.0000	19	127	0.1074	0.6809	0.0000
4	119	0.0014	0.0119	0.2050	20	53	0.0000	0.1140	0.0000
5	120	0.0022	0.0224	0.3792	20	157	0.0113	0.0279	0.0004
5	129	0.0022	0.0268	0.4612	21	22	0.0312	0.1629	0.0778
5	131	0.0000	0.0127	0.0000	21	127	0.0105	0.6414	0.0000
7	8	0.0004	0.0189	0.0000	22	38	0.0140	0.0540	0.0250
7	9	0.0017	0.0169	0.2872	22	39	0.0000	0.0493	0.0000
8	10	0.4591	1.0703	0.0000	22	40	0.0188	0.0717	0.0328
8	12	0.0106	0.0574	0.0000	22	41	0.0172	0.0850	0.0404
8	13	0.1274	0.4784	0.0000	23	24	0.0174	0.0511	0.0230
8	14	0.0473	0.3956	0.0000	23	60	0.0660	0.3093	0.0000
8	15	0.5035	1.7433	0.0000	24	25	0.0000	0.0340	0.0000
8	132	0.0252	0.2880	0.0000	24	28	0.0249	0.0725	0.0202
9	75	0.0013	0.0150	0.2682	24	45	0.0137	0.0725	0.0340
10	11	0.0051	0.0370	0.0716	25	26	0.0059	0.0583	0.9302
10	13	0.1299	0.6220	0.0000	25	27	0.0044	0.0410	0.8384
10	15	0.1275	0.7033	0.0000	26	74	0.0063	0.0607	0.9300
10	60	0.2525	1.2242	0.0000	26	75	0.0030	0.0322	0.5038
11	15	0.0285	0.1793	0.3484	26	76	0.0000	0.0082	0.0000
11	46	0.0142	0.1225	0.1876	27	31	0.0101	0.1273	0.0000
11	58	0.0170	0.1070	0.2074	27	62	0.0173	0.5810	0.0000
11	59	0.0071	0.0471	0.0852	27	65	0.0105	0.2764	0.0000
2	12	0.0008	0.0377	0.0000	27	125	0.0350	1.6845	0.0000
12	13	0.1038	0.3137	0.0000	27	126	0.0022	0.0225	0.0000
12	14	0.1598	0.6415	0.0000	27	127	0.1506	1.4355	0.0000
12	132	0.4486	1.5773	0.0000	28	29	0.0240	0.0965	0.0444
13	15	0.0440	0.3227	0.0000	29	30	0.0380	0.1500	0.0696
13	62	0.0098	0.1221	0.0000	29	31	0.0206	0.0833	0.0384
14	72	0.0107	0.0828	0.0000	30	32	0.0249	0.1005	0.0458
14	113	0.0063	0.0382	0.0000	32	33	0.0114	0.0448	0.0208
14	132	0.0057	0.0374	0.0000	33	34	0.0280	0.1140	0.0520
15	58	0.0115	0.0732	0.1420	33	35	0.0216	0.1070	0.0510
15	60	0.3907	1.6753	0.0000	33	36	0.0102	0.0536	0.0254
15	62	0.0084	0.0588	0.0000	34	40	0.0397	0.1517	0.0690
15	63	0.1704	1.4555	0.0000	34	77	0.0235	0.0896	0.0408
16	17	0.6017	1.4373	0.0000	35	40	0.0271	0.1341	0.0638

Table B-5. Line Data 2 of 3

From	To	R (p.u.)	X (p.u.)	B (p.u.)
36	67	0.0176	0.0924	0.0440
37	39	0.0039	0.0379	0.6700
37	126	0.0040	0.0381	0.6700
37	127	0.0040	0.0403	0.6832
39	42	0.0020	0.0186	0.3200
40	81	0.0300	0.3450	0.0038
40	82	0.0040	0.0190	0.0108
41	81	0.0370	0.3720	0.0058
41	83	0.0052	0.0256	0.0124
41	84	0.0057	0.0580	0.0292
42	109	0.0019	0.0196	0.3330
43	44	0.0188	0.0751	0.0348
43	103	0.0324	0.1702	0.0000
43	124	0.0293	0.1766	0.0000
43	125	0.1449	0.6509	0.0000
44	102	0.0130	0.0500	0.0236
44	103	0.0127	0.0510	0.0244
45	54	0.0108	0.0570	0.0272
46	47	0.0310	0.1378	0.0622
47	48	0.0251	0.1114	0.0502
47	49	0.0030	0.0120	0.0054
48	50	0.0336	0.1660	0.0780
48	51	0.0420	0.1300	0.0570
48	52	0.0540	0.1680	0.0740
49	87	0.0140	0.0680	0.0266
50	51	0.0300	0.0900	0.0410
50	123	0.4071	1.8543	0.0000
50	125	0.1337	0.6031	0.0000
51	141	0.0323	0.1000	0.0442
52	79	0.0623	0.2126	0.0940
52	106	0.0231	0.0717	0.0314
52	116	0.0060	0.0487	0.0256
52	117	0.0117	0.0493	0.0230
52	118	0.0000	0.0520	0.0000
11	53	0.0005	0.0200	0.0000
53	54	0.0275	0.1961	0.0956
53	55	0.0005	0.0026	0.0022
54	56	0.0174	0.0910	0.0430
54	57	0.0250	0.1237	0.0588
55	57	0.0462	0.1763	0.0802
55	149	0.0153	0.0671	0.0312
55	162	0.0040	0.0189	0.0098
56	67	0.0170	0.0894	0.0424
57	80	0.0272	0.1037	0.0472
58	61	0.0133	0.1018	0.1842
59	61	0.0106	0.0706	0.1210
60	61	0.0027	0.0653	-0.0022
60	61	0.0020	0.0393	0.0000
60	62	0.3674	0.9640	0.0000
60	65	0.1041	0.4144	0.0000

From	To	R (p.u.)	X (p.u.)	B (p.u.)
60	126	0.5367	1.8295	0.0000
61	62	0.0296	0.2275	0.3996
61	63	0.0043	0.0422	0.0764
62	63	0.0158	0.1702	0.0000
62	65	0.0040	0.0740	0.0000
62	126	0.0044	0.2969	0.0000
63	65	0.2409	1.9600	0.0000
64	65	0.0050	0.0571	0.9098
64	66	0.0033	0.0381	0.6066
65	126	0.0031	0.1536	0.0000
11	66	0.0000	0.0118	0.0000
67	68	0.0193	0.1013	0.0482
68	69	0.0068	0.0353	0.0168
69	77	0.0098	0.0374	0.0170
69	78	0.0114	0.0434	0.0196
69	79	0.0052	0.0433	0.0220
70	73	0.0000	0.0197	0.0000
70	149	0.0002	0.0018	0.0010
70	149	0.0002	0.0018	0.0010
71	85	0.0304	0.1506	0.0716
71	150	0.0196	0.0970	0.0462
72	113	0.0022	0.0130	0.0000
72	132	0.0028	0.0168	0.0000
72	152	0.0385	0.1800	0.0000
74	119	0.0031	0.0310	0.4822
75	128	0.0008	0.0087	0.1660
75	130	0.0004	0.0242	0.0000
78	79	0.0051	0.0336	0.0182
78	80	0.0244	0.0930	0.0422
74	79	0.0000	0.0180	0.0000
82	83	0.0053	0.0249	0.0130
84	93	0.0125	0.0826	0.0414
85	86	0.0211	0.1046	0.0498
86	87	0.0280	0.1120	0.0538
86	88	0.0440	0.2280	0.1090
88	96	0.0740	0.2500	0.0142
88	106	0.0079	0.0468	0.0232
86	89	0.0000	0.0570	0.0000
89	90	0.0690	0.1340	0.0140
90	96	0.1837	0.3590	0.0370
91	92	0.0156	0.0819	0.0376
91	93	0.0143	0.0895	0.0450
91	94	0.0145	0.0957	0.0480
92	102	0.0150	0.0610	0.0292
42	93	0.0000	0.0260	0.0000
93	108	0.0000	0.0154	0.0000
94	103	0.0227	0.1333	0.0660
94	107	0.0613	0.1891	0.0836
94	109	0.0000	0.0350	0.0000
91	95	0.0054	0.0458	-0.0036

Table B-6. Line Data 3 of 3

From	To	R (p.u.)	X (p.u.)	B (p.u.)
95	96	0.0870	0.2120	0.0860
95	97	0.1289	0.2809	0.0334
95	98	0.0071	0.0430	0.0224
95	99	0.0000	0.0685	0.0000
96	100	0.0690	0.1610	0.0186
96	101	0.0000	0.1031	0.0000
44	97	0.0051	0.1007	-0.0025
93	98	0.0006	0.0214	-0.0341
98	105	0.1485	0.2930	0.0310
100	104	0.0620	0.1450	0.0166
103	123	0.1820	0.7510	0.0000
103	124	0.0002	0.0167	0.0000
103	125	0.0279	0.1972	0.0000
34	104	0.0080	0.0637	-0.0033
38	105	0.0000	0.1160	0.0000
106	107	0.0196	0.0611	0.0268
107	122	0.0130	0.0621	0.0296
109	119	0.0060	0.0577	0.9290
109	124	0.0020	0.0222	0.3782
109	125	0.0070	0.0620	1.0000
110	111	0.0230	0.0990	0.0460
110	112	0.0000	0.0185	0.0000
110	114	0.0000	0.0768	0.0000
110	134	0.0032	0.0256	0.0134
110	141	0.0210	0.0649	0.0288
111	115	0.0527	0.2215	0.1030
112	120	0.0005	0.0044	0.0720
112	121	0.0000	0.0190	0.0000
113	132	0.0459	0.2911	0.0000
113	134	0.0008	0.0072	0.0038
115	117	0.0019	0.0154	0.0330
116	117	0.0048	0.0391	0.0214
116	119	0.0000	0.0090	0.0000
116	147	0.0035	0.0286	0.0156
117	147	0.0022	0.0175	0.0100
14	120	0.0003	0.0188	0.0000
120	128	0.0004	0.0051	0.1000
120	129	0.0003	0.0038	0.0652
122	123	0.0175	0.0835	0.0398
123	125	0.0423	0.2441	0.0000
124	125	0.0113	0.1585	0.0000
124	126	0.0577	0.8256	0.0000
125	126	0.0201	0.5915	0.0000
126	127	0.0877	0.7049	0.0000
72	128	0.0004	0.0180	0.0000
129	132	0.0004	0.0198	0.0000
133	134	0.0000	0.0410	0.0000
133	135	0.0109	0.0259	0.0004
133	136	0.0390	0.0990	0.0016
133	137	0.0134	0.0504	0.0010
135	138	0.0466	0.1182	0.0020
136	139	0.0260	0.0650	0.0010
137	140	0.0041	0.0156	0.0004
110	138	0.0000	0.0410	0.0000
138	139	0.0260	0.0650	0.0010
138	140	0.0251	0.0941	0.0018
138	145	0.0923	0.2338	0.0038
51	142	0.0000	0.1728	0.0000
142	143	0.1582	0.3919	0.0068
142	146	0.1618	0.3861	0.0070
143	144	0.0927	0.2322	0.0020
141	144	0.0000	0.0820	0.0000
144	145	0.0890	0.2210	0.0032
144	146	0.0680	0.2906	0.0058
116	148	0.0000	0.0410	0.0000
26	149	0.0000	0.0386	0.0000
26	149	0.0000	0.0386	0.0000
149	150	0.0010	0.0085	0.0020
149	151	0.0039	0.0262	0.0138
149	152	0.0253	0.1168	0.0544
151	161	0.0021	0.0138	0.0074
70	153	0.0000	0.0916	0.0000
70	153	0.0000	0.0916	0.0000
153	154	0.0710	0.2841	0.0054
153	155	0.0430	0.1856	0.0038
154	156	0.0155	0.0379	0.0008
154	160	0.0102	0.0429	0.0010
155	156	0.0176	0.0822	0.0014
156	157	0.0530	0.1273	0.0022
55	157	0.0000	0.0827	0.0000
157	158	0.0489	0.1404	0.0028
158	159	0.0339	0.0664	0.0012
159	160	0.0190	0.0811	0.0120
161	162	0.0022	0.0103	0.0054

Appendix C AR(3) Parameter Estimation

As mentioned in Chapter 6, an autoregressive model order three with a differentiation process of order one, or ARI(3,1), proved to be the model which best described the voltage phase angle data for the California System. A detailed description of how the parameter estimation for this model is carried out is presented in this Appendix.

An Autoregressive model order 3 has the following expression:

$$\theta_t = \phi_1\theta_{t-1} + \phi_2\theta_{t-2} + \phi_3\theta_{t-3} + e_t \tag{C.1}$$

solving for e_t the following equation is obtained:

$$e_t = \theta_t - \phi_3\theta_{t-3} - \phi_2\theta_{t-2} - \phi_1\theta_{t-1} \tag{C.2}$$

Knowing that the least squares estimator tries to minimize the value of squared sum of the random errors, the following objective function is obtained.

$$\min J(\phi) = \sum_{t=1}^{t=T}(e_t)^2 = \sum_{t=1}^{t=T}(\theta_t - \phi_3\theta_{t-3} - \phi_2\theta_{t-2} - \phi_1\theta_{t-1})^2 \tag{C.3}$$

Taking the first derivative with respect to ϕ_1 and setting it equal to zero:

$$\frac{d(J(\phi))}{d\phi_1} = -2\theta_{t-1}\sum_{t=1}^{t=T}(\theta_t - \phi_3\theta_{t-3} - \phi_2\theta_{t-2} - \phi_1\theta_{t-1}) = 0 \tag{C.4}$$

Simplifying and reorganizing equation (C.4):

$$\frac{d(J(\phi))}{d\phi_1} = \sum_{t=1}^{t=T}(\theta_t * \theta_{t-1} - \phi_3\theta_{t-3} * \theta_{t-1} - \phi_2\theta_{t-2} * \theta_{t-1} - \phi_1{\theta_{t-1}}^2) = 0 \tag{C.5}$$

Solving equation (C.5) for ϕ_1:

$$\phi_1 = \frac{\sum_{t=1}^{t=T} \theta_t * \theta_{t-1}}{\sum_{t=1}^{t=T} \theta_{t-1}^{\,2}} - \phi_3 \frac{\sum_{t=1}^{t=T} \theta_{t-3} * \theta_{t-1}}{\sum_{t=1}^{t=T} \theta_{t-1}^{\,2}} - \phi_2 \frac{\sum_{t=1}^{t=T} \theta_{t-2} * \theta_{t-1}}{\sum_{t=1}^{t=T} \theta_{t-1}^{\,2}} \tag{C.6}$$

Following the same procedure for ϕ_2 and ϕ_3 the next two expressions are found:

$$\phi_2 = \frac{\sum_{t=1}^{t=T} \theta_t * \theta_{t-2}}{\sum_{t=1}^{t=T} \theta_{t-2}^{\,2}} - \phi_3 \frac{\sum_{t=1}^{t=T} \theta_{t-3} * \theta_{t-2}}{\sum_{t=1}^{t=T} \theta_{t-2}^{\,2}} - \phi_1 \frac{\sum_{t=1}^{t=T} \theta_{t-1} * \theta_{t-2}}{\sum_{t=1}^{t=T} \theta_{t-2}^{\,2}} \tag{C.7}$$

$$\phi_3 = \frac{\sum_{t=1}^{t=T} \theta_t * \theta_{t-3}}{\sum_{t=1}^{t=T} \theta_{t-3}^{\,2}} - \phi_2 \frac{\sum_{t=1}^{t=T} \theta_{t-3} * \theta_{t-2}}{\sum_{t=1}^{t=T} \theta_{t-3}^{\,2}} - \phi_1 \frac{\sum_{t=1}^{t=T} \theta_{t-1} * \theta_{t-3}}{\sum_{t=1}^{t=T} \theta_{t-3}^{\,2}} \tag{C.8}$$

Organizing equations (C.6), (C.7) and (C.8) in matrix form:

$$\begin{bmatrix} \phi_1 \\ \phi_2 \\ \phi_3 \end{bmatrix} = \begin{bmatrix} 1 & \dfrac{\sum_{t=1}^{t=T} \theta_{t-2} * \theta_{t-1}}{\sum_{t=1}^{t=T} \theta_{t-1}^{\,2}} & \dfrac{\sum_{t=1}^{t=T} \theta_{t-3} * \theta_{t-1}}{\sum_{t=1}^{t=T} \theta_{t-1}^{\,2}} \\ \dfrac{\sum_{t=1}^{t=T} \theta_{t-1} * \theta_{t-2}}{\sum_{t=1}^{t=T} \theta_{t-2}^{\,2}} & 1 & \dfrac{\sum_{t=1}^{t=T} \theta_{t-3} * \theta_{t-2}}{\sum_{t=1}^{t=T} \theta_{t-2}^{\,2}} \\ \dfrac{\sum_{t=1}^{t=T} \theta_{t-1} * \theta_{t-3}}{\sum_{t=1}^{t=T} \theta_{t-3}^{\,2}} & \dfrac{\sum_{t=1}^{t=T} \theta_{t-3} * \theta_{t-2}}{\sum_{t=1}^{t=T} \theta_{t-3}^{\,2}} & 1 \end{bmatrix}^{-1} \begin{bmatrix} \dfrac{\sum_{t=1}^{t=T} \theta_{t} * \theta_{t-1}}{\sum_{t=1}^{t=T} \theta_{t-1}^{\,2}} \\ \dfrac{\sum_{t=1}^{t=T} \theta_{t} * \theta_{t-2}}{\sum_{t=1}^{t=T} \theta_{t-2}^{\,2}} \\ \dfrac{\sum_{t=1}^{t=T} \theta_{t} * \theta_{t-3}}{\sum_{t=1}^{t=T} \theta_{t-3}^{\,2}} \end{bmatrix} \quad \text{(C.9)}$$

Appendix D Transmission Lines

Table D-1 lists the transmission lines that have to be disconnected to isolate each coherent group from the system.

Table D-1. California - Transmission Lines

Group	From	To
Kramer	PISGAH 230	LUGO 230
	BAKER 115	MTN PASS 115
	BARRENRD 230	RINALDI 230
	KRAMER 230	LUGO 230
	VICTOR 230	LUGO 230
Vulcan 1	MIDWAY X 230	MIDWAY X 92
	HIGHLINE 230	HIGHLINE 92
Mnt. View	MNTVIEW 230	SANBRDNO 230
North-South	MIDWAY 500	VINCENT 500
Magunden	MAGUNDEN 230	ANTELOPE 230
	MAGUNDEN 230	PASTORIA 230
Diablo	DIABLO 2 25	DIABLO 500
	DIABLO 1 25	DIABLO 500
Morrobay	GATES 230	MORROBAY 230
	GATES 230	ARCO 230
	GATES 230	MIDWAY 230
	GATES 230	TEMPLETN 230
	GATES 70	GATS2_TP 70
	GATES 70	HURON 70
	GATES 70	JACALITO 70
	TEMPLT7 70	TEMPLETN 230
	HELM 70	HELM 230
	LOS BANS 70	WRGHT PP 70
	CHEVPIPE 70	LOS BANS 70
	ORO LOMA 70	ORO LOMA 115
	MENDOTA 70	MENDOTA 115
	SCHLNDLR 70	SCHINDLR 115
Haynes	HAYNES 230	ATWATER 230
	VELASCO 230	HAYNES 230
	STJOHN 230	HAYNES 230
	RIVER 230	HAYNES 230